AD-A016 439

INVESTIGATION OF RADAR RAIN CLUTTER CANCELLATION USING A POLARIZATION METHOD

R. W. Rice, et al

Tennessee University

Prepared for:

Rome Air Development Center

August 1975

RADC-TR-75-126
Final Technical Report
August 1975

INVESTIGATION OF RADAR RAIN CLUTTER CANCELLATION USING A POLARIZATION METHOD

University of Tennessee

Rome Air Development Center
Air Force Systems Command
Griffiss Air Force Base, New York 13441

This report has been reviewed by the RADC Information Office (OI) and is releasable to the National Technical Information Service (NTIS). At NTIS it will be releasable to the general public including foreign nations.

This report has been reviewed and is approved for publication.

APPROVED: Vincent Vannicola

VINCENT VANNICOLA
Project Engineer

APPROVED: Rudolf C. Paltauf

RUDOLF C. PALTAUF
Lt Col, USAF
Chief, Surveillance Division

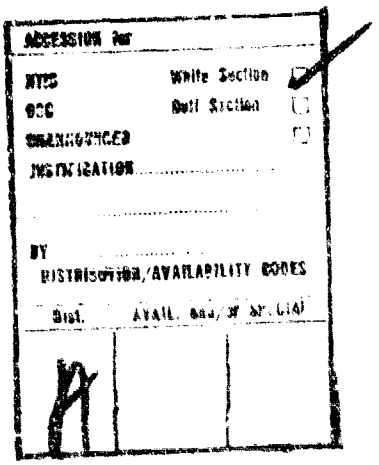

FOR THE COMMANDER: John P. Huss

JOHN P. HUSS
Acting Chief, Plans Office

Do not return this copy. Retain or destroy.

UNCLASSIFIED
SECURITY CLASSIFICATION OF THIS PAGE (When Data Entered)

REPORT DOCUMENTATION PAGE		READ INSTRUCTIONS BEFORE COMPLETING FORM
1. REPORT NUMBER RADC-TR-75-126	2. GOVT ACCESSION NO.	3. RECIPIENT'S CATALOG NUMBER
4. TITLE (and Subtitle) INVESTIGATION OF RADAR RAIN CLUTTER CANCELLATION USING A POLARIZATION METHOD		5. TYPE OF REPORT & PERIOD COVERED Final Technical Report Oct 73 - Dec 74 6. PERFORMING ORG. REPORT NUMBER N/A
7. AUTHOR(s) R. W. Rice P. Z. Peebles		8. CONTRACT OR GRANT NUMBER(s) F30602-74-C-0037
9. PERFORMING ORGANIZATION NAME AND ADDRESS University of Tennessee Knoxville TN 37916		10. PROGRAM ELEMENT, PROJECT, TASK AREA & WORK UNIT NUMBERS 62702F 45060188
11. CONTROLLING OFFICE NAME AND ADDRESS Rome Air Development Center (OCTS) Griffiss AFB NY 13441		12. REPORT DATE August 1975 13. NUMBER OF PAGES 157
14. MONITORING AGENCY NAME & ADDRESS(if different from Controlling Office) Same		15. SECURITY CLASS. (of this report) Unclassified 15a. DECLASSIFICATION/DOWNGRADING SCHEDULE N/A

16. DISTRIBUTION STATEMENT (of this Report)

Approved for public release; distribution unlimited.

17. DISTRIBUTION STATEMENT (of the abstract entered in Block 20, if different from Report)

Same

18. SUPPLEMENTARY NOTES

RADC Project Engineer:
Vincent Vannicola (OCTS)

19. KEY WORDS (Continue on reverse side if necessary and identify by block number)

Radar, Polarization Backscatter,
Rain Backscatter, Clutter

20. ABSTRACT (Continue on reverse side if necessary and identify by block number)

This work considers a new polarization method for possible reduction of rain clutter in monostatic radar. Basically, the proposed technique attempts to adjust the effective polarization of the receiver to match the average polarization of backscattered fields to improve the cancellation attainable from systems ordinarily using circular polarization.

DD FORM 1 JAN 73 1473 EDITION OF 1 NOV 65 IS OBSOLETE

UNCLASSIFIED
SECURITY CLASSIFICATION OF THIS PAGE (When Data Entered)

PREFACE

This report describes work performed at the Electrical Engineering Department of the University of Tennessee, Knoxville, Tennessee 37916, over the period 16 October 1973 to 31 December 1974. The work was performed for the Air Force Systems Command, Rome Air Development Center, Griffiss Air Force Base, New York 13441 under contract F30602-74-C-0037.

The overall effort related to the definition of a rain backscatter model and cancellation of radar rain clutter using a new polarization method. The work was conceived and guided by Dr. Peyton Z. Peebles, Jr., Associate Professor of Electrical Engineering. Most of the work on the rain cancellor was performed by Mr. R.W. Rice, a Graduate Research Assistant. Dr. Peebles did most of the work regarding the rain model, while Mr. H. Sakamoto, a Graduate Teaching Assistant, performed several literature searches. The final report was prepared by Dr. Peebles and Mr. Rice.

The technical contract officer for the Air Force was Mr. Vincent C. Vannicola. The authors express their appreciation to Mr. Vannicola for his support of the research.

CONTENTS

EVALUATOR'S MEMO

Project No: 45060188

Effort Title: Investigation of Radar Rain Clutter Using a Polarization Method

Contract No: F30602-74-C-0037

Contractor: University of Tennessee Knoxville, Tennessee

Radar backscatter from rain rapidly degrades the capability to detect aircraft targets. A most crucial situation exists with GCA (Ground Control Approach) and PAR (Precision Approach Radar) equipment during rain storms. This effort involved a method for cancelling the backscatter polarization from raindrops. In contrast to the ordinary circular polarization cancellation method this technique estimates the mean ellipticity and orientation of the backscattered polarization and in turn adjusts the receiver to null out this polarization. The target return will, on the average, lose about 3 dB while the loss in rain return will exceed that from ordinary CP by about 10 dB.

The results are in the form of simulations modeled from meteorological data. With a relatively simple scheme, equipments now employing CP can be converted to cancel the estimated mean polarization of the rain.

This work is in support of TPO-5, "EM Generation and Control."

Vincent Vannicola

VINCENT VANNICOLA
Project Engineer/OCTS

1.0 INTRODUCTION

1.1 Historical Development

In spite of improved performance due to advances in detection methods, low-noise receivers, waveform optimization, etc., the modern radar system often gives a much lower level of performance because of rain clutter.

Early radar systems were generally designed to emit and receive linearly polarized radiation. There is nothing inherent in the structure of the linearly polarized system to suppress the clutter caused by precipitation. Recognition of this problem prompted investigation into different types of systems. In 1947 Ridenour [1] proposed a significant new concept for the basic radar system. Ridenour noted that if rain particles could be correctly modeled as spheres then the use of circular polarization on both the transmitting and receiving antennas offered the possibility of significant clutter reduction. In the same discussion Ridenour was also able to offer experimental data that indicated that clutter reduction on the order of 26dB. was possible using circular polarization. Additionally Ridenour was able to point out that two limitations of this approach to clutter cancellation are rain particles which are not true spheres and radiation which is not exactly circular. In spite of the advantages offered by the use of circular polarization it was not immediately adopted. In fact, circular polarization was rediscovered in 1954 by White [2] while at the same time Hunter [3] reemphasized the limitations of the technique due to radiation which was not perfectly circular.

A necessary step in the process of correcting the errors introduced by non-circular polarization and non-spherical scatterers was that of obtaining an accurate model of the scattering particles and then obtaining a solution to the scattering of electromagnetic waves by an object whose shape is that of the model. From the literature one recognizes that interest in modeling rain particles preceeded the development of radar technology by many years. A recent paper by Pruppacher and Beard [4] offers a review of the efforts along this line while another paper by Pruppacher and Pitter [5] claims to offer the most accurate model yet available for rain. In simple terms, Pruppacher and Pitter claim that the oblate spheroid is a good approximation to the true shape of rain particles in many cases. Additional detail concerning particle shape will be discussed in Chapter 3.

The scattering of electromagnetic waves by bodies of various shapes is a problem that has also received considerable attention for many years. Logan [6] notes that some of the earliest work done in this area involved scattering by a sphere and was done by Clebsch in 1861. In the same article, Logan offers an excellent outline of the historical development of the theory of scattering by spheres. Another paper deserving mention at this point is a survey of scattering literature by Corriher and Pyron [7]. It should be noted however that none of the sources referenced by the two previously mentioned works considers the problem of scattering by an oblate spheroid. This problem was apparently first solved by Labrum [8] in 1952, and later Atlas, Kerker, and Mitschfield [9] offered concurring results.

1.2 Description of the Proposed Method

This report is an analysis of the system depicted in figure 1.2-1. In the block diagram, the transmitter is represented in the left hand portion of the figure, the propagating medium and scattering elements are shown in the center of the figure, and the receiver is depicted in the right hand portion of the diagram.

The features which distinguish this system from the ordinary circular system are indicated in the block diagram as elements T, R, and G. Elements T and R account for the magnitude and phase imperfections which prevent the ordinary system from being truly circularly polarized. G is a dynamic gain element which has been added in the effort to reduce the performance limitations of the ordinary system caused by non-spherical rain and non-circular polarization. A detailed description of G will be given in section 5.

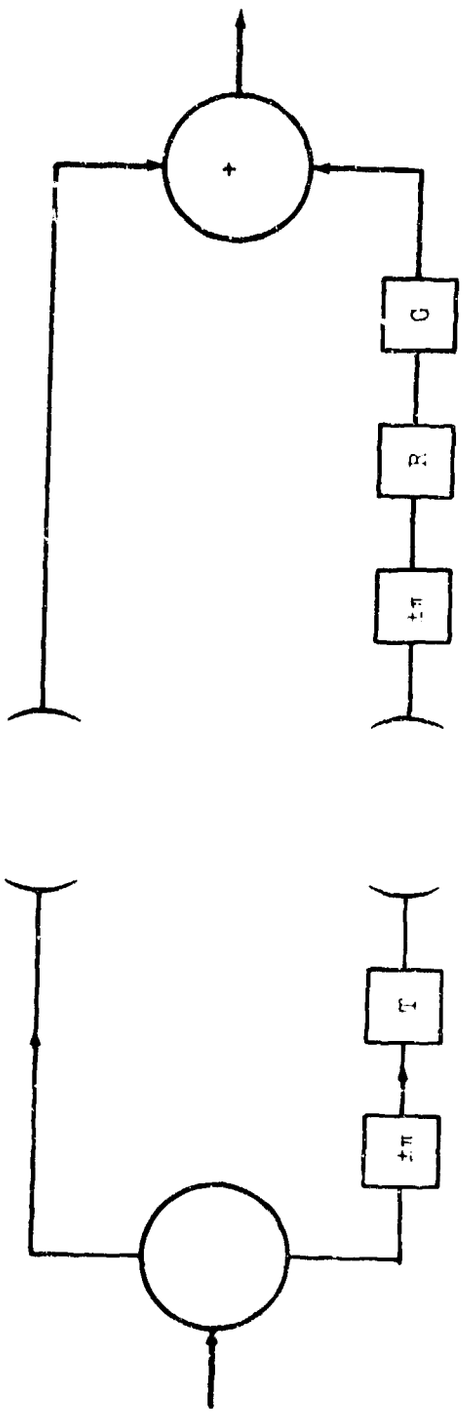

Fig. 1.2-1. The clutter cancellation system.

2.0 BACKGROUND THEORY AND ASSUMPTIONS

2.1 Basic Assumptions

Prior to detailed development of the concept which gives rain clutter cancellation it is helpful, indeed necessary, to first set down certain definitions, assumptions and preliminary theory applicable to the whole work. For example, to avoid confusion we shall use the word "signal" to imply either a waveform resulting from backscatter from a target or waveforms preceeding target or rain illumination while the word "clutter" will apply to waveforms resulting from rain backscatter. Other definitions are made clear in the course of developments.

We make the following basic assumptions throughout the effort.

1. Only rain clutter is present. Thus, noise, ground clutter, multipath and other interference sources are neglected. This assumption is approximately satisfied for a low-noise, narrow-beam system directed several beamwidths above the horizon.
2. Only a single target exists within the radar beam.
3. The target behaves as a point reflector, that is, the target size is small relative to the pulse length in space.
4. There are no multiple reflections between rain particles or between the rain and target.
5. The radar is a monostatic system. Generalization to the bistatic system is relatively straightforward and some of the developments are formulated in such a manner prior to specialization to the monostatic case.

6. The system is capable of transmitting and receiving two linearly polarized waves that are approximately space-orthogonal.
7. The antenna patterns have narrow main lobes, that is, beam-widths are on the order of a few degrees or less in any plane containing the boresight axis.
8. Antenna pattern sidelobes fall off with angle such that the dominant contribution to the rain clutter power comes from angles sufficiently near the direction of the mainlobe maximum that small-angle approximations may be made.

2.2 Coordinate Definitions

Figure 2.2-1 defines the coordinate system which interfaces the radar with its environment. The radar is at the origin of the X, Y, Z system and radiates in the Z (boreright) direction. Rain particles are assumed to fall, on the average, along a line parallel to O-x. This line is defined by angles ζ, called the rain heading, and ψ, called the rain fall angle. With these definitions the average wind vector lies in the O-x-y plane; it also lies in the X-Z plane (as shown) if the boresight axis is horizontal and the wind is entirely horizontal. In general, even for horizontal wind, the wind vector is tilted in the O-x-y plane when the boresight axis is elevated.

The above definitions apply to the fall geometry for raindrops which is determined by the wind. Locations of the drops are defined by spherical coordinates, radar centered. The coordinates for the ith drop are α_i, β_i analogous to ζ, ψ.

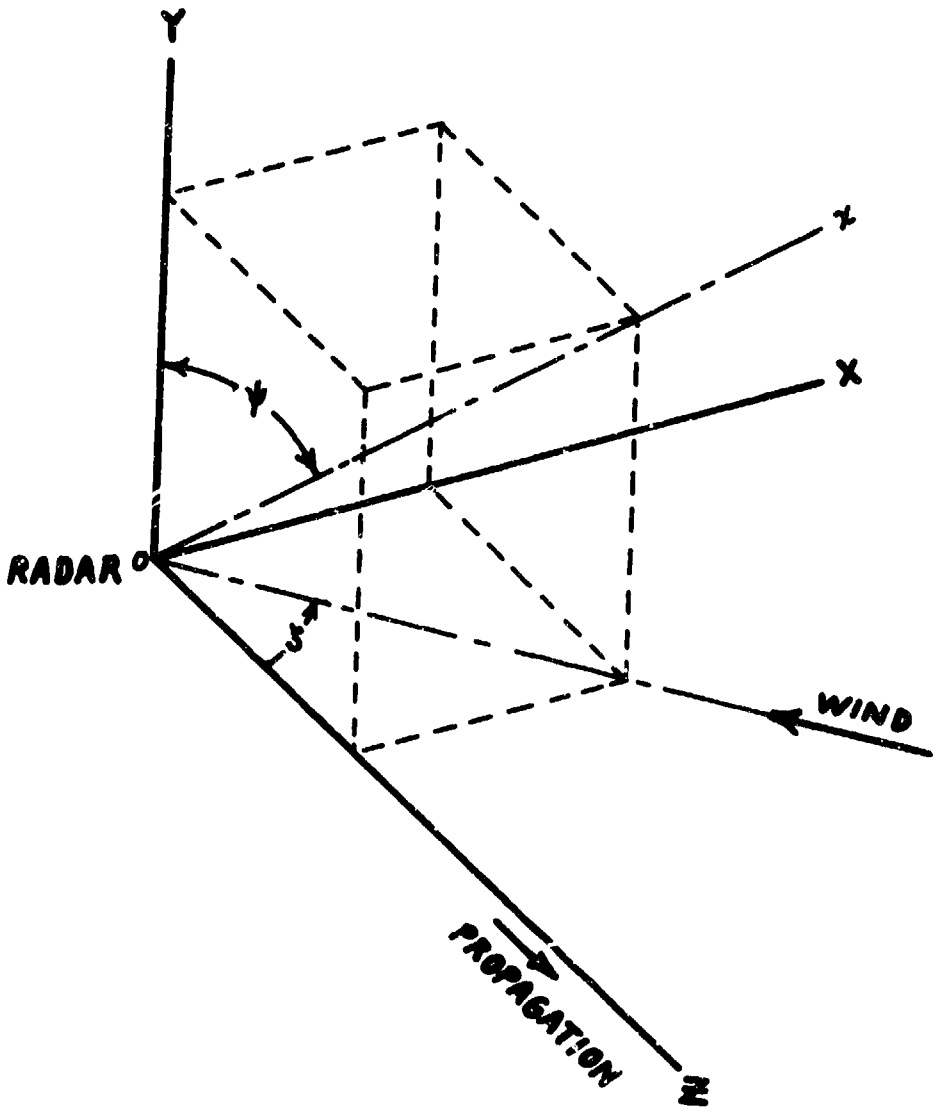

Fig. 2.2-1.

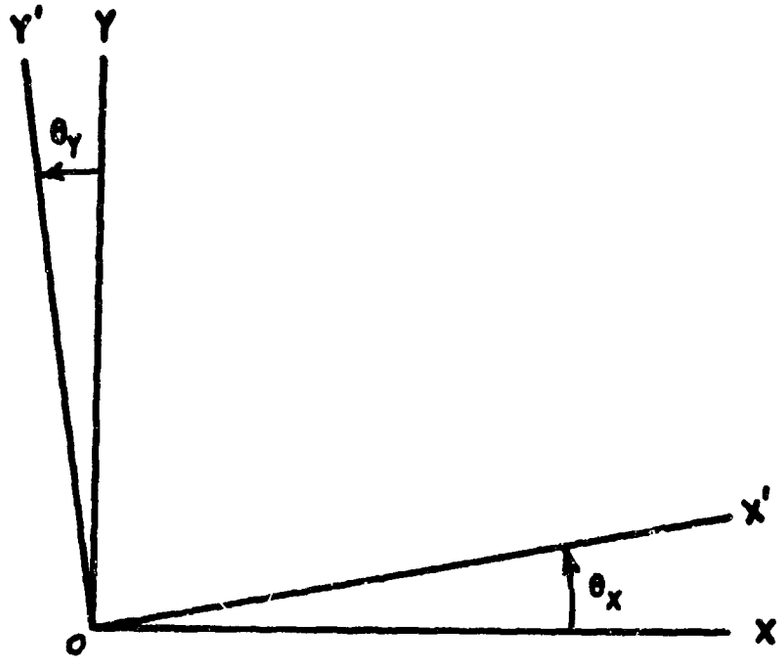

Fig. 2.2-2.

2.3 Scattering Theory

It is desirable to be able to write an equation relating the electric field incident upon and reflected by a scattering body such as a rain particle. The first step in the process of obtaining the desired equation is the specification of the nature of the scattering particle. For the purposes of the following calculations it shall be assumed that the scattering particle is a homogeneous oblate spheroid. Justification for the assumed shape is provided in section 3.

N.R. Labrum [8] has provided a fundamental solution to the problem of electromagnetic scattering by an oblate spheroid. His approach to the problem is based upon work done by Stratton [10], which has shown that where the ratio

$$\frac{\text{particle radius}}{\text{radiation wavelength}}$$

is small, the dipole moment induced in a sphere is the same for both static and time varying incident fields. Labrum's work relates the dipole moment induced in the scattering particle to the incident electric field. In turn, the reflected electric field may be related to the induced dipole moment, but this is unnecessary for the current work since the final equation will involve only ratios of this parameter which associates a reflected field with an incident field. Thus, the equations relating the reflected electric field to the incident electric field will be of the form

$$E^- = SE^+ \tag{2.3-1}$$

E^- = reflected electric field

E^+ = incident electric field

but S will not be unitless. As in Labrum's work, S will have the units

$$\frac{\text{dipole moment}}{\text{electric field intensity}} = \text{Farad} - \text{meter}^2 \tag{2.3-2}$$

Rice and Peebles [11] have extended Labrum's work to the case of circular polarization and homogeneous oblate spheroids. From the standpoint of notation, this extension is simplified if the field intensities are resolved into orthogonal components which may be entered as elements in a column matrix. Thus the following shall be used.

$$\begin{bmatrix} E_x^- \\ E_y^- \end{bmatrix} = \begin{bmatrix} S_{11} & S_{12} \\ S_{21} & S_{22} \end{bmatrix} \begin{bmatrix} E_x^+ \\ E_y^+ \end{bmatrix} \tag{2.3-3}$$

For the particles assumed, Rice and Peebles define the S_{ij} terms in the following manner.

$$\begin{aligned} S_{11} &= g_x \cos^2(\theta) + g_y \sin^2(\theta) \\ S_{12} &= (g_x - g_y) \cos(\theta) \cos(\psi) \\ S_{21} &= (g_x - g_y) \cos(\theta) \cos(\psi) \\ S_{22} &= g_x \cos^2(\psi) + g_y \sin^2(\psi) \end{aligned} \tag{2.3-4}$$

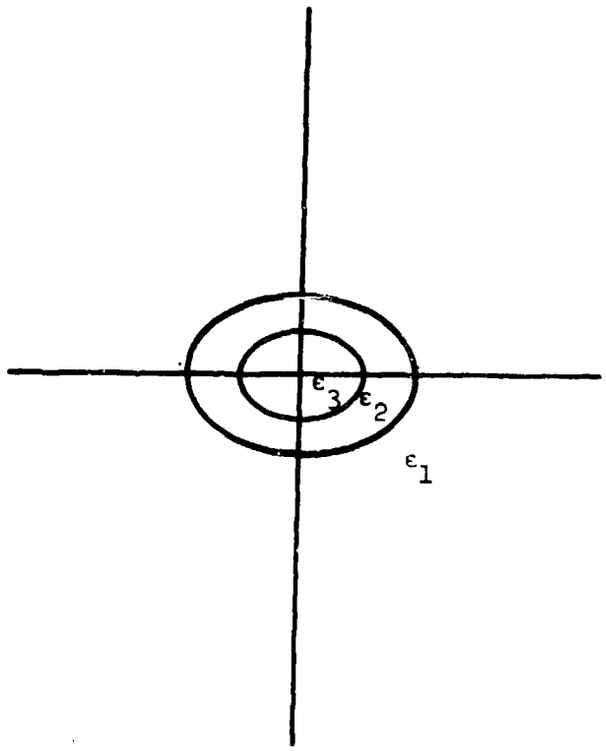

Fig. 2.3-1. Particle and related dielectric quantities.

$$g_x = \frac{8\pi\varepsilon_1}{3}\left[\frac{\rho(1-\rho^2)^{3/2}\,(\varepsilon_2-\varepsilon_1)b^3}{[2\sqrt{1-\rho^2} - \rho\pi + 2\rho\arctan\,(\rho/\sqrt{1-\rho^2})]\,(\varepsilon_2-\varepsilon_1) + 2\varepsilon_1(1-\rho^2)^{3/2}}\right]$$

$$g_y = \frac{8\pi\varepsilon_1}{3}\left[\frac{\rho(1-\rho^2)^{3/2}\,(\varepsilon_2-\varepsilon_1)b^3}{\rho[\frac{\pi}{2} - \rho\sqrt{1-\rho^2} - \arctan\,(\rho/\sqrt{1-\rho^2})]\,(\varepsilon_2-\varepsilon_1) + 2\varepsilon_1(1-\rho^2)^{3/2}}\right]$$

$\rho = a/b$

In equation (2.3-4), θ is a particle orientation parameter which is used by Labrum and is related to the coordinate parameters used in this work as indicated in equation (2.3-5).

$$\cos(\theta) = \sin(\zeta)\,\sin(\psi) \qquad (2.3\text{-}5)$$

The results of applying equation (2.3-5) to the definition of the S_{ij} terms given in equation (2.3-4) are provided in equation (2.3-6)

$$S_{11} = g_y + (g_x - g_y)\sin^2(\zeta)\sin^2(\psi)$$

$$S_{12} = (g_x - g_y)\sin(\zeta)\sin(\psi)\cos(\psi) \qquad (2.3\text{-}6)$$

$$S_{22} = g_x\cos^2(\psi) + g_y\sin^2(\psi)$$

With the S matrix elements defined as in equation (2.3-6), it is now possible to express the components of the scattered electric field in terms of the components of the incident electric field as indicated in equation (2.3-3). Note that the equation in this form

represents scattering from a single scattering particle. The effects of multiparticle scattering will be represented by a summation of the following form.

$$E_x^- = \sum_{i=1}^{N_k} (S_{11i}\, E_{xi}^+) + \sum_{i=1}^{N_k} (S_{12i}\, E_{yi}^+)$$
$$E_y^- = \sum_{i=1}^{N_k} (S_{21i}\, E_{xi}^+) + \sum_{i=1}^{N_k} (S_{22i}\, E_{yi}^+) \qquad (2.3\text{-}7)$$

In equation (2.3-7), the total number of scattering particles within the scattering volume of interest is N_k.

2.4 The Reference System

What will be called the reference system in this work is presented in block diagram form in Figure 2.4-1. The system is a linearly polarized monostatic radar, and the performance of the ordinary circularly polarized system and the cancellation system will be compared to the performance of this reference system.

From the theory of linear antennas [12], it can be shown that the electric field intensity in the far zone of a dipole radiator, e^+, is related to the driving point potential, e_T, as shown in equation (2.4-1).

$$e^+ = \frac{K_1\, e_T\, G_T}{Z}\, e^{-j\beta_0 Z} \qquad (2.4\text{-}1)$$

In the preceeding equation, K_1 is a complex constant, β_0 is the traditional phase constant, Z is the radial distance between the phase

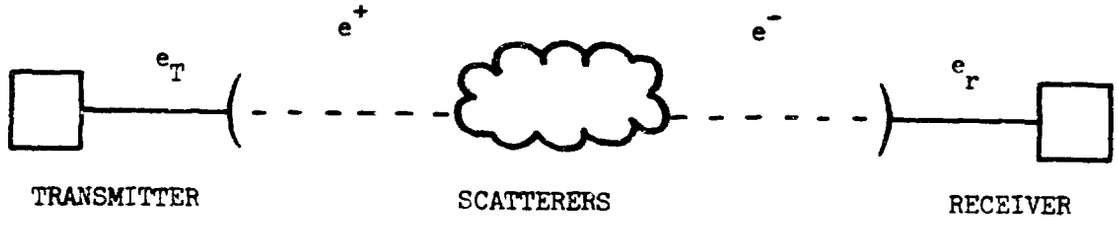

Fig. 2.4-1. Reference system diagram.

center of the antenna and the point where the field intensity is to be measured, and G_T is the radiation characteristic (voltage) of the transmitter antenna.

By the scattering theory of the preceeding, section, the scattered field at a distance Z' from the scattering body has an intensity, e^-, which is given by

$$e^- = \frac{S_{11}\, e^+}{Z'}\; e^{-j\beta_0 Z'} \tag{2.4-2}$$

where S_{11} is an element of the previously defined scattering matrix.

From the theory of reciprocity as it applies to linear antennas, the received signal, e_r, is

$$e_r = K_2 G_r e^- = \frac{K_2 G_r S_{11} e^+}{Z'}\; e^{-j\beta_0 Z'}$$

$$= \frac{K_2 K_1 G_r G_T S_{11} e_T}{Z \cdot Z'}\; e^{-j\beta_0 (Z+Z')} \tag{2.4-3}$$

For a monostatic radar, $G_r = G_T = G$ and $Z = Z'$, and to simplify notation let

$$K = K_2 \cdot K_1 \quad . \tag{2.4-4}$$

Thus the signal received as a result of scattering from one scattering body is given by equation (2.4-5).

$$e_r = \frac{K e_T S_{11}}{Z^2}\; G^2 e^{-j2\beta_0 Z} \tag{2.4-5}$$

Extending the analysis to cover multiparticle scattering involves only implementing a summation of returns from the individual scattering bodies. Such a summation is

$$e_r = \sum_{i=1}^{N_k} \frac{Ke_T S_{11i}(k) G_i^2}{Z_i^2} e^{-j2\beta_0 Z_i} \tag{2.4-6}$$

The receiver signal, e_r, indicated in equation (2.4-6) is a result of returns from all the scattering bodies lying within the range cell corresponding to the time at which e_r is evaluated. A convenient way of noting this fact is to specify the location of each particle with respect to the center of the range cell in which it lies. For the $i^{\underline{th}}$ particle in the $k^{\underline{th}}$ range cell this would be

$$Z_i(k) = Z(k) + \Delta Z_i \tag{2.4-7}$$

An approximation which will be used in the denominator of equation (2.4-6) is

$$Z_i(k) \simeq Z(k). \tag{2.4-8}$$

This approximation is in error by no more than 0.5 percent for a transmitter pulsewidth of one microsecond and a range of 16 km. Application of the approximation to equation (2.4-6) results in the following. Note that N_k is the total number of scattering particles in the $k^{\underline{th}}$ range cell.

$$e_r(k) = \frac{Ke_T}{Z_{(k)}^2} e^{-j2\beta_0 Z(k)} \sum_{i=1}^{N_k} S_{11i}(k) G_i^2 e^{-j2\beta_0 \Delta Z_i} \tag{2.4-9}$$

In summary, equation (2.4-9) is an expression for the output voltage resulting from clutter occuring in the $k^{\underline{th}}$ range cell for what will be called the reference system.

2.5 The Ordinary System

An ordinary system will be defined as a radar which radiates and receives the same-sense circular polarization to reduce rain clutter. Such a system is ideal if it radiates perfectly circular polarization of one sense and has zero response to a perfectly circular wave of the opposite sense. An imperfect ordinary system does not produce perfectly circular operation due to manufacturing and/or alignment errors.

By recognizing that a circularly polarized wave, indeed, even an elliptically polarized wave, may be considered to be comprised of two linearly polarized waves we may model the transmission and reception operations of the system as shown in Figure 2.5-1. A signal e_T is power-split with one signal driving an "antenna" representing the x-polarized pattern. The second signal passes through a complex gain constant T, representing the error that the transmitting function introduces relative to true circular polarization (T=1, ideally). This signal then passes through a $\pm \pi/2$ or $-\pi/2$ phase shifts to produce either left or right hand polarizations respectively when transmitted through an "antenna" representing the Y-polarized pattern. Similar, but reverse, operations exist in the receiver. The parameter R of the receiver equals T in a monostatic system.

If the true radiations e_X^+, and e_Y^+, are non-orthogonal, the components each couple to the desired space axes X and Y (see Figure 2.2-2). The coupling may be accounted for by use of a coupling matrix with elements t_{ij}, i and j=1 and 2. Thus,

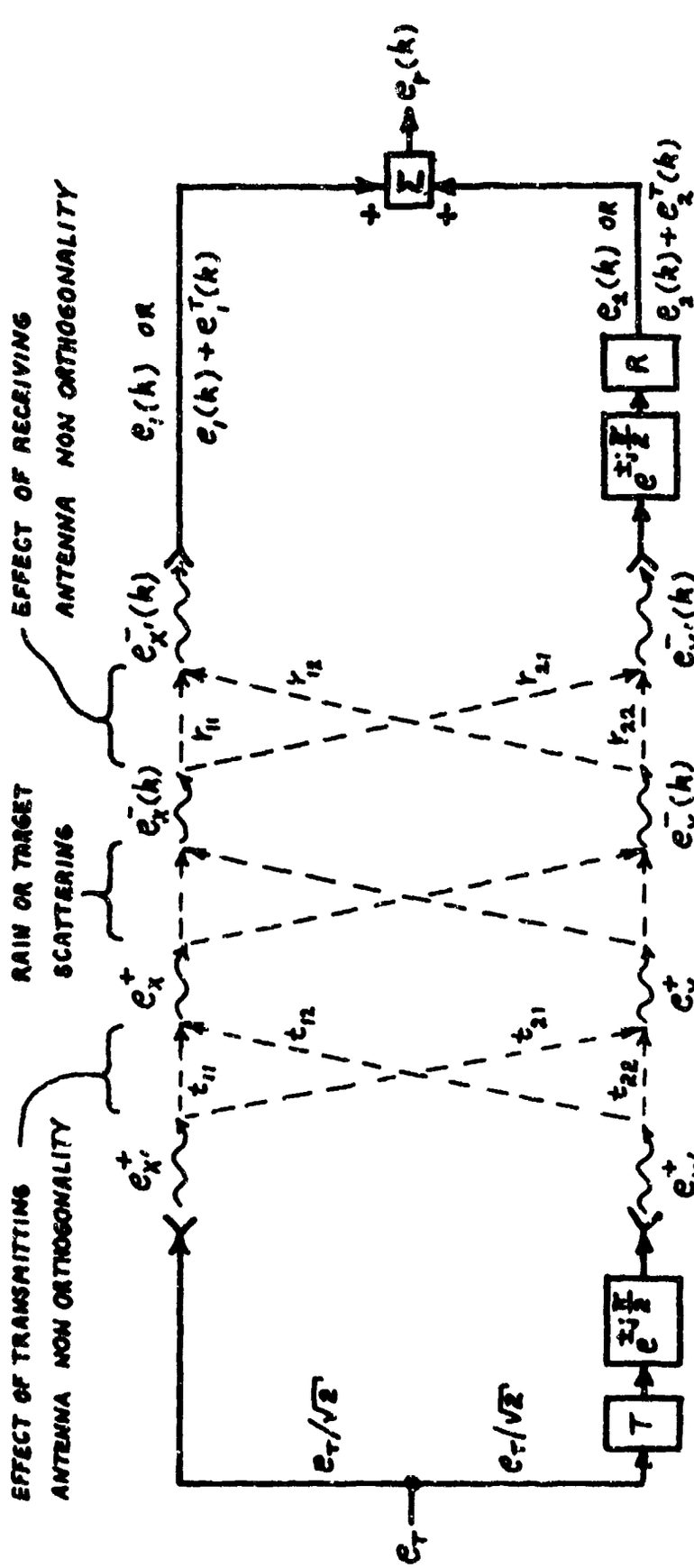
EFFECT OF TRANSMITTING ANTENNA NON ORTHOGONALITY
RAIN OR TARGET SCATTERING
EFFECT OF RECEIVING ANTENNA NON ORTHOGONALITY
e_T
$e_T/\sqrt{2}$
$e_T/\sqrt{2}$
T
$e^{\pm j\frac{\pi}{2}}$
$e^{\pm j\frac{\pi}{2}}$
R
e_x^+
$e_{x'}^+$
e_y^+
$e_{y'}^+$
t_{11}
t_{12}
t_{21}
t_{22}
$e_x^-(k)$
$e_{x'}^-(k)$
$e_y^-(k)$
$e_{y'}^-(k)$
$e_i(k)$ OR
$e_i(k)+e_i^T(k)$
$e_r(k)$
$e_2(k)$ OR
$e_2(k)+e_2^T(k)$

Fig. 2.5-1

$$\begin{bmatrix} e_X^+ \\ e_Y^+ \end{bmatrix} = \begin{bmatrix} t_{11} & t_{12} \\ t_{21} & t_{22} \end{bmatrix} \begin{bmatrix} e_{X'}^+ \\ e_{Y'}^+ \end{bmatrix} \quad . \tag{2.5-1}$$

Using Figure 2.2-2 we may find that

$$[t] = \begin{bmatrix} t_{11} & t_{12} \\ t_{21} & t_{22} \end{bmatrix} = \begin{bmatrix} \cos(\theta_X) & -\sin(\theta_Y) \\ \sin(\theta_X) & \cos(\theta_y) \end{bmatrix} \quad . \tag{2.5-2}$$

Another matrix accounts for either rain or target scattering. Still a third matrix accounts for the receiver non-orthogonal polarizations. For a monostatic radar the matrix, defined to have elements r_{ij}, i and j=1 and 2, relates received fields at the antenna to reflections from range cell k as follows:

$$\begin{bmatrix} e_{X'}^-(k) \\ e_{Y'}^-(k) \end{bmatrix} = \begin{bmatrix} r_{11} & r_{12} \\ r_{21} & r_{22} \end{bmatrix} \begin{bmatrix} e_X^-(k) \\ e_Y^-(k) \end{bmatrix} \tag{2.5-3}$$

where,

$$[r] = \begin{bmatrix} r_{11} & r_{12} \\ r_{21} & r_{22} \end{bmatrix} = \frac{\begin{bmatrix} \cos(\theta_X) & \sin(\theta_X) \\ -\sin(\theta_Y) & \cos(\theta_Y) \end{bmatrix}}{\cos(\theta_X - \theta_Y)} = \frac{[t]^t}{\cos(\theta_X - \theta_Y)} \tag{2.5-4}$$

Here $[\cdot]^t$ represents matrix transpose.

We now calculate the received waveforms for the system of Figure 2.5-1. We shall use the exponential (phasor) representation of waveforms. The transmitter excitation is then

$$e_T = E_T e^{j\omega_o t} \tag{2.5-5}$$

where E_T is the magnitude of e_T and ω_0 is radian frequency. Let $G_t^X(\alpha, \beta)$ and $G_t^Y(\alpha, \beta)$ be the transmit patterns for X´ and Y´ polarization components evaluated in directions α and β. The electric fields $e_{X'}^+$ and $e_{Y'}^+$ near the antenna become

$$e_{X'}^+ = K_1 G_t^X(\alpha, \beta)\, e_T/\sqrt{2} \tag{2.5-6a}$$

$$e_{Y'}^+ = \pm jTK_1 G_t^Y(\alpha, \beta)\, e_T/\sqrt{2} \tag{2.5-6b}$$

where K_1 is a proportionality constant.

To continue further we first assume scattering is from a single rain particle. Results are then extended to multiple-particle rain and target scattering.

Let rain particle i be located in range cell k at a distance

$$Z_i(k) = Z(k) + \Delta Z_i \tag{2.5-7}$$

where Z(k) is the distance to the center of the cell and ΔZ_i is particle position relative to cell center. By combining (2.5-5) with (2.5-1) the field components e_X^+ and e_Y^+ may be determined. If we then use the scattering matrix of the rain particle and include the attenuation factor due to distance we may write the received fields $e_X^-(k)$ and $e_Y^-(k)$ due to range cell k as

$$\begin{bmatrix} e_X^-(k) \\ e_Y^-(k) \end{bmatrix} = \begin{bmatrix} s_{11i}(k) & s_{12i}(k) \\ s_{21i}(k) & s_{22i}(k) \end{bmatrix} \begin{bmatrix} t_{11} & t_{12} \\ t_{21} & t_{22} \end{bmatrix} \begin{bmatrix} G_t^X(\alpha_i, \beta_i) \\ \pm jTG_t^Y(\alpha_i, \beta_i) \end{bmatrix} \frac{K_1 e_T e^{-j2\beta_0 Z_i(k)}}{Z_i^2(k)\sqrt{2}} \tag{2.5-8}$$

Here the rain scattering matrix [s] has elements $s_{mni}(k)$ for cell k.

We may next use (2.5-3) with 2.5-8) to obtain the fields in the polarization planes of the receiving antenna. The received waveforms $e_1(k)$ and $e_2(k)$ are related to these fields, $e_X^-(k)$ and $e_Y^-(k)$, by

$$e_1(k) = K_2 G_r^X(\alpha_i, \beta_i)\, e_X^-(k) \tag{2.5-9a}$$

$$e_2(k) = \pm jK_2 R G_r^Y(\alpha_i, \beta_i)\, e_Y^-(k) \tag{2.5-9b}$$

where K_2 is a proportionality constant. Combining and recognizing that R=T, $G_t^X = G_r^X = G^X$ and $G_t^Y = G_r^Y = G^Y$ for a monostatic system gives

$$\begin{bmatrix} e_1(k) \\ e_2(k) \end{bmatrix} = \begin{bmatrix} G^X(\alpha_i, \beta_i) & 0 \\ 0 & \pm jTG^Y(\alpha_i, \beta_i) \end{bmatrix} [t]^t [s][t] \begin{bmatrix} G^X(\alpha_i, \beta_i) \\ \pm jTG^Y(\alpha_i, \beta_i) \end{bmatrix} \cdot \frac{Ke_T e^{-j2\beta_0 Z_i(k)}}{Z_i^2(k)\sqrt{2}} \tag{2.5-10}$$

where $K = K_1 \cdot K_2$.

To be more explicit, (2.5-10) may be expanded to obtain $e_1(k)$ and $e_2(k)$ as

$$\begin{aligned} e_1(k) = G^X(\alpha_i, \beta_i) \Big\langle & \{t_{11}[t_{11}s_{11i}(k) + t_{21}s_{12i}(k)] \\ & + t_{21}[t_{11}s_{21i}(k) + t_{21}s_{22i}(k)]\}\, G^X(\alpha_i, \beta_i) \\ & \pm jT\{t_{11}[t_{12}s_{11i}(k) + t_{22}s_{12i}(k)] \\ & + t_{21}[t_{12}s_{21i}(k) + t_{22}s_{22i}(k)]\}\, G^Y(\alpha_i, \beta_i) \Big\rangle \cdot \frac{Ke_T e^{-j2\beta_0 Z_i(k)}}{\sqrt{2}\, Z_i^2(k)} \end{aligned} \tag{2.5-11a}$$

$$e_2(k) = \pm jTG^Y(\alpha_i, \beta_i)\Big\langle \{t_{12}[t_{11}s_{11i}(k) + t_{21}s_{12i}(k)]$$

$$+ t_{22}[t_{11}s_{21i}(k) + t_{21}s_{22i}(k)]\}\, G^X(\alpha_i, \beta_i)$$

$$\pm jT\{t_{12}[t_{12}s_{11i}(k) + t_{22}\, s_{12i}(k)]$$

$$+ t_{22}[t_{12}s_{21i}(k) + t_{22}s_{22i}(k)]\}\, G^Y(\alpha_i, \beta_i)\Big\rangle \cdot \frac{Ke_T e^{-j2\beta_0 Z_i(k)}}{\sqrt{2}\, Z_i^2(k)} \qquad (2.5\text{-}11b)$$

Certain special cases of these results are of interest. For example, most of our work will involve assuming the system polarizations are orthogonal ($\theta_X = 0$ and $\theta_Y = 0$ in Figure 2.2-2); with this assumption $t_{11} = t_{22} = 1$ and $t_{12} = t_{21} = 0$. Hence,

$$e_1(k) = G^X(\alpha_i, \beta_i)\, \{s_{11i}(k)\, G^X(\alpha_i, \beta_i) \pm jTs_{12i}(k)\, G^Y(\alpha_i, \beta_i)\}$$

$$\cdot \frac{Ke_T\, e^{-j2\beta_0 Z_i(k)}}{\sqrt{2}\, Z_i^2(k)} \qquad (2.5\text{-}12a)$$

$$e_2(k) = \pm jTG^Y(\alpha_i, \beta_i)\, \{s_{21i}(k) G^X(\alpha_i, \beta_i) \pm jTs_{22i}(k)\, G^Y(\alpha_i, \beta_i)\}$$

$$\cdot \frac{Ke_T e^{-j2\beta_0 Z_i(k)}}{\sqrt{2}\, Z_i^2(k)} \qquad (2.5\text{-}12b)$$

Another special case derives from an assumption that the patterns G^X and G^Y are identical. We have

$$G^X(\alpha_i, \beta_i) = G^Y(\alpha_i, \beta_i) = G(\alpha_i, \beta_i) \qquad (2.5\text{-}13)$$

giving

$$e_1(k) = G^2(\alpha_i, \beta_i)\ \{s_{11i}(k) \pm jTs_{12i}(k)\}\ \frac{Ke_T e^{-j2\beta_0 Z_i(k)}}{\sqrt{2}\ Z_i^2(k)} \qquad (2.5\text{-}14a)$$

$$e_2(k) = \pm jTG^2(\alpha_i, \beta_i)\ \{s_{21i}(k) \pm jTs_{22i}(k)\}\ \frac{Ke_T e^{-j2\beta_0 Z_i(k)}}{\sqrt{2}\ Z_i^2(k)} \cdot \qquad (2.5\text{-}14b)$$

Any of the single particle rain clutter results may be used for the multiple particle case by simply summing over all particles in cell k. The result of such a summation coupled with the simplification indicated in equation (2.4-8) is given below for equation (2.5-12).

$$e_1(k) = \frac{Ke_T e^{-j2\beta_0 Z(k)}}{\sqrt{2}\ Z^2(k)} \left\{ \sum_{i=1}^{N_k} s_{11i}(k)[G^X(\alpha_i, \beta_i)]^2\ e^{-j2\beta_0 \Delta Z_i} \right.$$

$$\left. \pm jT \sum_{i=1}^{N_k} s_{12i}(k) G^X(\alpha_i, \beta_i) G^Y(\alpha_i, \beta_i)\ e^{-j2\beta_0 \Delta Z_i} \right\} \qquad (2.5\text{-}15a)$$

$$e_2(k) = \pm jT\ \frac{Ke_T e^{-j2\beta_0 Z(k)}}{\sqrt{2}\ Z^2(k)} \left\{ \sum_{i=1}^{N_k} s_{21i}(k) G^X(\alpha_i, \beta_i) G^Y(\alpha_i, \beta_i) e^{-j2\beta_0 \Delta Z_i} \right.$$

$$\left. \pm jT \sum_{i=1}^{N_k} s_{22i}(k)[G^Y(\alpha_i, \beta_i)]^2\ e^{-j2\beta_0 \Delta Z_i} \right\} \cdot \qquad (2.5\text{-}15b)$$

Similarly, (2.5-14) becomes

$$e_1(k) = \frac{Ke_T e^{-j2\beta_0 Z(k)}}{\sqrt{2}\ Z^2(k)} \sum_{i=1}^{N_k} G^2(\alpha_i, \beta_i)\ [s_{11i}(k) \pm jTs_{12i}(k)] e^{-j2\beta_0 \Delta Z_i} \qquad (2.5\text{-}16a)$$

$$e_2(k) = \pm jT\ \frac{Ke_T e^{-j2\beta_0 Z(k)}}{\sqrt{2}\ Z^2(k)} \sum_{i=1}^{N_k} G^2(\alpha_i, \beta_i)\ [s_{21i}(k) \pm jTS_{22i}(k)] e^{-j2\beta_0 \Delta Z_i} \qquad (2.5\text{-}16b)$$

If a target exists in cell k the received signals are given by (2.5-11) in general if the $s_{mni}(k)$ are replaced by the corresponding target scattering matrix elements $S^T_{mn}(k)$. For the special case of m monostatic system with orthogonal radiations we use (2.5-12) to obtain

$$e^T_1(k) = \frac{Ke_T e^{-j2\beta_0 Z(k)}}{\sqrt{2}\, Z^2(k)} \left\{ [G^X(\alpha, \beta)]^2 S^T_{11}(k) \pm jTG^X(\alpha, \beta)G^Y(\alpha, \beta)S^T_{12}(k) \right\} \tag{2.5-17a}$$

$$e^T_2(k) = \pm jT \frac{Ke_T e^{-j2\beta_0 Z(k)}}{\sqrt{2}\, Z^2(k)} \left\{ G^X(\alpha, \beta)G^Y(\alpha, \beta)S^T_{21}(k) \pm jT[G^Y(\alpha, \beta)]^2 S^T_{22}(k) \right\} . \tag{2.5-17b}$$

If, in addition, all beam patterns are identical we use (2.5-14) and get

$$e^T_1(k) = \frac{Ke_T e^{-j2\beta_0 Z(k)}}{\sqrt{2}\, Z^2(k)} G^2(\alpha, \beta)[S^T_{11}(k) \pm jTS^T_{12}(k)] \tag{2.5-18a}$$

$$e^T_2(k) = \pm jT \frac{Ke_T e^{-j2\beta_0 Z(k)}}{\sqrt{2}\, Z^2(k)} G^2(\alpha, \beta)[S^T_{21}(k) \pm jTS^T_{22}(k)]. \tag{2.5-18b}$$

In all these target signals we shall most often assume the target is located on the beam axis so X = 0 and Y = 0.

3.0 THEORETICAL RAIN MODEL

In this section a rain model is developed which is used in sections 4, 5 and 6 for calculating performance of ordinary and cancellation systems. The model is built around the specification of raindrop shape, size distribution and orientation with respect to wind velocity components.

3.1 Drop Shape

It is well known that falling raindrops are not spherical [4, 14, 16, 20]. The drops become flattened on the bottom as they fall and may even develop a small "dimple" at the center of the flattened surface [13] as shown in Figure 3.1-1(a). Very small droplets fall with the least distortion. Distortion becomes more severe the larger the raindrop and is significant for drops of 2mm equivalent spherical diameter[1] or larger. Above about 2 mm the dimple occurs and becomes more severe as equivalent spherical diameter increases up to about 4.5mm where drops tend to break up, even in quiet air, [15].

Being more specific, it is found [5] that for equivalent spherical diameters less than about 0.17mm the drop is spherical with negligible error. Between 0.17mm and 0.5mm the drops are oblate spheroids. Above 0.5mm to about 4.5 mm the drops are asymetrical spheroids.

---

[1] The equivalent sphere is that having the same volume as the distorted drop.

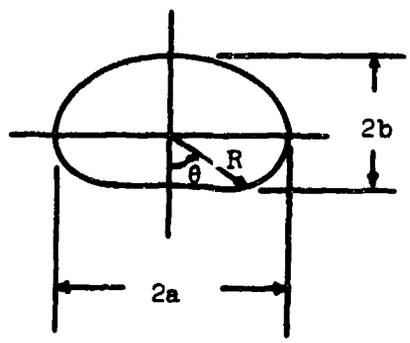

(a)

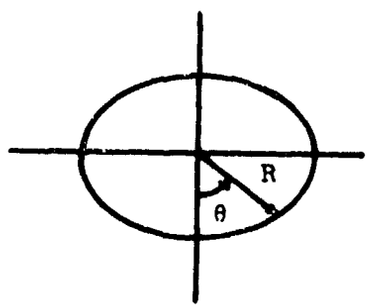

(b)

Fig. 3.1-1. Raindrop crossections. (a) Large heavily distorted drop, and (b) oblate spheroid model for drops with medium distortion.

Pruppacher and Pitter [5] have given an excellent model for raindrop shape. It appears to fit measured results quite well except for the largest raindrops where the actual deformations are slightly underestimated by the model. We shall next describe the shape model of Pruppacher and Pitter (P&P model) and justify that our use of the oblate spheroid is a reasonable second-order approximation to the P&P model.

The P&P model is a refinement of work due to Savic [17]. Actual drops will have a cross-section such as shown in Figure 3.1-1(a). The drop, of course, has rotational symmetry about the vertical axis. The radial distance to the surface from some interior point is $r(\theta)$. The P&P model consists of expanding $r(\theta)$ as an arbitrary (but necessarily single-valued) function into a Fourier series[1]

$$r(\theta) = b_0[1 + \sum_{n=0}^{\infty} c_n \cos(n\theta)] \qquad (3.1\text{-}1)$$

and finding the "distortion coefficients" c_n which correspond to a balance of forces (aerodynamic pressure, hydrostatic pressure gradients in the drop, pressure across the surface and surface tension) on the falling drop. Here b_0 is the radius of the equivalent sphere having the same volume as the deformed drop and the c_n were found under a constant-volume constraint. It results that $c_1 = 0$ may be assumed without loss in generality.

[1] Notation of [5] has been altered to agree with that used here.

The solutions of [5] for the c_n values are plotted in Figure 3.1-2 as a function of b_0. The actual deformation ratio b/a, with b and a defined in Figure 3.1-1(a), is a function of b_0 as shown in Figure 3.1-3. Notice how excellent the fit is to experimental data.

We now show that an oblate spheroid is a reasonable approximation to the more exact P&P model. The reason for using the oblate spheroid in analysis is that analytical solutions for the backscattered fields exist [8] in relatively simple forms.

Consider expanding $r(\theta)$ for an oblate spheroid having the cross-section of Figure 3.1-1(b). Since the cross-section is an ellipse

$$r^2(\theta) = \frac{b^2}{1 - \epsilon^2 \sin^2(\theta)} \quad , \tag{3.1-2}$$

where

$$\epsilon^2 = 1 - (b/a)^2 < 1 \tag{3.1-3}$$

is the eccentricity of the ellipse. We select the two free parameters, a and b, for the oblate spheroid first to make its volume equal to that in the P&P model and second to make the ratio b/a nearly equal to that of the P&P model. In the latter case, the actual relationship between b/a and b_0 is the solid line of Figure 3.1-3. We shall choose b/a according to

$$\frac{b}{a} = \left[1 + \left(\frac{b_0}{2.5}\right)^2\right]^{-1/2} \quad , \; b_0 \text{ in mm}, \tag{3.1-4}$$

which is shown dashed. This function is a good approximation to the

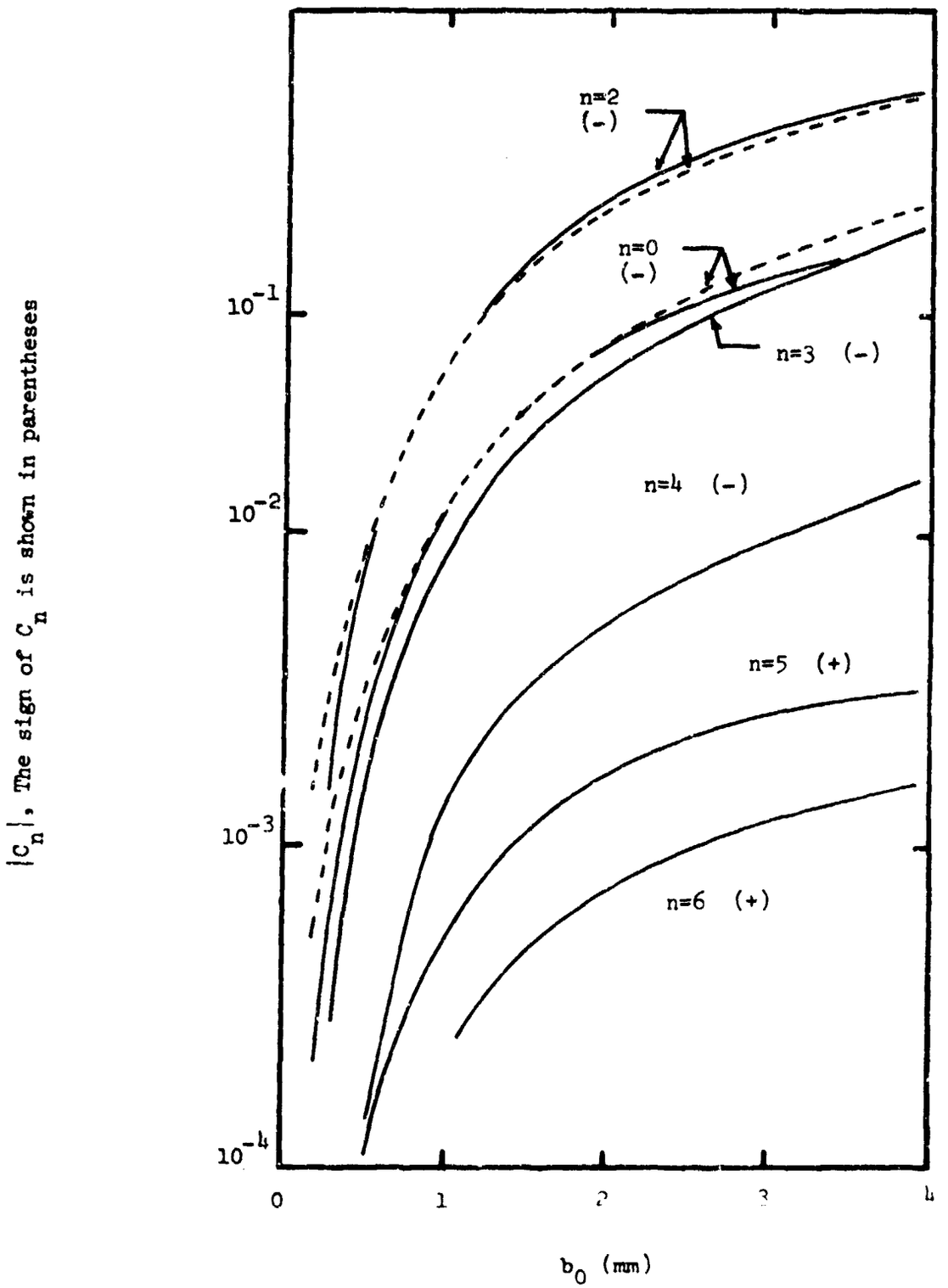

Fig. 3.1-2. Coefficients in the expansion of the shape of raindrops (solid curves) and the coefficients of the expansion of the oblate spheroid (dotted).

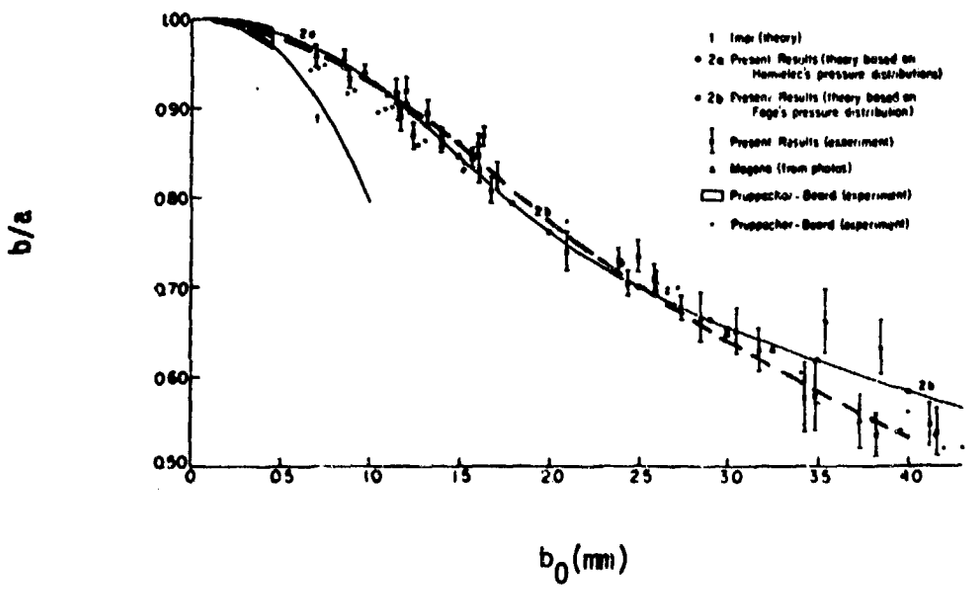

Fig. 3.1-3. Variation of drop deformation with drop size: Comparison of theory and experiment. Figure from Pruppacher and Pitter [5].

P&P model except for large b_0 where it actually approximates the measured data better than the P&P model.

By equating the volume $4\pi a^2 b/3$ [18] of an oblate spheroid to the volume $4\pi b_0^3/3$ of an equivalent sphere we find that

$$b^3 = b_0^3(1 - \varepsilon^2) \tag{3.1-5}$$

for a constant volume constraint and any $\varepsilon < 1$. The constraint that ε must be chosen to approximate that of the P&P model requires that ε be given by (3.1-3) using (3.1-4). From (3.1-2) using (3.1-5) we get

$$r^2(\theta) = \frac{b_0^2 (1 - \varepsilon^2)^{2/3}}{1 - \varepsilon^2 \sin^2(\theta)} \quad . \tag{3.1-6}$$

This function has even symmetry and has two cycles of behavior in the interval $(-\pi, \pi)$. Thus, the Fourier series representing (3.1-6) has only terms for $n = 0, 2, 4, \ldots$ when the expansion is over $(-\pi, \pi)$. The series may be written in the form

$$r(\theta) = b_0 \{1 + \bar{c}_0 + \sum_{\substack{n=2 \\ (n \text{ even})}}^{\infty} \bar{c}_n \cos(n\theta)\} \quad . \tag{3.1-7}$$

Solutions for the coefficients $\bar{c}_n$ involve elliptic integrals and are slightly involved to determine. The first two are

$$\bar{c}_0 = -1 + \frac{2(1-\varepsilon^2)^{1/3}}{\pi} K(\varepsilon) \tag{3.1-8a}$$

$$\bar{c}_2 = 2(1+\bar{c}_0) - \frac{8(1-\varepsilon^2)^{1/3}}{\pi} D(\varepsilon) \tag{3.1-8b}$$

where $K(\varepsilon)$ and $D(\varepsilon)$ are complete elliptic integrals defined by [19]

$$K(\varepsilon) = \int_0^{\pi/2} \frac{d\theta}{\sqrt{1-\varepsilon^2\sin^2(\theta)}} \qquad (3.1\text{-}9)$$

$$D(\varepsilon) = \int_0^{\pi/2} \frac{\sin^2(\theta)d\theta}{\sqrt{1-\varepsilon^2\sin^2(\theta)}} \quad . \qquad (3.1\text{-}10)$$

We may now demonstrate that the oblate spheroid is a reasonable approximation to the P&P drop shape model. By comparing (3.1-7) for the oblate spheroid with (3.1-1) for theP&P model we see that the $\bar{c}_n$ should be nearly equal to the c_n for all n. Two values of $\bar{c}_n$, as given in (3.1-8), are plotted in Figure 3.1-2 as dashed curves. Excellent agreement is seen for all even values of n. The main loss in using the oblate spheroid is the loss of odd numbered terms for $n \geq 3$. There is only one odd term in the P&P model of any significance (n = 3) however, so the loss is small. (The term for N = 5 is well over two orders of magnitude smaller than unity for all values of b_0).

3.2 Drop-Size Distributions

The various mechanisms that cause rain to have a given drop-size distribution are so complicated as to prohibit analysis. Indeed, there is such variation in measured distributions in the literature that one may conclude that no one distribution can describe all rain cases. The best that one can hope for is to find a raindrop distribution model which is simple, easy to work with, and represents a more or less average of many rain situations. With these facts in mind we shall discuss

various measured data from the literature, consider available proposed models, and finally select the model which seems to present the best compromise in the desired behavior.

Before proceeding it is helpful to classify the forms of distributions according the Figure 3.2-1. We define these forms as types A, B, C, and D. The general behavior is all that is important in these definitions and some variations may be expected.

Measured Data

Measurements of raindrop sizes were first made as early as 1895 in Germany by J. Wiesner using an absorbent paper method. For our purposes, however, the most significant early paper was due to Laws and Parsons [21] who used a flour pellet method developed by W.A. Bentley in 1904, an American. Their data, taken in 1938 and 1939 in Washington, D.C. on surface rain, were approximately type C below drop diameters of about 1 (at 2.5mm/hr rain rate) and 2 (25mm/hr) mm, and type B above these diameters.

Marshall and Palmer [22] analyzed surface data taken in Ottawa, Canada [23] in 1946 using the filter paper method. They obtained a good fit to their data and data of [21], for $1 \leq I \leq 25$ mm/hr using their famous distribution

$$n(d_0) = Ae^{-\lambda d_0} \ m^{-3} \ mm^{-1} \tag{3.2-1}$$

where

$$A = 8000 m^{-3} mm^{-1} \tag{3.2-2}$$

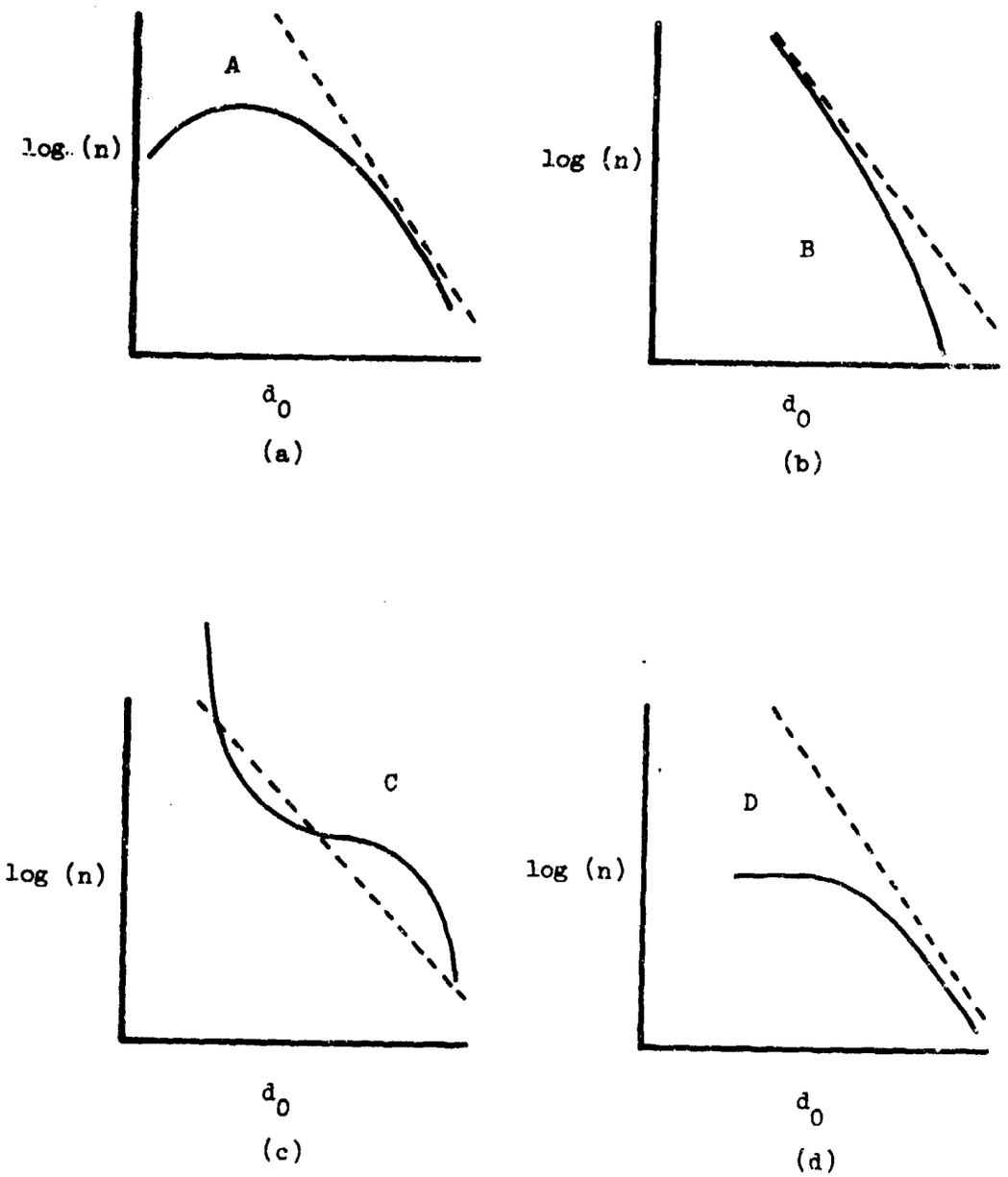

Fig. 3.2-1. Representative raindrop distributions.

$$\lambda = 4.1\ I^{-0.21}\ \text{mm}^{-1} \quad . \qquad (3.2\text{-}3)$$

Here $n(d_0)$ is the number of drops per unit volume (in m^3) having diameters from d_0 to $d_0 + dd_0$, I is rain intensity in mm/hr of water rate and d_0 is in mm.

Blanchard [24], using the filter paper method, has given average distributions for a large number (113) of measurements taken in Hawaii in 1952. Some of the data were taken at or near the dissipating edge of non-freezing orographic clouds. Other data corresponds to rain at the base of a non-freezing orographic cloud while some applied to non-orographic rain (probably due to snow falling through the melting level). Orographic data were mainly type B for low rain rates (<2mm/hr) and type D for higher rates. The non-orographic data were type C.

Mason and Ramanadham [25] have given surface data on rain taken apparently in England with a photoelectric spectrometer which is quite similar to that in [4].

Monsoon rain data in India (1956) have been reported by Murty and Gupta [26] which resulted from the filter paper method. Average drop-size distribution curves based upon 229 sets of measurements were given for rain intensities I from 2 to 140 mm/hr. The data were type C and quite similar to the non-orographic data of [24].

One of the most comprehensive studies of raindrop distributions is discussed by Fujiwara [27, 28]. Data taken with a raindrop camera related to data taken at Miami, Florida and Champaigne, Illinois on a large number of storms. The data are too numerous to discuss in detail. However, one of the most important observations to be made is on how variable drop-size distribution can be. It can vary from a

unimodal structure (with maximum at about 1 to 2 mm diameter) to multimodal with many peaks; of course, the exponential decreasing structure (type B) is also found. The variation (fluctuations) may even be pronounced for a single distribution measurement so results do not usually form smooth functions. Another important observation is that distributions always decreased for small drop sizes (type A). Fujiwara also shows time evolution of distributions which indicate great variability in only short time periods (as small as 1 min.). Most of the data of [27] were for thunderstorms., rainshowers and continuous rains.

More data on tropical rains are given by Sivaramakrishnan [29]. The filter paper mtehod was used to measure surface drop distributions at Poona, India. The data, for non-freezing rain and rain from melting snow were generally of type B but considerable fluctuation existed along the curves.

Additional data on rain from a melting band is given by Hardy [30]. Relatively steady rain at Flegstaff, Arizona on 31 July 1961 produced distributions of type A for I from 0.11 to 3.4 mm/hr. These results were mostly smooth curves with the peak occuring near 1 mm drop diameter. Measurements were made with a photoelectric raindrop-size spectrometer.

The photoelectric spectrometer was also used by Dingle [31] to measure thunderstorm rain of 8 October 1959 at Ann Arbor, Michigan. Results were type B where the slope decreases as I increases for I from 0.18 to 51.6 mm/hr. A Marshall-Palmer (M-P) model is a farily good fit to these data. Other data for a heavy shower on 23 October 1959 and for showers of 16 June 1960 also indicated reasonable agreement with the M-P distribution, especially when the data were averaged (16 June results).

Using at 3.2 cm doppler radar during 1960 and 1961 at Pershore, England, Caton [32] analyzed 83 of 107 observations of continuous rain from melting levels in an excellent paper. The rains were related to three warm fronts, four cold fronts and three low pressure centers. Melting level varied from 1.0 to 3.3 km above ground. Humidity was nearly always high and evaporation below 750 m was negligible. Median distributions at altitude are quite smooth in their behavior, which is type A. The M-P distribution fits the data only over the mid-range of drop diameter and overestimates both small and large diameter drop numbers. Caton also gives bounding curves, within which, 90% of all drop concentrations fall. These bounds are also smooth curves. Data were for I from 0.1 to 5.6 mm/hr.

Distributions for high-intensity rains have been assembled by Blanchard and Spencer [33]. Their data are taken from Mueller and Sims [34] and Hudson [35]. Data of [34] were taken from several types of rain using a raindrop camera at several locations around the world (Miami, Florida; Franklin, North Carolina; and the Marshall Islands). One set of three curves representing about 10 sample distributions (type A), and corresponding to I of 170, 205 and 216 mm/hr, show close agreement to the M-P function for dorp diameters from 1 to about 3.5 mm. For diameters outside this range the M-P function overestimates the drop density. A curve, for I = 300 mm/hr, of data from [35] were quite similar to the data near 200 mm/hr from [34] (again type A, the curve averaged 9 samples). For I = 500 mm/hr, data based on averaging 3 samples [35] again gave similar performance except the peak moved from near 1 mm diameter out to near 2 mm. All data from [35] were taken at Miami, Florida.

Discussion of Measurement Data

Including Russian data, to be commented upon subsequently, we have discussed measurements from all over the world (U.S., England, Canada, Hawaii, India, Russia, Africa and the Marshall Islands) covering intensities from a few tenths of a mm/hr to 500 mm/hr. The data apply to rain at various spatial positions (within rain cloud, at rain cloud base, at edge of cloud, between cloud base and earth's surface and at the surface) and correspond to nearly every type of rain generation mechanism (from melting band for snow, hail, sleet, from non-freezing clouds, frontal storms, showers, convective storms and both freezing and non-freezing orographic rain). Thus, it can be concluded that sufficient results are given to represent nearly all typical rain situations which can occur.

The factors which cause a particular rain situation are extremely complex. Some of these are: temperature and humidity profiles, time and spatial location of points of interest, spatial extent of rain cloud, intensity, accretion (important in non-freezing clouds), coalescence and drop breakup (related to intensity), evaporation (related to humidity), orography, and the generation mechanism. Because of the complex nature of the problem we make no effort to determine why, where or how a particular situation arises. We only here attempt to correlate the best rain model to fit an <u>average</u> rain situation. Thus, we place the averaged data of [20], [24], [26], [30], [31], [32] and [33].

It is helpful to first divide all cases into two categories: orographic and non-orographic. Typical distributions in the former case are markedly different from those of the latter. They typically behave

as type B (with steep slope) for low intensity rain and as type D for heavier rains.

For non-orographic rain it is again convenient to place data in two categories. The first contains results obtained by the flour pellet and filter paper methods. The second has data from photoelectric spectrometer, radar and raindrop camera methods. An immediately obvious difference in distribution form between the two categories is seen. For small drop diameters the former shows increasing concentrations (type C) while the latter shows decreasing concentrations (type A). One is tempted to suspect that splashing of large drops causes the increase in the filter paper method (perhaps even the flour method). However, as pointed out by Caton [32] the splashing problem has been considered by at least one researcher and was ruled out. It is, of course, possible that both categories of measurement method are correct. On the other hand, a radar man tends to place more confidence in radar data. Caton has carefully considered his radar system and concludes the weight of evidence supports distributions of the second category for moderate and heavy rains. Regardless of how the above suspicion is resolved, at least one thing is clear from nearly all of the data of both categories: below some drop size, typically in the 1 to 3 mm diameter range, actual rain drop densities tend to be overestimated by the M-P distribution (An exception would be very light rain during very high humidity).

In the mid-range of raindrop size the M-P distribution is a fair to good approximation to all measurement data. The region of close agreement varies with intensity and Dyer [36] suggests it is from 0.75 to 2.25 mm for near 1 mm/hr, 1.25 to 3 mm for near 5 mm/hr and 1.5 to

4.5 mm for near 25 mm/hr. In the light of data shown here, those upper limits are perhaps optimistic.

For larger drops, measured distributions almost always are overestimated by the M-P curve. This fact is not surprising since there is a practical size limit to drops caused by break-up.

The above results may broadly be summarized as follows. A reasonable model for the drop-size distribution of average rainfall has these characteristics: (1) a peaked behavior occurs with the peak typically occuring to 0.5 to 1.0 mm diameter for intensities up to about 300 mm/hr, the peak moves nearer to 2.0 for higher intensities; (2) for drop diameters below the peak region, the M-P curve overestimates the number of drops; (3) for drop diameters above the peak region and up to a value from about 2 to 4 mm depending on intensity (up to 300 mm/hr) the M-P distribution gives results nearly equal to measured values (typically within a factor of 2); (4) for diameters above the 2 to 4mm region the actual results are overestimated by the M-P curve.

Drop-Size Distribution Models

Having determined the desirable characteristics of a model we look at the various models suggested in the literature.

The Marshall-Palmer [22] model already introduced is the oldest and still remains widely used because of its simplicity in calculations. Another reason is that it is a good approximation in the mid-range of drop sizes, which contribute greatly to radar cross-section because of the d_0^6 power relationship. An often played game is to find the best A and λ to fit given data. Some examples are given in [36] from various researchers. Perhaps one of these examples should be mentioned. Using

data of [26] for orographic rain

$$A = 7500\ I^{-0.25} \tag{3.2-4}$$

$$\lambda = 4.5\ I^{-0.27} \tag{3.2-5}$$

are derived. Since our desired model characteristics are referred to the M-P curve we use it to compare other models.

Best [17] gave a rain model in 1950. It may be written in the form

$$n(d_0) = \frac{6Wn}{\pi} \frac{d_0^{n-4}}{a^n} e^{-(d_0/a)^n} \tag{3.2-6}$$

where

$$a = AI^p \tag{3.2-7}$$

$$W = CI^r \tag{3.2-8}$$

with A, C, p, r and n constants. Here W is the amount of liquid water per unit volume of air and I is rain intensity. If d_0 is in mm, I in mm/hr and W in mm^3/m^3 the mean constant values are A = 1.3, C = 67, p = 0.232, r = 0.846 and n = 2.25, and $n(d_0)$ is in $m^{-3}mm^{-1}$. The constants may vary appreciably from their means, especially n if rain is showery or orographic [37].

Taking the average constant values (3.2-6) becomes

$$n(d_0) = \frac{13.5W}{\pi a^4} \left(\frac{d_0}{a}\right)^{-1.75} e^{-(d_0/a)^{2.25}} \tag{3.2-9}$$

Plots of (3.2-9) show clearly that the Best model does not fit our model requirements (it is more like type C behavior). It may be better in its more general form, however, we seek not only a good but also a simple model if possible.

In 1956 Litvinov [38] proposed the following model as discussed in [39]*.

$$n(d_0) = Ne^{-\lambda d_0^3/2} \tag{3.2-10}$$

where N and λ are constants as far as intensity is concerned, but vary with rain type. Thus, for a given rain type, this model is not flexible since it does not depend upon I. It is not considered further.**

Litvinov [39] also describes a model due to E.A. Polyakova and K.S. Shifrin. The model (P-S) is also described by Krasyuk, et. al. [41]. It is

$$n(d_0) = Ad_0^2 e^{-\gamma d_0} \tag{3.2-11}$$

where A and γ are given in Table 3.2-1. Litvinov

Table 3.2-1

Type Rain	$A(m^{-3}mm^{-3})$	$\gamma(mm^{-1})$
Thawing of Pellets (Hail)	$64500I^{-0.5}$	$6.95I^{-0.27}$
Thawing of Granular Snow (Sleet)	$11750I^{-0.29}$	$4.87I^{-0.2}$
Thawing of NonGranular Snow (Snow)	$2820I^{-0.18}$	$4.01I^{-0.19}$

* This article was translated by Mr. Jim Elliott of the University of Tennessee.

** In a later paper by Litvinov [40], as translated by Irving Emin, N and λ are said to be functions of intensity but not of the usual form $\alpha I^{-\beta}$. This case would appear to be true with [38] having either a typographical or translation error. At any rate (3.2-10) does not account for the decrease of distribution for very small drop size and is not considered further.

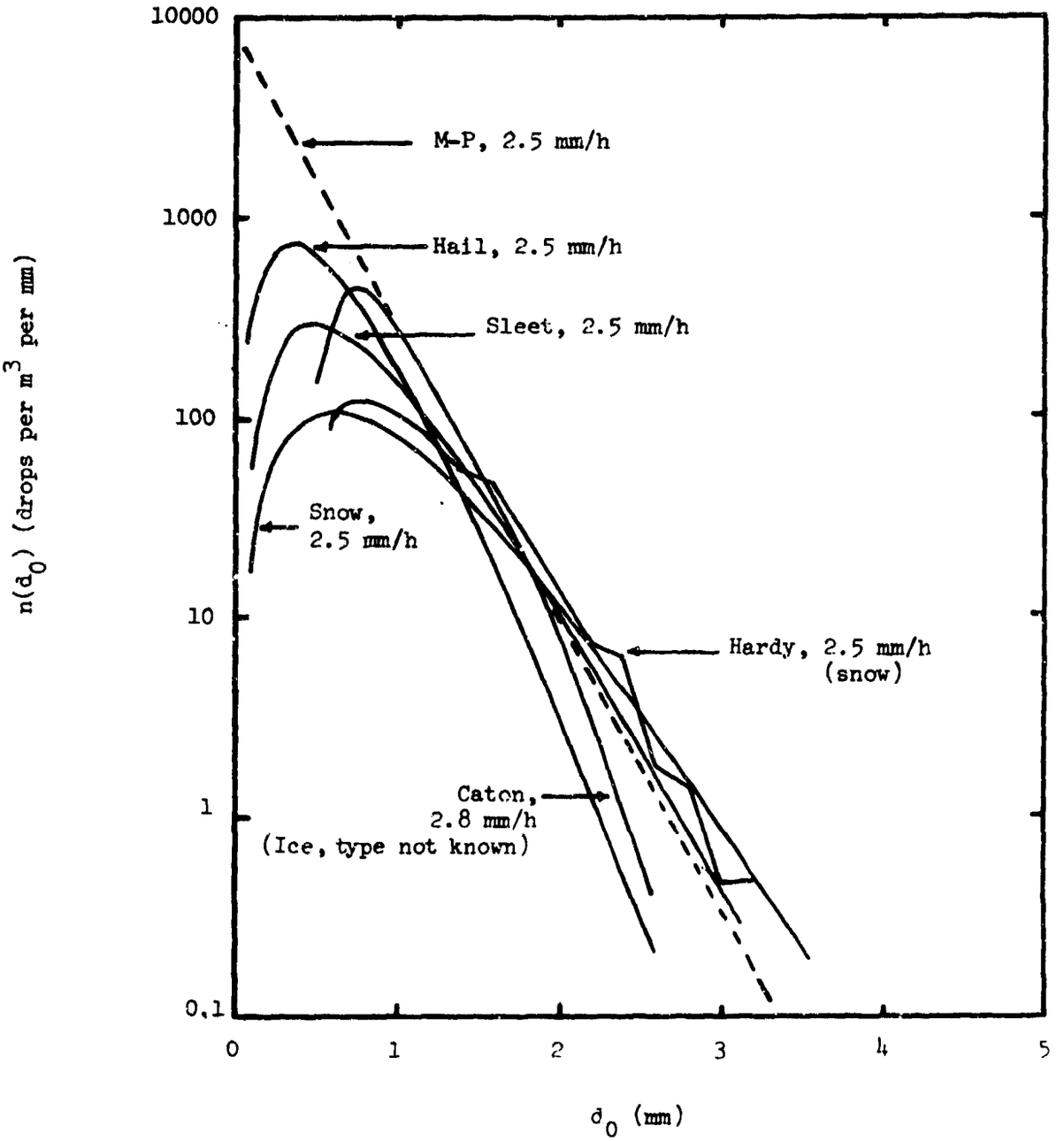

Fig. 3.2-2. P-S model compared to measured data near 2.5 mm/h rain intensity.

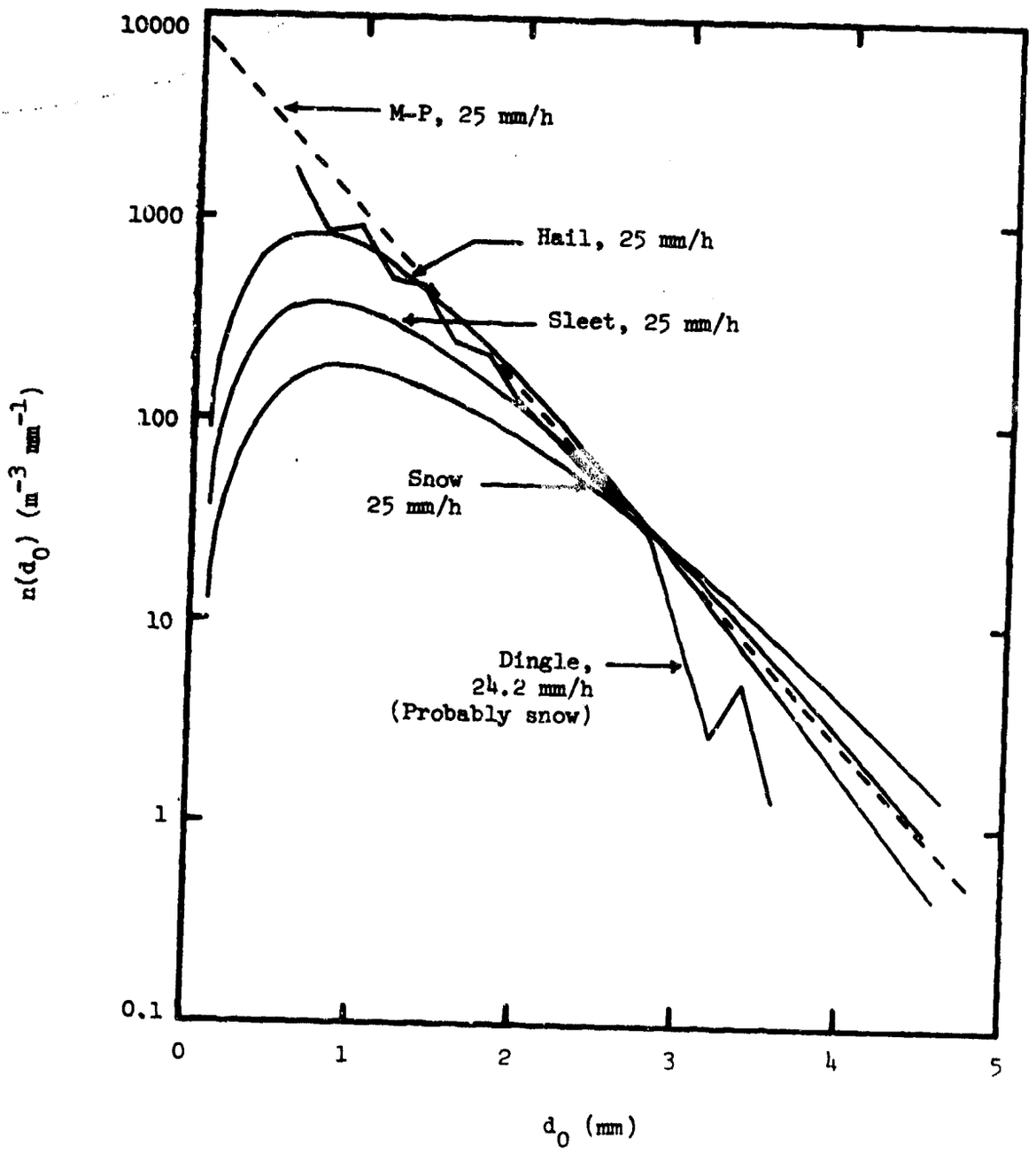

Fig. 3.2-3. P-S model compared to measured data near 25 mm/h rain intensity.

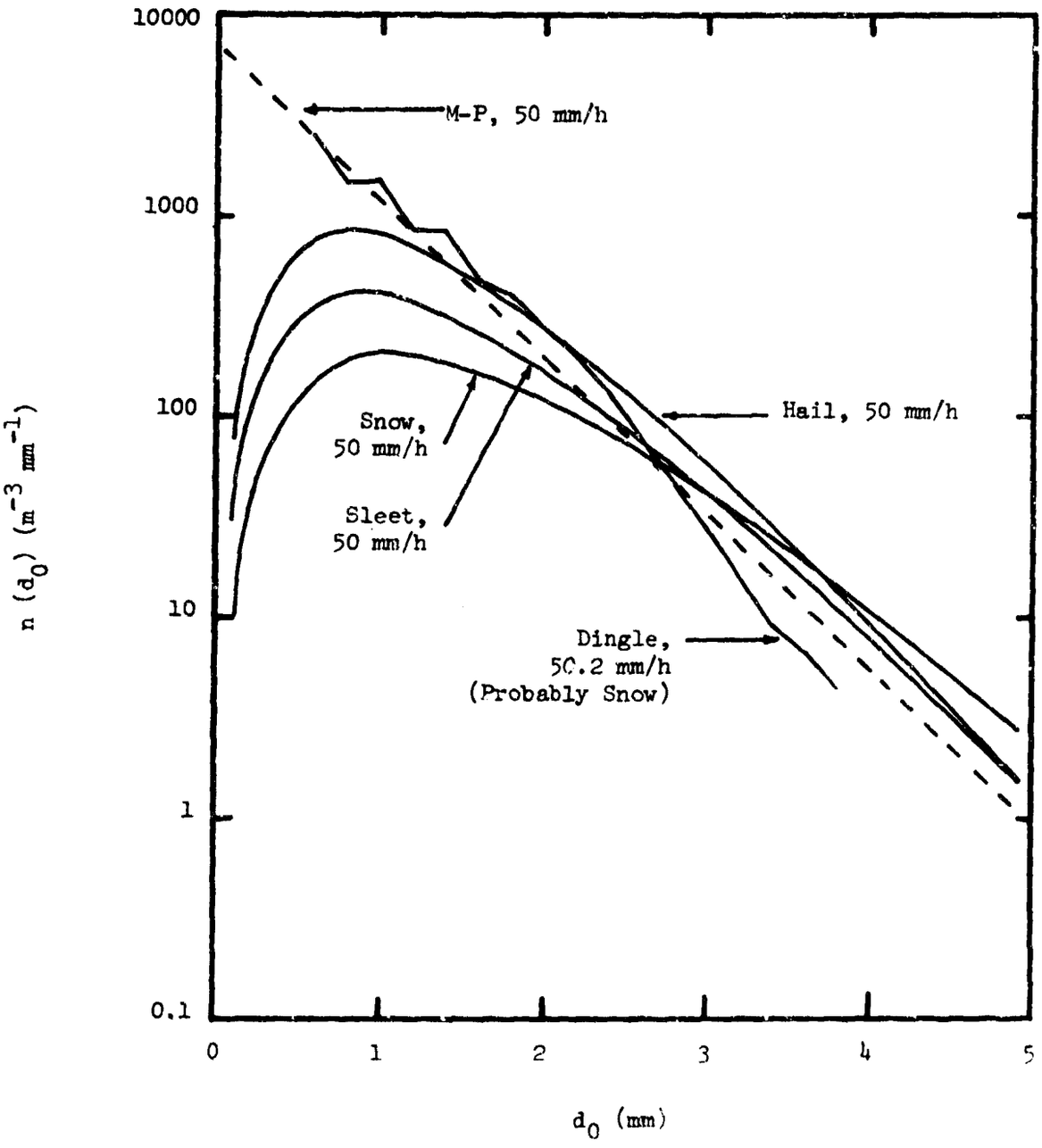

Fig. 3.2-4. P-S model compared to measured data near 50 mm/hr rain intensity.

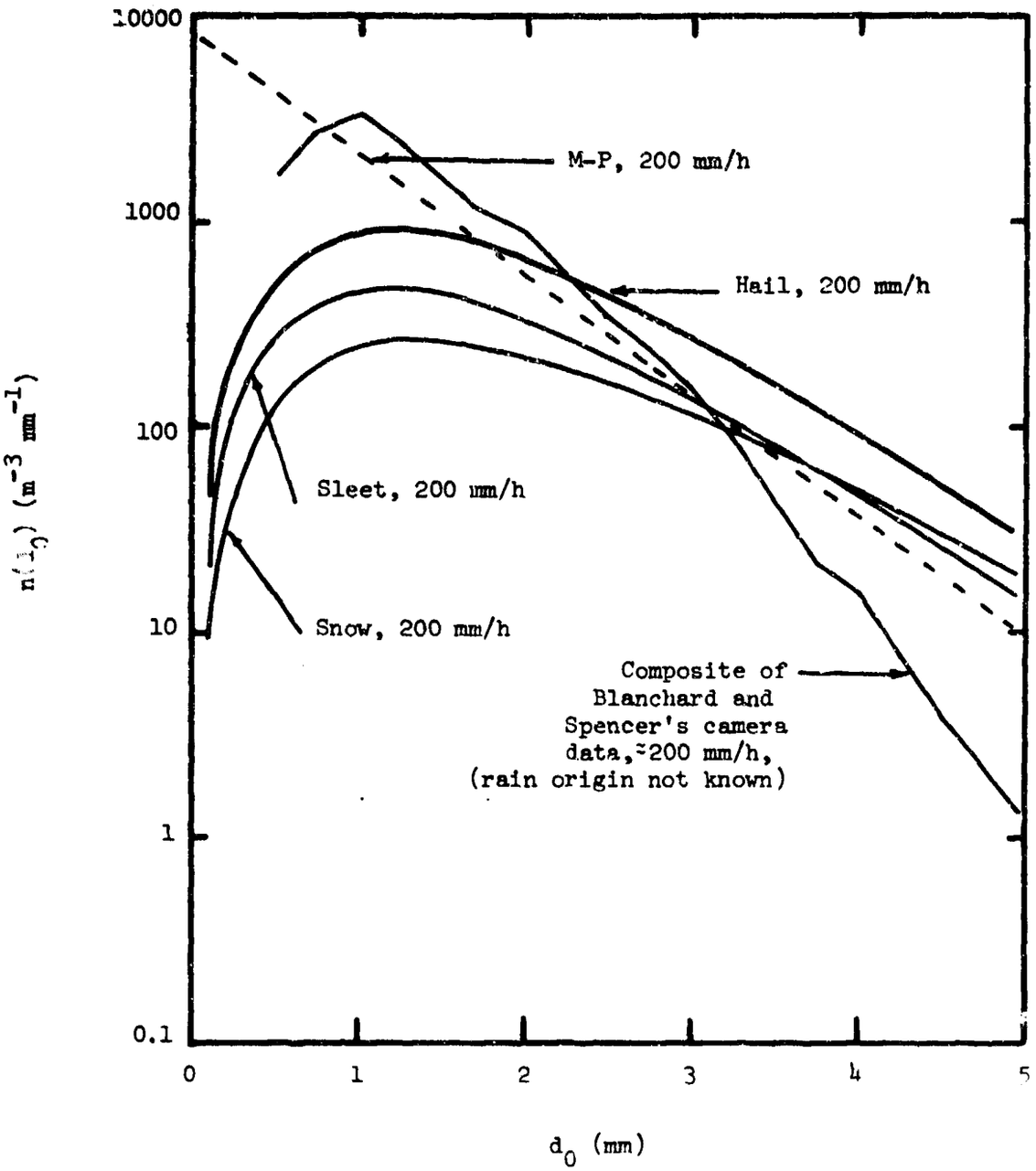

Fig. 3.2-5. P-S model compared to measured data near 200 mm/h rain intensity.

has shown Russian data for all three types of rain which are fit excellently using (3.2-11). Figures 3.2-2, 3, 4 and 5 illustrate the P-S model for I = 2.5, 25, t0 and 200 mm/hr respectively. Spotted on these figures are various average data described earlier; also shown where possible are the estimated origins of the rain, that is, whether originating from melted snow, sleet or hail, etc. For moderate rain*, using Figure 3.2-2, there is excellent agreement with averaged data, especially if we assume the Caton data (taken from August to December 1961 in England) originated as hail. For heavy rain the model does not fit average data too well as seen from Figure 3.2-3, if Dingle's data are from melting snow. On the other hand, if the data are from melting hail, the agreement is quite good. Similar comments may be made about excessive rain from Figure 3.2-4. For deluge rain Figure 3.2-5 shows the model is a poor fit regardless of the rain's origin.

To better place bounds upon the usefulness of (3.2-11) we have replotted some of Litvinov's measured data [39] in Figures 3.2-6, 7. The first figure is for rain originating from hail. Excellent agreement is seen for intensities from 1.5 to 15.2 mm/hr. (Litvinov also shows curves for 3.47 and 7.25 mm/hr which also show close agreement). The curve for I = 1.5 represents an average of 77 measurements while only a single sample applies to the I = 15.2 curve. The second figure shows excellent agreement of data and theory for rain from melting snow for

* We define intensities as: drizzle, 0-0.5 mm/hr; light rain, 0.5-2.0 mm/hr; moderate rain, 2.0-8.0 mm/hr; heavy rain, 8-32 mm/hr; excessive rain, 32-128 mm/hr; deluge rain, 128 mm/h higher.

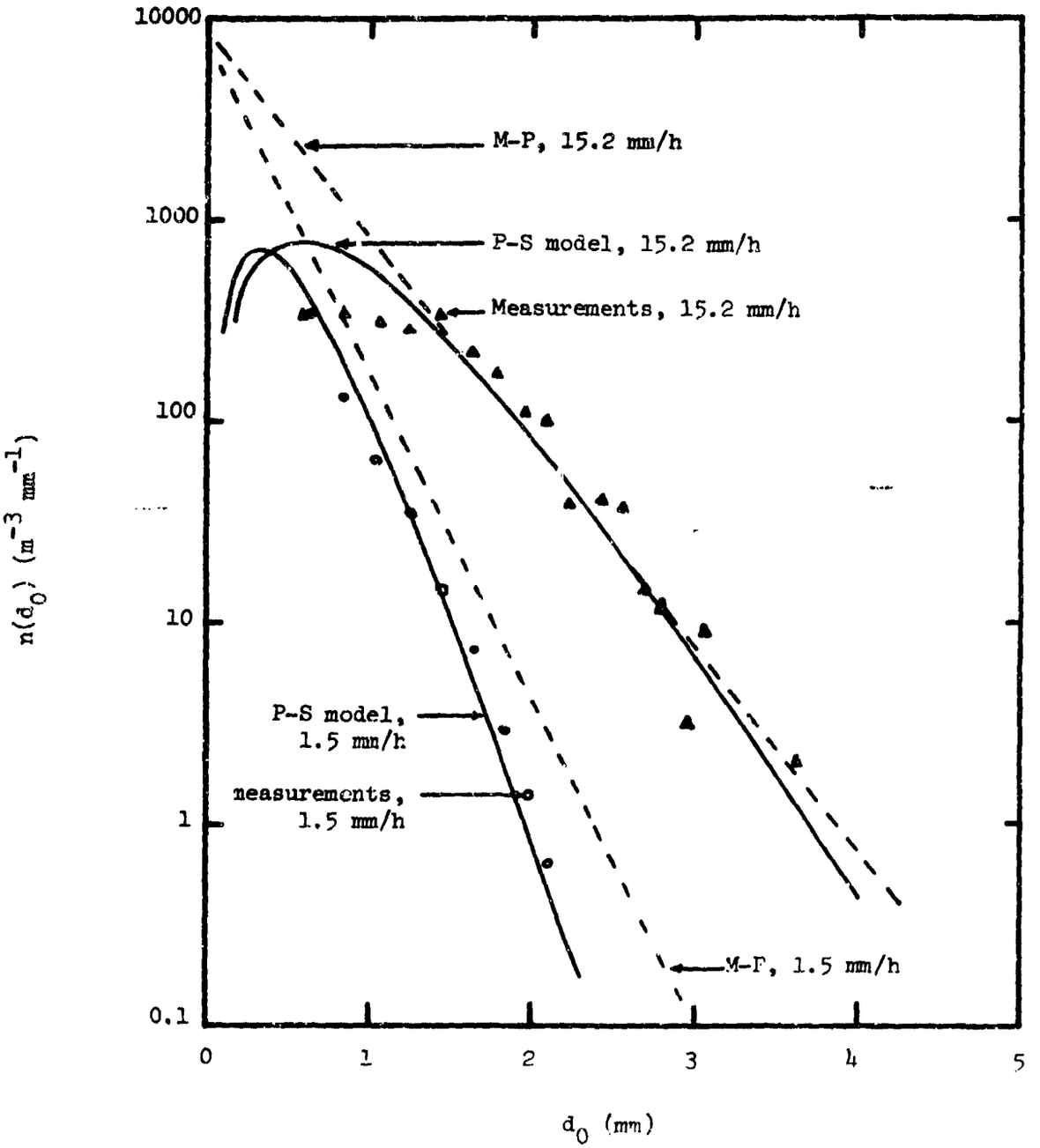

Fig. 3.2-6. P-S model compared to measured data at rain intensities of 1.5 and 15.2 mm/h.

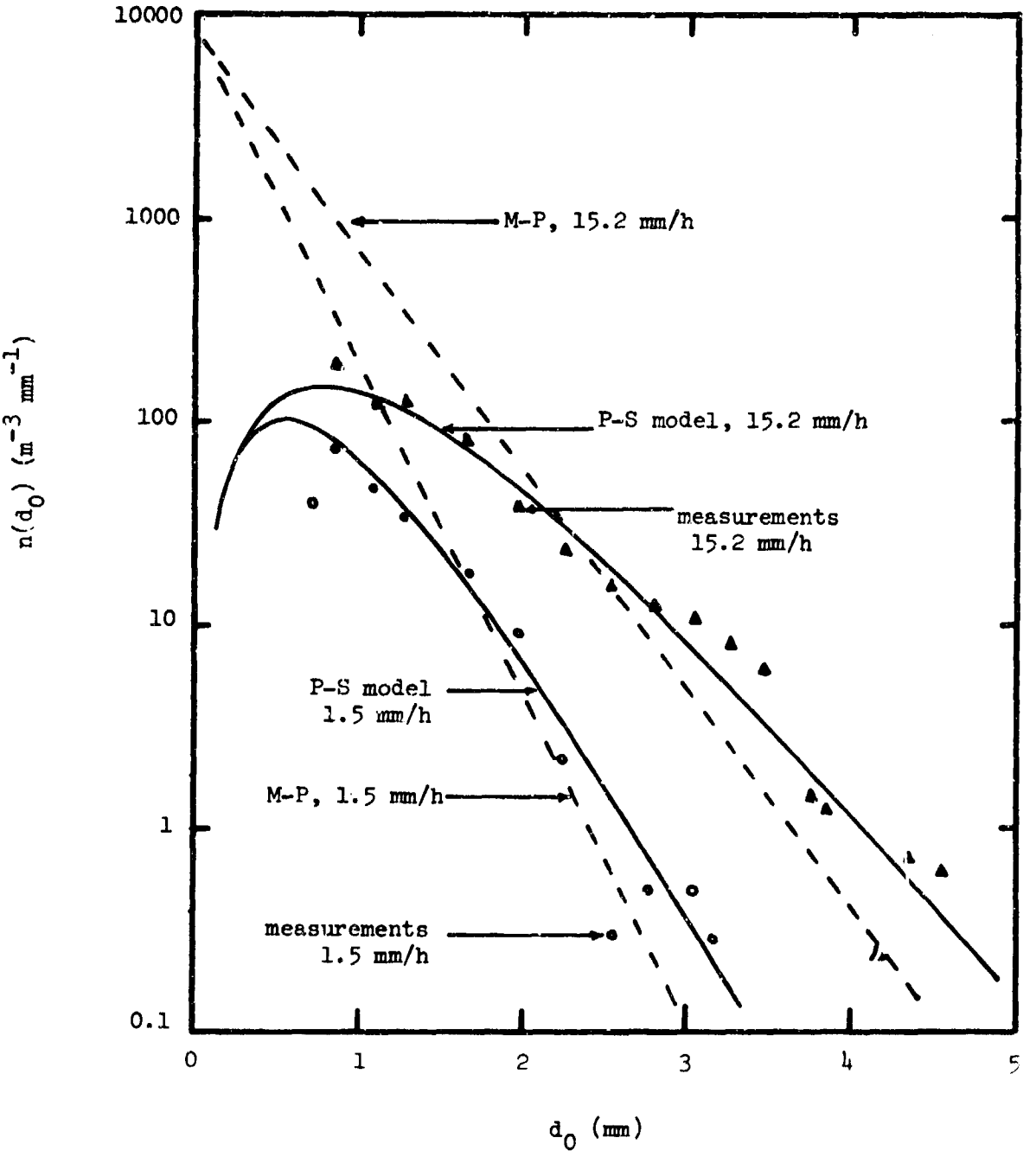

Fig. 3.2-7. P-S model compared to measured data at rain intensities of 1.5 and 15.2 mm/h.

intensities from 1.5 to 11.1 mm/hr (curves are average of 4 and 14 samples respectively). Excellent agreement is obtained for intermediate intensities of 3.52 and 7.47 mm/hr as well [39]. Finally, Litvinov also gives results for rain from granular snow (sleet) which verify agreement of the model with measurements for intensities from 1.56 to 10.88 mm/hr.

Thus, in summary, the P-S model appears to represent average raindrop size distributions quite well up to intensities of at least 15 mm/hr. There is some doubt as to its validity for intensities near 25 to 50 mm/hr and it is not a good model for intensities near 200 mm/hr. It can probably serve useful analytical purpose for rains through the heavy region.

Fujiwara [27] has given a model involving four variable parameters and is applicable to fitting individual storms. It is

$$n(d_0) = \frac{NS}{a^S} (d_0 - D_0)^{S-1} e^{-(d-D_0)^S/a^S} \quad , \quad D_0 \leq d_0 \quad , \qquad (3.2\text{-}12)$$

where N is the total number of drops per unit volume; D_0 is a "mode shift" parameter, typically around 0.8 mm on the average; S is a "skewness" parameter usually varying from 1 to 3; a is a "broadness" parameter which is related to rainfall rate, and, from fitting of measurement data, ranges from 1 to 3.5 mm. Because of the number of parameters having unclear relationships with intensity and rain type (3.2-12) is difficult to work with. Fujiwara shows a good fit to many data and (3.2-12) may be very useful model when these relationships are developed. However, until the developments are available we shall not consider (3.2-12) a useful simple model.

Finally, we briefly discuss the log-normal model. According to Dyer [36] it is the most universally applicable distribution. However,

Litvinov [39] finds it to be non-applicable to rain from melting snow, sleet and hail. He later [40] shows explicitly that it does not fit data from melting hail. Incidently, according to [40], the log-normal distribution was suggested by Levine [42]. Because of Litvinov's conclusions we do not consider the log-normal distribution further.

Summary of Drop-Size Distribution Models

The Marshall-Palmer model of (3.2-1) remains a reasonable model for most average rains over the important mid-range of drop sizes. It can give useful analytical results because it is easy to work with.

For orographic rains the M-P distribution with A and λ given by (3.2-4) and (3.2-5) has been developed [36] from measurement data.

For non-orographic rains, such as rain from the melting layer, the Polyakova-Shifrin model of (3.2-11) gives excellent agreement with many measurements and does not appear to be difficult to work with.

During this study all analytical work will assume either the M-P or P-S distribution for non-orographic rain.

3.3 Probability Density Function for Drop-Size

Let $n(d_0)$ be a drop size distribution. The total number of drops N is

$$N = \int_0^\infty n(d_0)dd_0 \quad . \tag{3.3-1}$$

For the M-P distribution

$$N = \int_0^\infty \Lambda e^{-\lambda d_0} dd_0 = \Lambda/\lambda \quad . \tag{3.3-2}$$

For the P-S distribution

$$N = \int_0^\infty A d_0^2 e^{-\gamma d_0} \, dd_0 = 2A/\gamma^3 \quad . \tag{3.3-3}$$

We shall define the probability density function for a drop diameter by

$$p(d_0) = \frac{n(d_0)}{N} \quad . \tag{3.3-4}$$

For the M-P and P-S models

$$p(d_0) = \lambda e^{-\lambda d_0} \quad , \quad M - P \quad , \tag{3.3-5}$$

$$p(d_0) = \frac{\gamma^3}{2} d_0^2 e^{-\gamma d_0} \quad , \quad P - S \quad . \tag{3.3-6}$$

Since $p(d_0)$ is a function of rain intensity I through λ and γ, it must be considered as a conditional density if I is random.

4.0 ORDINARY SYSTEM PERFORMANCE

When a linearly polarized radar operates in rain, using a frequency above a few gigahertz, there may be undesirable clutter from backscatter due to raindrops. The usual way of reducing this clutter is to resort to circular polarization. If the system transmits and receives perfectly circular polarization in all directions, and if raindrops are all spherical, the clutter may be totally cancelled in theory. Neither of these conditions is satisfied in reality and the purpose of this section is to determine approximate bounds on the practical clutter cancellation achievable by a system designed to radiate and receive approximately circular polarization. Practical effects of raindrop shape, size distribution, and drop orientation are determined for various rain intensities from 0.5 to 128 mm/hr.

Two situations are developed. First, the raindrops are assumed to be perfectly spherical and the effect of system polarization tolerance is found. Second, the system polarization is assumed perfectly circular and the limits due to practical rain are found. In the latter case, both the Marshall-Palmer (M-P) and Polyakova-Shifrin)P-S) raindrop models are used to achieve numerical data.

4.1 System Model

The system model is that shown in Figure 2.5-1, and described in Section 2.5. The matrices [t] and [r] are chosen to give orthogonal space polarizations

4.2 System Clutter Powers

Ordinary System

Cancellation ratio CR will be defined as the ratio of clutter powers P_{ref}/P_{ord} where P_{ord} is the output clutter power of an ordinary or circularly polarized system. P_{ref} is the clutter power of a "reference" system defined as having a single polarization (say X), the same pattern and transmitter power as the ordinary system and operating in the same rain environment.

Using complex notation, P_{ord} is the expected value of $|e_r|^2$ in Figure 2.5-1, where we henceforth drop the functional dependence of all quantities on k since we deal only with a typical cell. Now $e_r = e_1 + e_2$, where e_1 and e_2 are produced by the sums of the backscattered fields from the N particles in cell k. Carrying out the necessary algebra leads to the ordinary system power

$$P_{ord} = |A|^2 \sum_{i=1}^{N} \left\{ |G(\alpha_i, \beta_i)|^4 \, |s_{11i} \pm j2Ts_{12i} - T^2 s_{22i}|^2 \right\} \quad . \quad (4.2\text{-}1)$$

Here

$$A = \frac{Ke_T \, e^{-j2\beta Z}}{\sqrt{2}\, Z^2} \quad , \quad (4.2\text{-}2)$$

Z is the radial distance to the center of cell k, K is a constant related to the range equation, $\beta = 2\pi/\lambda$, λ is wavelength, and $j = \sqrt{-1}$.

In arriving at (4.2-1), use has been made of the fact that $s_{12i} = s_{21i}$. Also, it has been recognized that radial position of raindrops is unifromly distributed over a range cell, which is large relative

to λ, and position is independent of all other random quantities. Hence the expected value with respect to radial drop position has already been taken.

Reference System

The reference system clutter power is most easily obtained by setting $s_{12i} = 0$ and $s_{22i} = 0$ in (4.2-1) and adding a factor 2 to account for the fact that the two systems must radiate the same total power

$$P_{ref} = |A|^2 \, 2E\left\{ \sum_{i=1}^{N} |G(\alpha_i \, \beta_i)|^4 \, |s_{11i}|^2 \right\} . \qquad (4.2\text{-}3)$$

4.3 Clutter Cancellation Ratio

Clutter cancellation ratio CR becomes the ratio of (4.2-3) to (4.2-1). The expression simplifies by observing that the raindrop location angles α_i and β_i may be considered statistically independent of all other random quantities which are related to drop scattering properties. It is furthermore reasonable to presume the same statistical distribution function for these angles applies to all drops. With these considerations we have

$$CR = \frac{2E\{\sum_{i=1}^{N} |s_{11}|^2\}}{E\{\sum_{i=1}^{N} |s_{11} \pm j2Ts_{12} - T^2 s_{22}|^2\}} . \qquad (4.3\text{-}1)$$

Further simplification follows the assumption that N is nonrandom. Such a situation is true if the rain intensity I is taken as constant.

Making this assumption, and noting that the same statistical distribution applies to all raindrops, we get

$$CR = \frac{2\, E\{|s_{11}|^2\}}{E\{|s_{11} \pm j2T\, s_{12} - T^2\, s_{22}|^2\}} \quad . \tag{4.3-2}$$

Here we have dropped the subscript denoting particle i since it is no longer required. We consider two special cases of (4.3-2).

Ideal Rain Case

For spherical raindrops $s_{12} = 0$ and $s_{11} = s_{22}$. Cancellation ratio becomes

$$CR = \frac{2}{|1 - T^2|^2} \quad . \tag{4.3-3}$$

This result describes the performance of a nonideal system operating in light, drizzle-type, rain since drops become more nearly spherical as rain intensity decreases. Figure 4.3-1 is a plot of CR from (4.3-3) as a function of $|T|$ with the phase of T as a parameter. To obtain 30 dB of cancellation, a system must not have more than 0.2 dB of amplitude unbalance in the two linear polarization components for zero phase unbalance. Phase unbalance rapidly decreases the allowable amplitude tolerance.

Ideal System Case

It can be shown that the functions s_{mn} are all real. With $T = 1$ (4.3-2) simplifies to

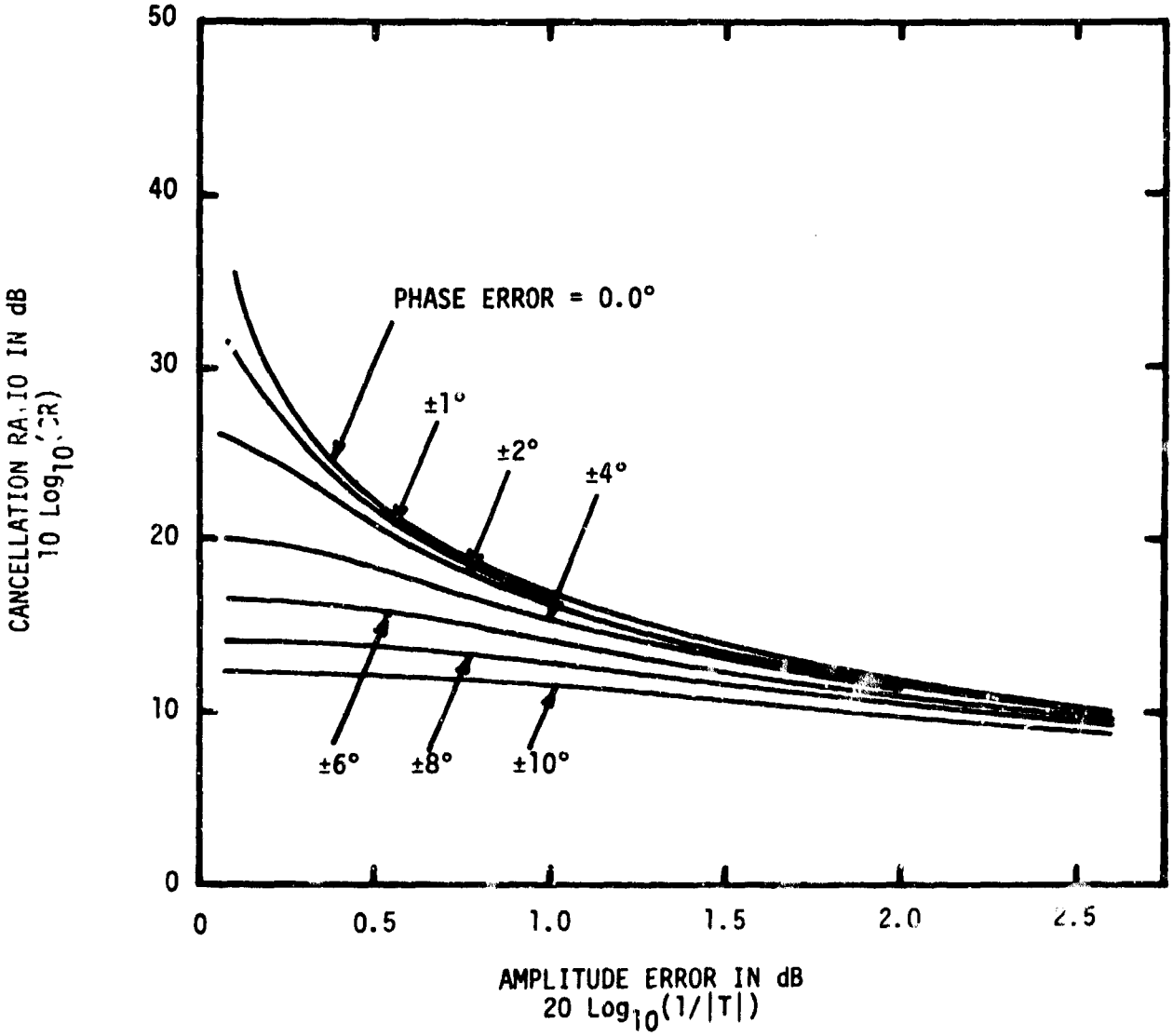

Fig. 4.3-1. Effect of Polarization Amplitude and Phase Unbalance on Cancellation Ratio for Operation in Drizzle Type Rain Having Spherical Raindrops.

$$CR = \frac{2\,E\{s_{11}^2\}}{E\{(s_{11} - s_{22})^2 + 4\,s_{12}^2\}} \quad . \tag{4.3-4}$$

The calculation of CR can not be carried further until the scattering parameters s_{mn} are determined for a typical raindrop. These relationships were given in (2.3-6). We use these expressions and assume in all following work that the radar beam is pointed horizontally and radiating in the Z direction with polarizations in the X and Y directions. Equation (4.3-4) will reduce to

$$CR = \frac{2E\{[g_y + (g_x - g_y)\sin^2(\zeta)\sin^2(\psi)]^2\}}{E\{(g_x - g_y)^2[\sin^2(\zeta)\sin^2(\psi) + \cos^2(\psi)]^2\}} \tag{4.3-5}$$

where g_x and g_y are functions of drop equivalent diameter d_0. They are given approximately by

$$g_x = \frac{B\,d_0^3}{\frac{1}{\varepsilon_r - 1} + \left(\frac{1+x^2}{x^2}\right)[1 - x\tan^{-1}(x)]} \tag{4.3-6}$$

$$g_y = \frac{2B\,d_0^3}{\frac{2}{\varepsilon_r - 1} - \left(\frac{1}{x}\right)^2 + \left(\frac{1+x^2}{x^3}\right)\tan^{-1}(x)} \quad . \tag{4.3-7}$$

Here

$$x = d_0/5 \tag{4.3-8}$$

$$B = -\pi\varepsilon_1(10^{-9})/6, \tag{4.3-9}$$

ε_1 is the dielectric constant of air, ε_r is the dielectric constant of rainwater (relative to air), and d_0 is in millimeters. The angles ζ and ψ define the fall-path of the raindrop with ζ being the azimuthal angle of the vertical plane containing the trajectory of the drop while ψ is the fall angle measured from vertical.

It is quite difficult to solve (4.3-5) exactly. Part of the difficulty arises because ζ and ψ are complicated nonlinear functions of wind components and ψ is additionally a function of d_0 through the drop terminal velocity. In general, the winds should be treated as random quantities. Other difficulties derive from the complicated behavior of g_x and g_y. Most of these problems can be avoided if we seek to calculate <u>bounds</u> on performance, rather than calculate CR exactly.

For the lower bound on CR we may show by direct calculation that $(g_x - g_y)$ is positive while g_y is negative and $|g_x - g_y| \leq |g_y|$ for all d_0. Thus, as a function of ζ, (4.3-5) is minimum when $\sin^2(\zeta) = 1$. Presuming this to be true for the moment, the resulting expression is minimum as a function of ψ when $\sin^2(\psi) = 1$. We define the final function as CR_{min}. It is given by

$$CR_{min} = \frac{2\, E\{g_x^2\}}{E\{(g_x - g_y)^2\}} \quad . \tag{4.3-10}$$

More careful study of the behavior of ζ and ψ shows that (4.3-10) results if we make the simple assumptions that all winds are constant (nonrandom) and that a strong horizontal wind blows.

For the upper bound, (4.3-5) is maximum, as a function of ζ, for $\sin^2(\zeta) = 0$. The resulting expression becomes maximum as $\cos(\psi)$ approaches zero. Again assuming nonrandom winds with a strong horizontal component V_r, the upper bound, defined as CR_{max}, becomes

$$CR_{max} = \frac{2 V_r^4 E\{g_y^2\}}{E\{(g_x-g_y)^2(V_\infty-V_v)^4\}} \quad . \tag{4.3-11}$$

Here V_v is the vertical wind speed and V_∞ is the drop terminal velocity, which is approximately given by

$$V_\infty = 10.105[1 - e^{-d_0/2}] \tag{4.3-12}$$

if d_0 is in millimeters.

A final situation supposes all winds are zero. The (22) reduces to

$$CR_{no} = \frac{2E\{g_y^2\}}{E\{(g_x-g_y)^2\}} \quad \text{(no winds)} \quad . \tag{4.3-13}$$

4.4 Ideal System Numerical Results

Calculation of (4.3-10), (4.3-11) and (4.3-13) is still not a simple task due to the form of the expressions for g_x and g_y. However, direct calculation of the functions g_x^2, g_y^2 and $(g_x-g_y)^2$ has shown: 1) that sensitivity to the parameter ε_r is small and, 2) they may be approximated closely with simple functions which lead to closed-form solutions for the various expectations. Thus, approximations were developed and expectations were taken assuming raindrops distributed

according to both the M-P distribution and the P-S distribution.

Marshall-Palmer Distribution

The applicable distribution probability density is (3.3-5) where λ is given by

$$\lambda = 4.1I^{-0.21} \tag{4.4-1}$$

where I is rain intensity (mm/hr). With this density function (4.3-10), (4.3-11) and (4.3-13) evaluate to

$$CR_{min} = \frac{122.77\ \lambda[1.405 - 1.656\lambda + \lambda^3]}{155.63 + \lambda^2} \tag{4.4-2}$$

$$CR_{max} = \left(\frac{V_r}{10.105}\right)^4 \frac{123.96\ [0.753 + \lambda^2]}{X_1 + (155.63X_2/\lambda^2)} \tag{4.4-3}$$

$$CR_{no} = \frac{123.96\ \lambda^2[0.753 + \lambda^2]}{155.63 + \lambda^2} \tag{4.4-4}$$

Assuming $V_v = 0$. Here

$$X_1 = 1 - \frac{4}{[1 + (0.5/\lambda)]^9} + \frac{6}{[1 + (1/\lambda)]^9} - \frac{4}{[1 + (1.5/\lambda)]^9} + \frac{1}{[1 + (2/\lambda)]^9} \tag{4.4-5}$$

$$X_2 = 1 - \frac{4}{[1 + (0.5/\lambda)]^{11}} + \frac{6}{[1 + (1/\lambda)]^{11}} - \frac{4}{[1 + (1.5/\lambda)]^{11}} + \frac{1}{[1 + (2/\lambda)]^{11}} \tag{4.4-6}$$

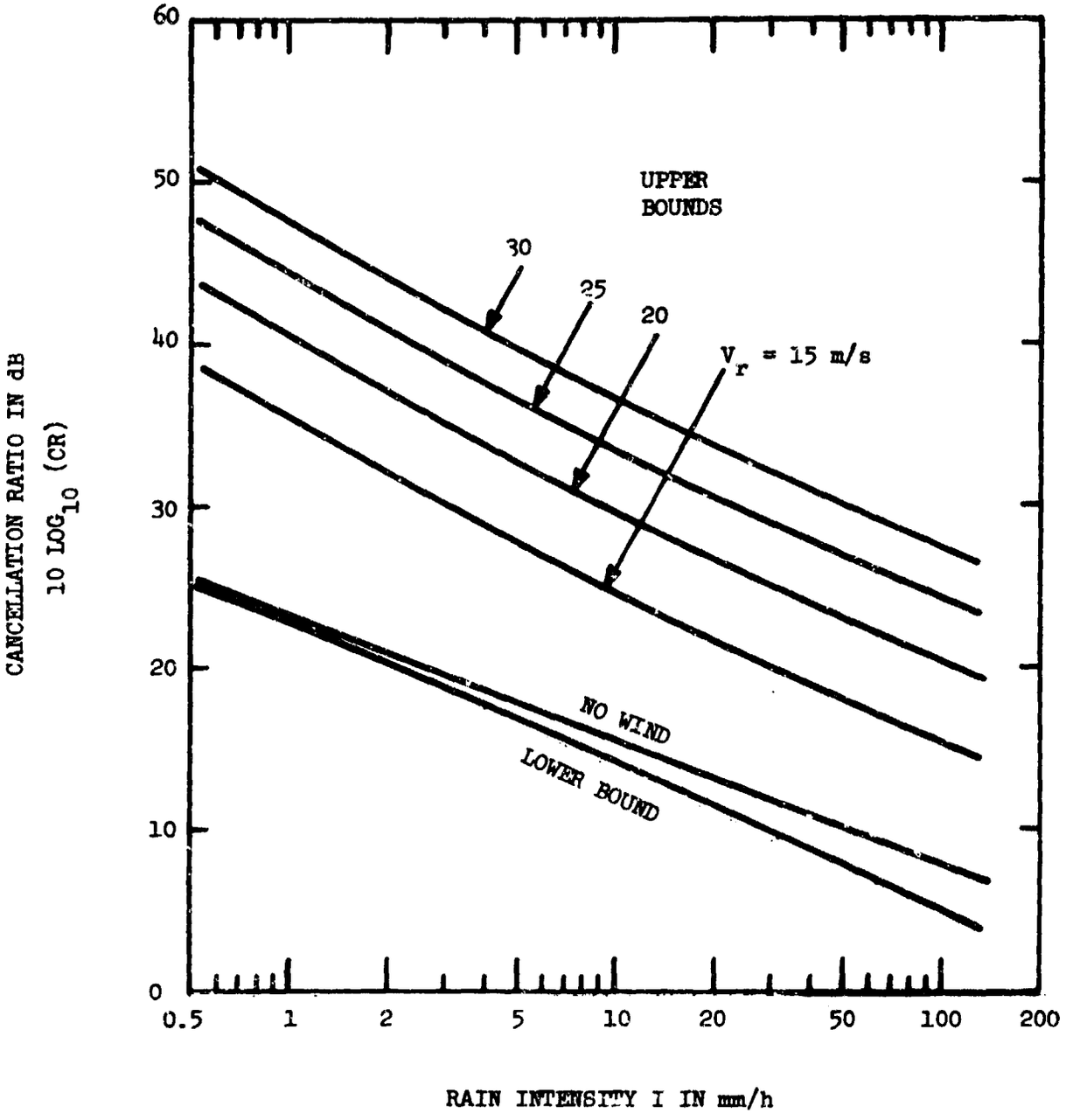

FIG 4.4-1. Bounds on rain cancellation ratio for a system having perfectly circular polarization when operating in rain described by the Marshall-Palmer drop-size distribution.

Figure 4.4-1 illustrates plots of (4.4-2), (4.4-3) and (4.4-4).

Polyakova-Shifrin Distribution

Here the probability density function of drop diameters is given by (3.3-6) and γ is given in Table 3.2-1. Calculation now produces

$$CR_{max} = \left(\frac{V_r}{10.105}\right)^4 \frac{77.21\ (1.21 + \gamma^2)}{X_1 + (228.467 X_2/\gamma^2)} \qquad (4.4\text{-}7)$$

$$CR_{min} = \frac{76.469\ \gamma\ (2.76 - 2.662\ \gamma + \gamma^3)}{228.467 + \gamma^2} \qquad (4.4\text{-}8)$$

$$CR\ (\text{no wind}) = \frac{77.21\ \gamma^2 (1.21 + \gamma^2)}{228.467 + \gamma^2} \qquad (4.4\text{-}9)$$

where

$$X_1 = 1 - \frac{4}{[1 + (0.5/\gamma)]^{11}} + \frac{6}{[1 + (1/\gamma)]^{11}} - \frac{4}{[1 + (1.5/\gamma)]^{11}} + \frac{1}{[1 + (2/\gamma)]^{11}} \qquad (4.4\text{-}10)$$

$$X_2 = 1 - \frac{4}{[1 + (0.5/\gamma)]^{13}} + \frac{6}{[1 + (1/\gamma)]^{13}} - \frac{4}{[1 + (1.5/\gamma)]^{13}} + \frac{1}{[1 + (2/\gamma)]^{13}} \ . \qquad (4.4\text{-}11)$$

The expressions (4.4-7) through (4.4-9) are plotted in Figures 4.4-2 through 4.4-4 for rain from melting snow, sleet and hail.

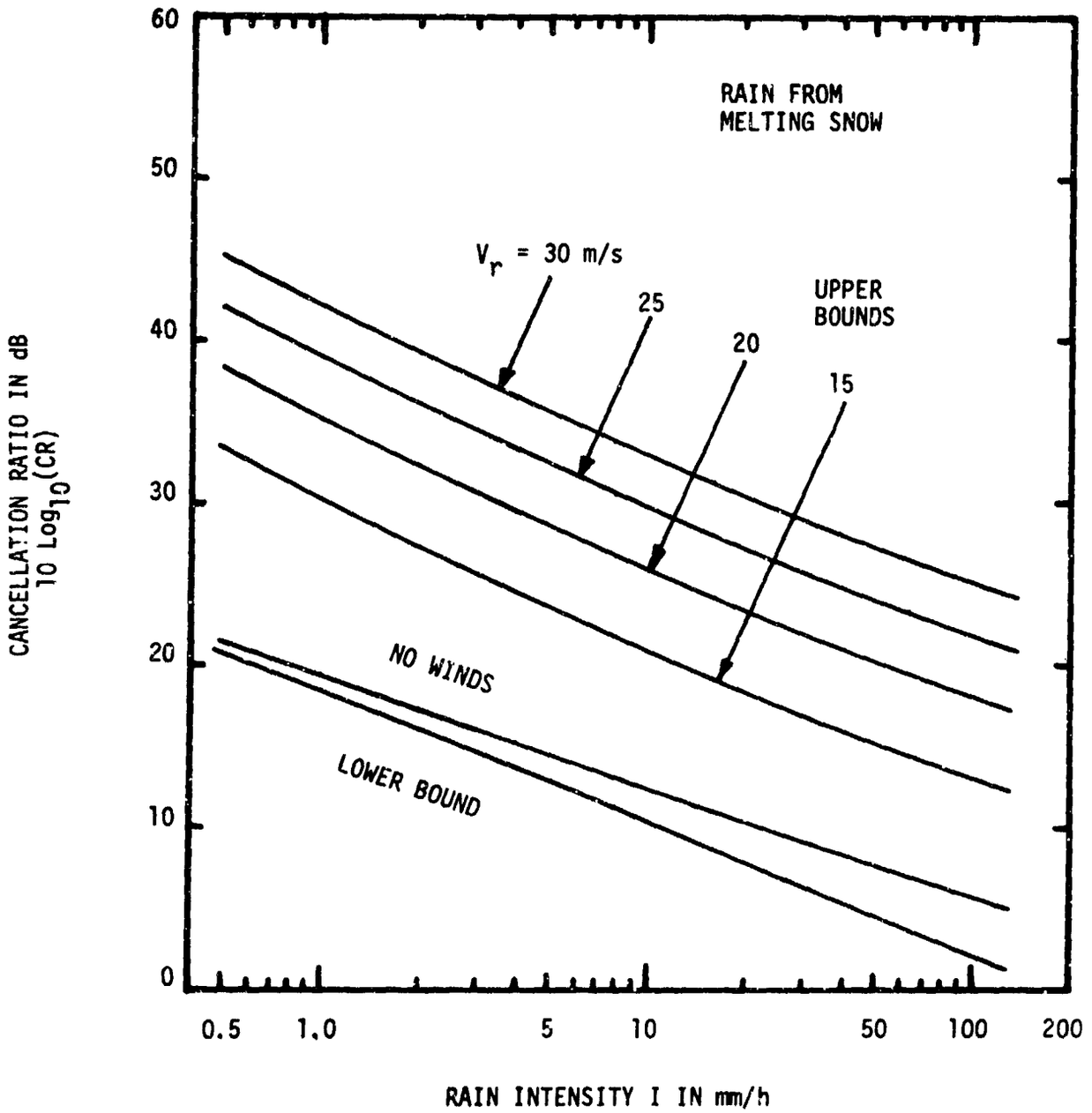

Fig. 4.4-2. Cancellation Ratio Bounds for a System Having Perfectly Circular Polarization Operating in Rain From Melting Snow.

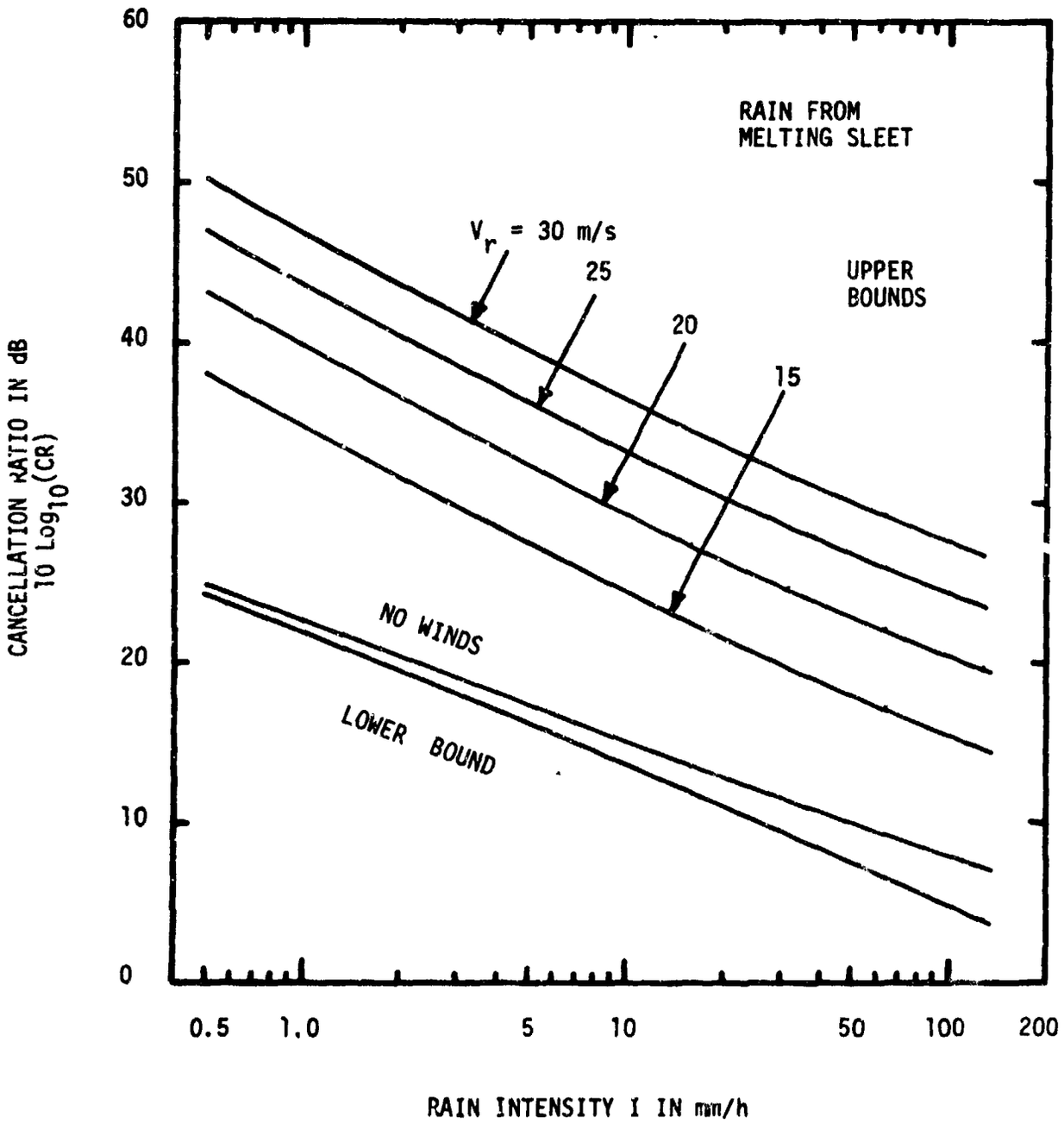

Fig. 4.4-3. Cancellation Ratio Bounds for a System Having Perfectly Circular Polarization Operating in Rain From Melting Sleet.

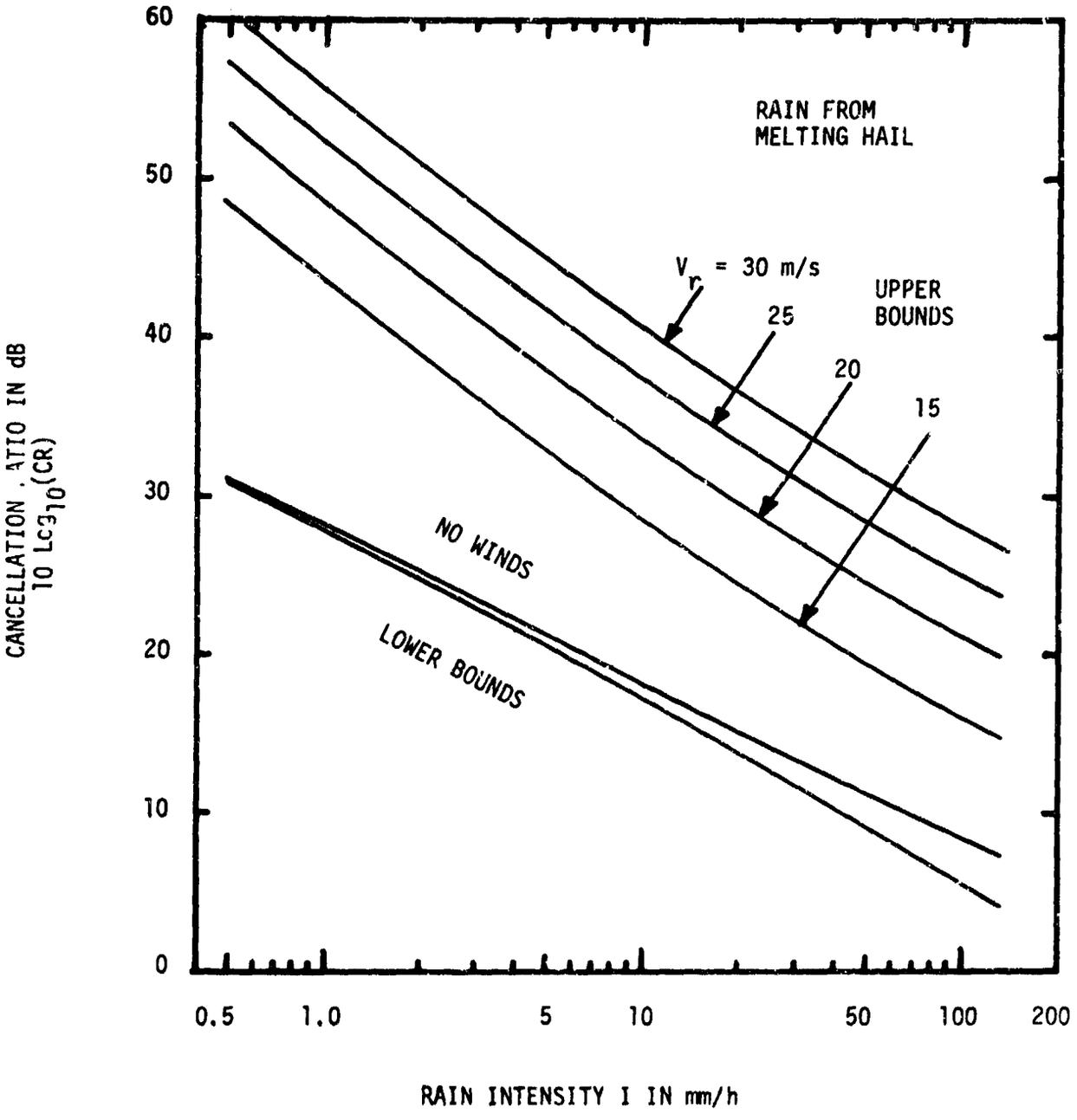

Fig. 4.4-4. Cancellation Ratio Bounds for a System Having Perfectly Circular Polarization Operating in Rain From Melting Hail.

5.0 PERFORMANCE OF CANCELLATION SYSTEM WITH UNIFORM RAIN CHARACTERISTICS

5.1 Rain Characteristics

As in section 3 we consider rain particles to be nonspherical in this section. However, unlike chapter 3, we shall here assume particles all have uniform shape, size, and orientation.

5.2 System Equations

The cancellation system is shown in block diagram form in Figure 5.2-1. At the left of the diagram, the transmitter signal is split in a power sense. Half of the signal power is directed to the antenna which generates the X component of the radiation field. The other half of the signal power is directed through the lower channel and eventually is used to generate the Y component of the radiation field. However, this second portion of the signal is modified in magnitude and phase by the element T. It is this element T which represents the basic system imperfections which prevent the transmission of a truly circularly polarized field. Finally the signal in the Y channel is shifted in phase by $\pm \pi/2$ with the $+\pi/2$ corresponding to polarization of a left hand sense and the $-\pi/2$ producing polarization of a right hand sense.

The quantities e_x^+ and e_y^+ represent the electric fields produced by the X and Y antennas respectively. By using equation (2.4-1), one may express these fields as indicated in equation (5.2-1).

$$e_x^+ = \frac{K_1 e_T G_T^X}{\sqrt{2}\, Z} e^{-j\beta_0 Z} \tag{5.2-1a}$$

$$e_y^+ = \frac{\pm jTK_1 e_T G_T^Y}{\sqrt{2}\, Z} e^{-j\beta_0 Z} \tag{5.2-1b}$$

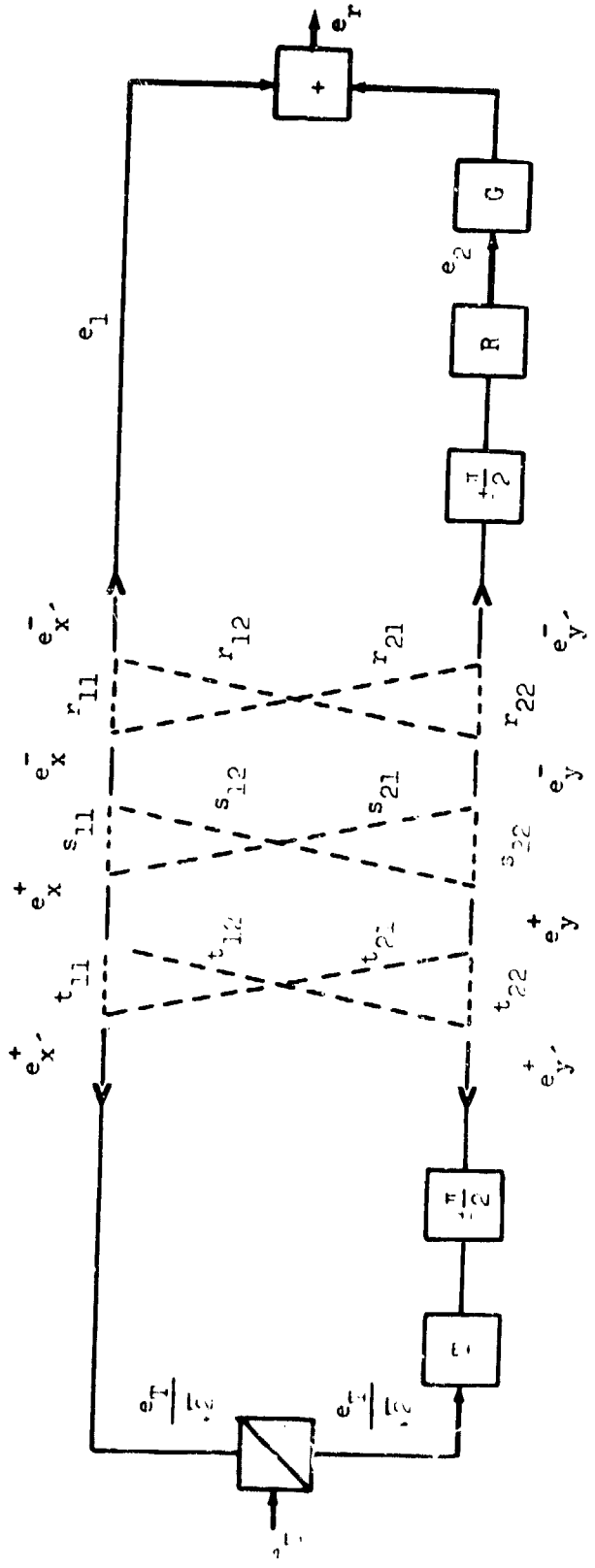

Fig. 5.2-1. Cancellation system diagram.

If the transmitter antennas are not perfectly orthogonal then a cross coupling of the electric field components occurs as indicated by the t_{ij} factors in Figure 5.2-1. This cross coupling is expressed mathematically in equation (2.5-1), and the t_{ij} terms are defined in equation (2.5-2). Thus, the true orthogonal components, e_x^+ and e_y^+, may be expressed as

$$e_x^+ = t_{11}e_{x'}^+ + t_{12}e_{y'}^+ \qquad \text{and} \qquad (5.2\text{-}2a)$$

$$e_y^+ = t_{21}e_{x'}^+ + t_{22}e_{y'}^+ \quad . \qquad (5.2\text{-}2b)$$

The relationship between the incident field components, e_x^+ and e_y^+, and the reflected or scattered field components is given by equation (2.3-3) with the S_{ij} terms defined in equation (2.3-6). These equations together with equation (2.4-2) which indicates the propagational magnitude and phase effects may be used to express the scattered field components at a distance Z' from the particle as

$$e_x^- = \frac{\left(S_{11}e_x^+ + S_{12}e_y^+\right)}{Z'} e^{-j\beta_0 Z'} \qquad (5.2\text{-}3a)$$

$$e_y^- = \frac{(S_{21}e_x^+ + S_{22}e_y^+)}{Z'} e^{-j\beta_0 Z'} \qquad (5.2\text{-}3b)$$

As in the case of the transmitter antennas, the axes of the receiver antennas may not be perpendicular to one another so that cross coupling of the field components occurs. The mathematical basis for this effect is given in equation (2.5-3), and the representation used

in this work is shown in equation (5.2-4).

$$e_{x'}^{-} = r_{11}e_{x}^{-} + r_{12}e_{y}^{-} \qquad (5.2\text{-}4a)$$

$$e_{y'}^{-} = r_{21}e_{x}^{-} + r_{22}e_{y}^{-} \qquad (5.2\text{-}4b)$$

Receiver signals e_1 and e_2 may be determined by application of equation (2.4-3).

$$e_1 = K_2 G_r^X e_{x'}^{-} = K_2 G_r^X [r_{11}e_x^{-} + r_{12}e_y^{-}]$$

$$= \frac{K_2 G_r^X \left[r_{11}(S_{11}e_x^{+} + S_{12}e_y^{+}) + r_{12}(S_{21}e_x^{+} + S_{22}e_y^{+})\right]}{Z'} e^{-j\beta_0 Z'}$$

$$= \frac{K_2 G_r^X \left[r_{11}(S_{11}\left\langle t_{11}e_{x'}^{+} + t_{12}e_{y'}^{+}\right\rangle + S_{12}\left\langle t_{21}e_{x'}^{+} + t_{22}e_{y'}^{+}\right\rangle)\right.}{Z'}$$

$$\left. + r_{12}\,(S_{21}\left\langle t_{11}e_{x'}^{+} + t_{12}e_{y'}^{+}\right\rangle + S_{22}\left\langle t_{21}e_{x'}^{+} + t_{22}e_{y'}^{+}\right\rangle)\right] e^{-j\beta_0 Z'}$$

$$= \frac{K_1 K_2 e_T G_r^X}{\sqrt{2}\cdot Z\cdot Z'} \left[r_{11}(S_{11}\left\langle t_{11}G_T^X \pm jTt_{12}G_T^Y\right\rangle + S_{12}\left\langle t_{21}G_T^X \pm jTt_{22}G_T^Y\right\rangle)\right.$$

$$\left. + r_{12}\,(S_{21}\left\langle t_{11}G_T^X \pm jTt_{12}G_T^Y\right\rangle + S_{22}\left\langle t_{21}G_T^X \pm jTt_{22}G_T^Y\right\rangle)\right] e^{-j\beta_0(Z+Z')}$$

(5.2-5a)

$$e_2 = \frac{\pm jRK_1K_2e_TG_r^Y}{\sqrt{2}\ Z\cdot Z'}\left[r_{21}\left(S_{11}\left\langle t_{11}G_T^X \pm jTt_{12}G_T^Y\right\rangle + S_{12}\left\langle t_{21}G_T^X \pm jTt_{22}G_T^Y\right\rangle\right)\right.$$

$$\left. + r_{22}\left(S_{21}\left\langle t_{11}G_T^X \pm jTt_{12}G_T^Y\right\rangle + S_{22}\left\langle t_{21}G_T^X \pm jTt_{22}G_T^Y\right\rangle\right)\right] e^{-j\beta_0(Z+Z')} \qquad (5.2\text{-}5b)$$

For the case of a monostatic radar the following relationships are valid.

$$Z = Z'$$

$$R = T$$

$$e_T^X = G_R^X \equiv G^X$$

$$G_T^Y = G_R^Y \equiv G^Y$$

The assumption that the antenna axes are orthogonal results in a significant simplification in equations (5.2-5a) and (5.2-5b). This simplified form is given in equations (5.2-6a) and (5.2-6b).

$$e_1 = \frac{K_1K_2e_TG^X}{\sqrt{2}\ Z^2}\left[G^XS_{11} \pm jTG^YS_{12}\right] e^{-j2\beta_0Z} \qquad (5.2\text{-}6a)$$

$$e_2 = \frac{\pm jRK_1K_2e_TG^Y}{\sqrt{2}\ Z^2}\left[G^XS_{21} \pm jTG^YS_{22}\right] e^{-j2\beta_0Z} \qquad (5.2\text{-}6b)$$

Use of the definition in equation (2.4-4) along with the assumption that the X and Y radiation characteristics, G^X and G^Y, are identical results in a further simplification for the terms representing the signals received as a result of scattering by one particle.

$$e_1 = \frac{Ke_T G^2(\alpha, \beta)}{\sqrt{2}\, Z^2} \left[S_{11} \pm jTS_{12}\right] e^{-j2\beta_0 Z} \quad , \text{ and} \tag{5.2-7a}$$

$$e_2 = \frac{\pm jTKe_T G^2(\alpha, \beta)}{\sqrt{2}\, Z^2} \left[S_{21} \pm jTS_{22}\right] e^{-j2\beta_0 Z} \tag{5.2-7b}$$

where

$$G^X = G^Y = G(\alpha, \beta) \quad . \tag{5.2-8}$$

In the process of evaluating actual radar system performance in the presence of rain, it will be necessary to consider multiparticle scattering. As pointed out in section 2.4, the multiparticle effect is evidenced by a summation of individual particle returns such as those of equation (5.2-7). Expressions for e_1 and e_2 for multiparticle scattering with the same assumptions as used in equations (5.2-7a) and (5.2-7b) are given in equations (5.2-9a) and (5.2-9b).

$$e_1(k) = \frac{Ke_T e^{-j2\beta Z_k}}{\sqrt{2}\, Z_k^2} \sum_{i=1}^{N_k} G^2(\alpha_i, \beta_i)\left[S_{11i}(k) \pm jTS_{12i}(k)\right] e^{-j2\beta_0 \Delta Z_i} \tag{5.2-9a}$$

$$e_2(k) = \frac{\pm jTKe_T e^{-j2\beta Z_k}}{\sqrt{2}\, Z_k^2} \sum_{i=1}^{N_k} G^2(\alpha_i, \beta_i) \left[S_{21i}(k) \pm jTS_{22i}(k)\right] e^{-j2\beta_0 \Delta Z_i} \tag{5.2-9b}$$

Before it will be possible to continue the analysis of the cancellation system, one must define the G element in the system block diagram. The original definition of G was provided by Rice and Peebles, and it is provided below.

$$G(k) = \frac{-1}{(2M+1)} \sum_{\ell=k-M}^{k+M} \frac{e_1(\ell)}{e_2(\ell)} \qquad (5.2\text{-}10)$$

The value of G at the time the system is processing the returns from the $k^{\underline{th}}$ range cell is determined by the negative of the average value of the ratio e_1/e_2. This ratio is evaluated in the M cells before cell k, cell k itself, and the M cells after cell k.

Using the definitions of e_1 and e_2 provided by equations (5.2-9a) and (5.2-9b), one obtains the following expression for G.

$$G(k) = \frac{-1}{\pm jT(2M+1)} \sum_{\ell=k-M}^{\ell=k+M} \frac{\sum_{i=1}^{N_k} G^2(\alpha_i, \beta_i)[S_{11i}(\ell) \pm jTS_{12i}(\ell)]\, e^{-j2\beta_0 \Delta Z_i}}{\sum_{i=1}^{N_k} G^2(\alpha_i, \beta_i)[S_{21i}(\ell) \pm jTS_{22i}(\ell)]\, e^{-j2\beta_0 \Delta Z_i}} \qquad (5.2\text{-}11)$$

If all the particles within a given range cell have the same size, shape, and orientation then

$$G(k) = \frac{-1}{\pm jT(2M+1)} \sum_{\ell=k-M}^{k+M} \frac{[S_{11}(\ell) \pm jTS_{12}(\ell)]}{[S_{21}(\ell) \pm jTS_{22}(\ell)]} \cdot \qquad (5.2\text{-}12)$$

G may be expressed by a yet simpler form by requiring cell-to-cell uniformity in all particle parameters. This assumption gives

$$G(k) = \frac{-1}{\pm jT(2M+1)} \; (2M+1) \frac{[S_{11} \pm jTS_{12}]}{[S_{21} \pm jTS_{22}]} = \frac{-1}{\pm jT} \frac{[S_{11} \pm jTS_{12}]}{[S_{21} \pm jTS_{22}]}$$

(5.2-13)

All of the equations developed thus far in this section pertain to the situation in which only clutter is present in the cells being observed. In the event that a target appears within one of the cells of interest, one obtains the following expressions for e_1, e_2, and G.

$$e_1(k) = e_1^c(k) + e_1^T(k) \tag{5.2-14}$$

$$e_2(k) = e_2^c(k) + e_2^T(k) \tag{5.2-15}$$

The quantities $e_1^c(k)$ and $e_2^c(k)$ are the clutter contributions to the total backscattered signal and will in general be expressed in the form indicated in equations (5.2-9a) and (5.2-9b). Target contributions to the backscattered signal are indicated by $e_1^T(k)$ and $e_2^T(k)$ and these terms find expression in equations (2.5-17a) and (2.5-17b). Application of equations (5.2-14) and (5.2-15) to general definition of G in equation (5.2-10) gives

$$G(k) = \frac{-1}{(2M+1)} \sum_{\ell=k-M}^{k+M} \frac{e_1(\ell)}{e_2(\ell)} = \frac{-1}{(2M+1)} \left[\sum_{\substack{\ell=k-M \\ \ell \neq k}}^{k+M} \frac{e_1(\ell)}{e_2(\ell)} + \frac{e_1(k)}{e_2(k)} \right] \tag{5.2-16}$$

Finally, using the appropriate combination of expressions for e_1, e_2, and G, one may express the receiver output, e_r, in general.

$$e_r(k) = e_1(k) + G(k)e_2(k) \tag{5.2-17}$$

5.3 Evaluation of Performance

In this section, the output of the cancellation system as indicated generally in equation (5.2-17) will be evaluated for several different situations. These situations are itemized below.

1. Only clutter is present in the radar system's field of view.
2. Both a target and clutter are in the system's field of view, and target occurs in the range cell presently being examined.
3. Both a target and clutter are in the system's field of view. The target occurs in a range cell whose returns are used in the evaluation of the present G function, but that cell is not the cell presently being examined.

For the first case, the needed expressions for e_1, e_2, and G are provided by equations (5.2-9a), (5.2-9b), and (5.2-13). The receiver output signal is

$$e_r(k) = e_1(k) + G(k)\, e_2(k). \tag{5.3-1}$$

Equation (5.2-13) reflects the assumption of cell-to-cell uniformity, and when this concept is applied to the definitions of e_1 and e_2 a simplification in form results.

$$e_1(k) = \frac{Ke_T e^{-j2\beta_0 Z_k}}{\sqrt{2}\, Z_k^2} [S_{11} \mp jTS_{12}] \sum_{i=1}^{N_k} G^2(\alpha_i, \beta_i) e^{-j2\beta_0 \Delta Z_i} \tag{5.3-2a}$$

$$e_2(k) = \frac{\mp jTKe_T e^{-j2\beta_0 Z_k}}{\sqrt{2}\, Z_k^2} [S_{21} \mp jTS_{22}] \sum_{i=1}^{N_k} G^2(\alpha_i, \beta_i) e^{-j2\beta_0 \Delta Z_i} \tag{5.3-2b}$$

$$G(k) = \frac{-1}{\pm jT} \frac{[S_{11} \pm jTS_{12}]}{[S_{21} \pm jTS_{22}]} \tag{5.3-3}$$

One may now evaluate the system output under the assumption of cell-to-cell uniformity by substituting the above expressions for e_1, e_2, and G into the system output equation, (5.3-1).

$$e_r(k) = \frac{Ke_T e^{-j2\beta_0 Z_k}}{\sqrt{2}\, Z_k^2} [S_{11} \pm jTS_{12}] \sum_{i=1}^{N_k} G^2(\alpha_i, \beta_i) e^{-j2\beta_0 \Delta Z_i}$$

$$+ \left(\frac{-1}{\pm jT}\right) \frac{[S_{11} \pm jTS_{12}]}{[S_{21} \pm jTS_{22}]} \frac{(\pm jT) Ke_T e^{-j2\beta_0 Z_k}}{\sqrt{2}\, Z_k^2} [S_{21} \pm jTS_{22}]$$

$$\cdot \sum_{i=1}^{N_k} G^2(\alpha_i, \beta_i) e^{-j2\beta_0 \Delta Z_i} = 0 \tag{5.3-4}$$

In the second case, the appropriate expressions for e_1, e_2, and G come from (5.2-14), (5.2-15) and (5.2-16).

$$e_r(k) = e_1(k) + G(k) e_2(k)$$

$$= e_1(k) + \left(\frac{-1}{2M+1}\right) \left[\sum_{\substack{\ell=k-M \\ \ell \neq k}}^{k+M} \frac{e_1(\ell)}{e_2(\ell)} + \frac{e_1(k)}{e_2(k)} \right] e_2(k) \tag{5.3-5}$$

$$= \left(\frac{2M}{2M+1}\right) e_1(k) + \left(\frac{-1}{2M+1}\right) \left[\sum_{\substack{\ell=k-M \\ \ell \neq k}}^{k+M} \frac{e_1(\ell)}{e_2(\ell)} \right] e_2(k) \tag{5.3-6}$$

$$= \left(\frac{2M}{2M+1}\right) \left[e_1(k) - \left(\frac{1}{\pm jT}\right) \frac{(S_{11} \pm jTS_{12})}{(S_{21} \pm jTS_{22})} e_2(k) \right] \tag{5.3-7}$$

$$= \left(\frac{2M}{2M+1}\right) \left[\left\langle e_1^C(k) + G_1(k) e_2^C(k) \right\rangle + \left\langle e_1^T(k) + G_1(k) e_2^T(k) \right\rangle \right] \tag{5.3-8}$$

What seems to be a new parameter, $G_1(k)$, appears in the last step of equation (5.3-8). Actually, comparison of $G_1(k)$ with the $G(k)$ of equation (5.2-13) leads one to conclude that the two parameters are the same. This latter observation simplifies evaluating equation (5.3-8) since the first part of the equation,

$$e_1^C(k) + G_1(k) e_2^C(k) ,$$

should now be recognized as being the same as equation (5.3-4). Thus,

$$e_r(k) = \left(\frac{2M}{2M+1}\right) [e_1^T(k) + G_1(k) e_2^T(k)] \tag{5.3-9}$$

The statement defining the third case specifies that while the target is not in the cell presently being examined it is located in one of the cells being used to evaluate G. It is assumed for this analysis that the target is in cell m, and thus $e_1(k)$ and $e_2(k)$ are given by equations (5.3-2a) and (5.3-2b) respectively while

$$G(k) = \left(\frac{1}{2M+1}\right) \left[\sum_{\substack{\ell=k-M \\ \ell \neq m}}^{k+M} \frac{e_1(\ell)}{e_2(\ell)} + \frac{e_1(m)}{e_2(m)} \right] . \tag{5.3-10}$$

This expression for G along with the specified expressions for e_1 and e_2 may be used to obtain the following expression for e_r.

$$e_r(k) = e_1(k) + G(k)e_2(k) = \left(\frac{1}{2M+1}\right)\left[e_1^C(k) - \left(\frac{e_1(m)}{e_2(m)}\right) e_2^C(k)\right] \qquad (5.3\text{-}11)$$

$$\frac{e_1(m)}{e_2(m)} = \frac{e_1^C(m) + e_1^T(m)}{e_2^C(m) + e_2^T(m)} \qquad (5.3\text{-}12)$$

Equation (5.3-11) will be further analyzed for two special situations. The first situation, which might be referred to as the high-noise environment, corresponds to the mathematical statements

$$e_1^C(m) >> e_1^T(m) \quad \text{and} \qquad (5.3\text{-}13a)$$

$$e_2^C(m) >> e_2^T(m) \quad . \qquad (5.3\text{-}13b)$$

When equations (5.3-13a) and (5.3-13b) are applied to equation (5.3-12), the following approximations are valid.

$$\frac{e_1(m)}{e_2(m)} \simeq \frac{e_1^C(m)}{e_2^C(m)} \qquad (5.3\text{-}14)$$

$$e_r(k) \simeq \left(\frac{1}{2M+1}\right)\left[e_1^C(k) - \left(\frac{e_1^C(m)}{e_2^C(m)}\right) e_2^C(k)\right] \qquad (5.3\text{-}15)$$

The following results are useful in working with equation (5.3-15).

$$\frac{e_1^C(m)}{e_2^C(m)} = \left(\frac{1}{\pm jT}\right) \frac{[S_{11} \pm jTS_{12}]}{[S_{21} \pm jTS_{22}]} \qquad (5.3\text{-}16)$$

$$\left(\frac{e_1^C(m)}{e_2^C(m)}\right) e_2^C(k) = \frac{TKe_T e^{-j2\beta_0 Z_k}}{\sqrt{2}\, Z_k^2} [S_{11} \pm jTS_{12}] \sum_{i=1}^{N_k} G^2(\alpha_i, \beta_i) e^{-j2\beta_0 \Delta Z_i}$$

$$= e_1^C(k) \qquad (5.3\text{-}17)$$

The result of applying equation (5.3-17) to equation (5.3-15) is given in equation (5.3-18).

$$e_r(k) \simeq \left(\frac{1}{2M+1}\right) [e_1^C(k) - e_1^C(k)] = 0 \qquad (5.3\text{-}18)$$

A second interesting situation arises for equation (5.3-11) when

$$e_1^T(m) >> e_1^C(m) \quad \text{and} \qquad (5.3\text{-}19a)$$

$$e_2^T(m) >> e_2^C(m) \quad . \qquad (5.3\text{-}19b)$$

These assumptions lead to what might be called the large signal environment, and the output signal, e_r, is determined to be

$$e_r(k) \simeq \left(\frac{1}{2M+1}\right) \left[e_1^C(k) - \left(\frac{e_1^T(m)}{e_2^T(m)}\right) e_2^C(k)\right] \quad . \qquad (5.3\text{-}20)$$

5.4 Comparison of Performance

In section 5.3, expressions were developed for the output of the cancellation system under various conditions, and in this section, the results obtained for the cancellation system shall be compared with the appropriate results for the reference system. The basis of comparison, in most cases, shall be the ratio CR which is defined below.

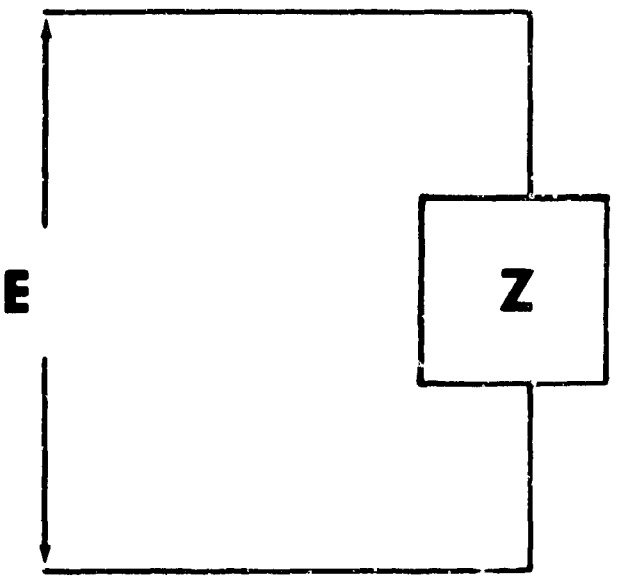

Fig. 5.4-1. Output voltage and load impedance.

$$CR = \frac{\text{output power of the reference system}}{\text{output power of the cancellation system}} \qquad (5.4\text{-}1)$$

The method of power calculation requires some discussion. Figure (5.4-1) shows a potential, E, applied across the terminals of a general impedance, Z. From the theory of netowrk analysis [43], one recalls that when E and Z are represented in phasor notation the complex power delivered to or absorbed by Z is

$$P = \frac{|E|^2}{Z} \quad . \qquad (5.4\text{-}2)$$

In the present analysis, E represents the output signal of the radar receiver, and Z corresponds to load impedance of the network driven by the receiver output. Now apply the following definitions.

$e_r(k)_{REF}$ ≡ output signal from reference receiver.

Z_{REF} ≡ the load impedance of the reference receiver.

P_{REF} ≡ the output power of the reference receiver.

$e_r(k)_{CAN}$ ≡ output signal from cancellation receiver.

Z_{CAN} ≡ the load impedance of the cancellation receiver.

P_{CAN} ≡ the output power of the cancellation receiver.

$$CR = \frac{P_{REF}}{P_{CAN}} \qquad (5.4\text{-}3)$$

$$= \frac{|e_r(k)_{REF}|^2 \cdot Z_{CAN}}{|e_r(k)_{CAN}|^2 \cdot Z_{REF}} \quad . \qquad (5.4\text{-}4)$$

If $Z_{CAN} = Z_{REF}$ then

$$CR = \frac{|e_r(k)_{REF}|^2}{|e_r(k)_{CAN}|^2} \quad . \tag{5.4-5}$$

It is the form of CR indicated in equation (5.4-5) that will be evaluated in the following material.

Equation (5.3-4) shows that the output of the cancellation system is zero when only clutter appears in the field of view of the radar, and thus

$$|e_r(k)_{CAN}|^2 = 0 \tag{5.4-6}$$

The output of the reference system given the same constraints imposed on equation (5.3-4) is

$$e_r(k)_{REF} = \frac{Ke_T S_{11}}{Z_k^2} e^{-j2\beta_0 Z_k} \sum_{i=1}^{N_k} G^2(\alpha_i, \beta_i) e^{-j2\beta_0 \Delta Z_i} \tag{5.4-7}$$

$$= \alpha e^{j\theta} \tag{5.4-8}$$

Thus,

$$|e_r(k)_{REF}|^2 = \alpha^2 \neq 0 \quad , \text{ and} \tag{5.4-9}$$

the cancellation ratio may be shown to be

$$CR = \frac{\alpha^2}{0} = \infty \quad . \tag{5.4-10}$$

The significance of equation (5.4-10) is that it states that the cancellation system offers infinite improvement in clutter cancellation when compared to the reference system.

The radar system output under the conditions outlined in case two of section 5.3 contains both a desired component, referred to as the signal, and an undesired component, called noise. When the system output contains both desired and undesired components, one finds that an excellent criterion for judging system performance is a ratio which indicates the relative strength of the signal to the noise. This criterion is referred to as a signal-to-noise ratio [44], and the ratio is defined in equation (5.4-11).

$$\text{SNR} = \frac{\text{output signal power}}{\text{output noise power}} \tag{5.4-11}$$

The reference system has an output

$$e_r(k) = e^C(k) + e^T(k) \tag{5.4-12}$$

where $e^C(k)$ is the noise or clutter component, and $e^T(k)$ is the signal or target component. This leads to the signal-to-noise ratio for the reference system given in equation (5.4-13).

$$\text{SNR} = \frac{|e^T(k)|^2}{|e^C(k)|^2 + 2\text{Re}\left\langle e^C(k)\, e^T(k)\right\rangle} \tag{5.4-13}$$

It is evident from equation (5.3-9) that the cancellation system output contains no noise or clutter component so that the signal-to-noise ratio for the cancellation system is infinite.

When the operating conditions satisfy the specifications of the third situation in section 5.3, one wishes to minimize the system output since any output under these conditions amounts to noise. The cancellation ratio will again be used a the criterion of performance, and the following expressions are used in evaluating the cancellation ratio

$$e_r(k)_{REF} = \frac{Ke_T S_{11}}{Z_k^2} e^{-j2\beta_0 Z_k} \sum_{i=1}^{N_k} G^2(\alpha_i, \beta_i) e^{-j2\beta_0 \Delta Z_i} = AS_{11}B \qquad (5.4\text{-}14)$$

$$A = \frac{Ke_T}{Z_k^2} e^{-j2\beta_0 Z_k} \qquad (5.4\text{-}15)$$

$$B = \sum_{i=1}^{N_k} G^2(\alpha_i, \beta_i) e^{-j2\beta_0 \Delta Z_i} \qquad (5.4\text{-}16)$$

$$|e_r(k)_{REF}|^2 = |AB|^2 S_{11}^2 \qquad (5.4\text{-}17)$$

The output of the cancellation system in a high noise environment as given by equation (5.3-18) is zero, and thus, the output noise power is zero. Thus,

$$CR = \frac{|AB|^2 S_{11}^2}{0} = \infty \qquad (5.4\text{-}18)$$

If the large signal environemnt assumptions are used, one finds that the output of the cancellation system is given by equation (5.3-20). The notation may be simplified if the following definitions are applied.

$$e_1^C(k) = ABC/\sqrt{2} \qquad (5.4\text{-}19)$$

$$e_2^C(k) = \pm jTADB/\sqrt{2} \qquad (5.4\text{-}20)$$

$$C = S_{11} \pm jTS_{12} \qquad (5.4\text{-}21)$$

$$D = S_{21} \pm jTS_{22} \qquad (5.4\text{-}22)$$

$$F = e_1^T(m)/e_2^T(m) \qquad (5.4\text{-}23)$$

The cancellation system output in the above notation is

$$e_r(k)_{CAN} = \frac{AB}{\sqrt{2}\,(2M+1)} \; [C \mp jFTD] \tag{5.4-24}$$

$$|e_r(k)_{CAN}| = \frac{|AB|^2}{2(2M+1)^2} \; [|C|^2 \mp 2\mathrm{Im}(C^* FTD) + |FTD|^2] \tag{5.4-25}$$

The large number of parameters in this equation makes it difficult to see the nature of overall variations. The following assumptions are restrictive in nature but do aid in clarifying the system effects.

$$T = 1.0 \tag{5.4-26}$$

$$F = e^{j\theta} = \cos(\theta) + j \sin(\theta) \tag{5.4-27}$$

One further point bears mentioning before the analysis is continued. Since the output of both the reference system and the cancellation system is random in nature, theoretical correctness demands that the expression used for output power be a statistical expectation. Thus equation (5.4-5) becomes

$$CR = \frac{E\{|e_r(k)_{REF}|^2\}}{E\{|e_r(k)_{CAN}|^2\}} \tag{5.4-28}$$

where $E\{\cdot\}$ denotes a statistical expectation [15].

$$E\{|e_r(k)_{REF}|^2\} = E\{|AB|^2\} \cdot S_{11}^2 \tag{5.4-29}$$

$$E\{|e_r(k)_{CAN}|^2\} = \frac{E\{|AB|^2\}}{2(2M+1)^2} \cdot [|C|^2 \mp 2\mathrm{Im}(C^* De^{j\theta}) + |D|^2] \tag{5.4-30}$$

$$CR = \frac{2S_{11}^2(2M+1)^2}{[|C|^2 \pm 2\mathrm{Im}(C^* D e^{j\theta}) + |D|^2]} \qquad (5.4\text{-}31)$$

$$= \frac{2(2M+1)^2 S_{11}^2}{\left[S_{11}^2 + 2S_{12}^2 + S_{22}^2 \pm 2 \left\langle (S_{11}S_{21} + S_{12}S_{22})\sin(\theta) \pm (S_{11}S_{22} - S_{12}^2)\cos(\theta) \right\rangle\right]} \qquad (5.4\text{-}32)$$

An interesting result is obtained if the cancellation ratio is evaluated with the output of the ordinary system replacing the output of the reference system and if θ equals 180 degrees. Under the stated conditions

$$CR = (2M+1)^2 \qquad (5.4\text{-}33)$$

6.0 PERFORMANCE OF THE CANCELLATION SYSTEM WITH A REALISTIC RAIN MODEL

6.1 The Rain Model

There are basically two major areas involved in specifying a rain model. The first area is concerned with describing the individual rain particle, and this aspect of rain modeling has been delt with in chapter 3 where a major emphasis was on defining particle size and shape. Particle size and shape affect the radar system equations through the S matrix elements defined in equation (2.3-6), and nothing in this chapter will be done to alter the nature of the influence that particle size and shape have on the system equations.

The second aspect of rain modeling is concerned with the nature of large scale rain systems. Here individual particle characteristics are lost and only overall effects are noted. In chapter 5 it was assumed that the rain system was characterized by overall uniformity, but the present goal is to establish a less restrictive and more realistic model for the rain system. In pursuit of the stated goal, the following assumptions will be applied.

1. The rain particles exhibit a uniform spatial distribution over the range cells.
2. Particle size and orientation will be treated as random variables, and it is assumed that they are statistically independent of the particle position parameters. The distribution of particle size presented in chapter 3 will be used here.
3. The number of particles occuring in a range cell is strictly random, and the distribution function for the number of particles will be determined in later work. It is assumed that

the number of particles is statistically independent of particle size, shape, orientation and location.

4. Although several parameters relating to the rain are random in nature, it is assumed that the statistical distributions describing the various parameters are invariant in time and space.

5. It is assumed that the clutter returns from one range cell are statistically independent of the clutter returns from any other range cell.

6.2 System Equations

The physical system bieng analyzed here is the same as the one presented in Figure 5.2-1, and so the definitions for $e_1(k)$, $e_2(k)$, and $G(k)$ given in equations (5.2-9a), (5.2-9b), and (5.2-10) respectively are valid here. However, for several reasons including both ease of notation and statistical considerations the following forms will be used.

$$e_1(k) = \frac{A}{\sqrt{2}}\left(X_1(k) + jY_1(k)\right) \tag{6.2-1}$$

$$e_2(k) = \frac{\pm\sqrt{TA}}{\sqrt{2}}\left(X_2(k) + jY_2(k)\right) \tag{6.2-2}$$

$$G(k) = \left(\frac{-1}{2M+1}\right)\sum_{\ell=k-M}^{k+M}\frac{e_1(\ell)}{e_2(\ell)} = \left(\frac{-1}{2M+1}\right)\left[\sum_{\substack{\ell=k-M\\ \ell\neq k}}^{k+M}\frac{e_1(\ell)}{e_2(\ell)} + \frac{e_1(k)}{e_2(k)}\right]$$

$$= \left(\frac{-1}{2M+1}\right)\left[G'(k) + \frac{e_1(k)}{e_2(k)}\right] \tag{6.2-3}$$

The quantities X_1, Y_1, X_2, and Y_2 are determined by the following.

$$S_{11i}(k) \pm jTS_{12i}(k) = \alpha_{1i}(k)\, e^{j\gamma_{1i}(k)} \tag{6.2-4}$$

$$S_{21i}(k) \pm jTS_{22i}(k) = \alpha_{2i}(k)\, e^{j\gamma_{2i}(k)} \tag{6.2-5}$$

$$2\beta_0 \Delta Z_i = \theta_i \tag{6.2-6}$$

$$X_1(k) = \sum_{i=1}^{N_k} G^2(\alpha_i, \beta_i)\alpha_{1i}(k) \cos\left(\gamma_{1i}(k) - \theta_i\right) \tag{6.2-7}$$

$$Y_1(k) = \sum_{i=1}^{N_k} G^2(\alpha_i, \beta_i)\alpha_{1i}(k) \sin\left(\gamma_{1i}(k) - \theta_i\right) \tag{6.2-8}$$

$$X_2(k) = \sum_{i=1}^{N_k} G^2(\alpha_i, \beta_i)\alpha_{2i}(k) \cos\left(\gamma_{2i}(k) - \theta_i\right) \tag{6.2-9}$$

$$Y_2(k) = \sum_{i=1}^{N_k} G^2(\alpha_i, \beta_i)\alpha_{2i}(k) \sin\left(\gamma_{2i}(k) - \theta_i\right) \tag{6.2-10}$$

Equations (6.2-1) through (6.2-10) may be used to express the system output as well as the magnitude squared of the system output.

$$e_r(k) = e_1(k) + G(k) \cdot e_2(k) = e_1(k) + \left(\frac{-1}{2M+1}\right)\left[G'(k) + \frac{e_1(k)}{e_2(k)}\right] e_2(k)$$

$$= \left(\frac{2M}{2M+1}\right) e_1(k) - \frac{G'(k) \cdot e_2(k)}{(2M+1)} \tag{6.2-11}$$

$$|e_r(k)|^2 = e_r(k) \cdot e_r^*(k) = \left(\frac{2M}{2M+1}\right)^2 |e_1(k)|^2 - \frac{4M}{(2M+1)^2} \mathrm{Re}\left\langle e_1^*(k) e_2(k) G'(k)\right\rangle$$

$$+ \frac{|G'(k)|^2\, |e_2(k)|^2}{(2M+1)^2} \tag{6.2-12}$$

$$|e_1(k)|^2 = \frac{|A|^2}{2}\left[X_1^2(k) + Y_1^2(k)\right] \tag{6.2-13}$$

$$|e_2(k)|^2 = \frac{|T|^2\,|A|^2}{2}\left[X_2^2(k) + Y_2^2(k)\right] \tag{6.2-14}$$

$$e_1^*(k)\,e_2(k) = \frac{\pm jT|A|^2}{2}\left[\left(X_1(k)\,X_2(k) + Y_1(k)\,Y_2(k)\right) + j\left(X_1(k)\,Y_2(k) - X_2(k)\,Y_1(k)\right)\right] \tag{6.2-15}$$

$$\begin{aligned} G'(k) &= \sum_{\substack{\ell=k-M \\ \ell\neq k}}^{k+M} \frac{[X_1(\ell) + jY_1(\ell)]}{(\pm jT)[X_2(\ell) + jY_2(\ell)]} \\ &= \pm \sum_{\substack{\ell=k-M \\ \ell\neq k}}^{k+M} \frac{\mathrm{Re}(T)\left(X_2(\ell)Y_1(\ell) - X_1(\ell)Y_2(\ell)\right) - \mathrm{Im}(T)\left(X_1(\ell)X_2(\ell) + Y_1(\ell)Y_2(\ell)\right)}{|T|^2\left(X_2^2(\ell) + Y_2^2(\ell)\right)} \\ &\quad \mp j \sum_{\substack{\ell=k-M \\ \ell\neq k}}^{k+M} \frac{\mathrm{Re}(T)\left(X_1(\ell)X_2(\ell) + Y_1(\ell)Y_2(\ell)\right) + \mathrm{Im}(T)\left(X_2(\ell)Y_1(\ell) - X_1(\ell)Y_2(\ell)\right)}{|T|^2\left(X_2^2(\ell) + Y_2^2(\ell)\right)} \end{aligned} \tag{6.2-16}$$

$$\begin{aligned} |G'(k)|^2 = &\left(\sum_{\substack{\ell=k-M \\ \ell\neq k}}^{k+M}\left[\frac{\mathrm{Re}(T)\left(X_2(\ell)Y_1(\ell) - X_1(\ell)Y_2(\ell)\right) + \mathrm{Im}(T)\left(X_2(\ell)Y_1(\ell) - X_1(\ell)Y_2(\ell)\right)}{|T|^2\left(X_2^2(\ell) + Y_2^2(\ell)\right)}\right]\right)^2 \\ &+\left(\sum_{\substack{\ell=k-M \\ \ell\neq k}}^{k+M}\left[\frac{\mathrm{Re}(T)\left(X_1(\ell)X_2(\ell) + Y_1(\ell)Y_2(\ell)\right) + \mathrm{Im}(T)\left(X_2(\ell)Y_1(\ell) - X_1(\ell)Y_2(\ell)\right)}{|T|^2\left(X_2^2(\ell) + Y_2^2(\ell)\right)}\right]\right)^2 \end{aligned} \tag{6.2-17}$$

The relationship given in equation (6.2-18) will be useful in later work with equation (6.2-17).

$$\left(\sum_{i=1}^{N} a_i\right)^2 = \sum_{i=1}^{N} a_i^2 + \sum_{\substack{i=1 \\ i\neq j}}^{N} \sum_{j=1}^{N} a_i a_j \qquad (6.2\text{-}18)$$

As a result of the random nature of the rain as outlined in the preceeding section, much of the evaluation done in this chapter will be done in a statistical sense. This means that power will be defined as $E\{|x|^2\}$ where the operator $E\{\cdot\}$ is the expectation operator presented by Thomas [45]. Thus the output noise power of the cancellation system is

$$E\{|e_r(k)|^2\} = \left(\frac{2M}{2M+1}\right)^2 E\{|e_1(k)|^2\} - \frac{4M}{(2M+1)^2} E\{Re\ \langle e_1^*(k)e_2(k)G'(k)\rangle\}$$

$$+ \left(\frac{1}{2M+1}\right)^2 E\{|G'(k)|^2\ |e_2(k)|^2\} \qquad (6.2\text{-}19)$$

Now consider, in order, the three expectation terms appearing on the right hand side of the equality in equation (6.2-19).

$$E\{|e_1(k)|^2\} = E\left\{\frac{|A|^2}{2}\left[X_1^2(k) + Y_1^2(k)\right]\right\} \qquad (6.2\text{-}20)$$

Examination of equation (5.4-15) reveals that A is not random in nature so that

$$E\{|e_1(k)|^2\} = \frac{|A|^2}{2}\left[E\{X_1^2(k)\} + E\{Y_1^2(k)\}\right] . \qquad (6.2\text{-}21)$$

From appendix A,

$$E\{X_1^2(k)\} = E\{N_k\}\ E\left\{\frac{G^4(\alpha,\beta)}{2}\right\} E\{\alpha_1^2\}\ , \text{ and} \qquad (6.2\text{-}22)$$

$$E\{Y_1^2(k)\} = E\{N_k\}\ E\left\{\frac{G^4(\zeta,\psi)}{2}\right\} E\{\alpha_1^2\}\ . \qquad (6.2\text{-}23)$$

Appendix B shows that

$$E\{N_k\} = K_1 V_k I_0^{K_2} \quad , \tag{6.2-24}$$

and appendix C indicates that

$$E\{G^4(\alpha,\beta)\} = 0.70808 \quad . \tag{6.2-25}$$

Consider the remaining unknown factor $E\{\alpha_1^2\}$. From equation (6.2-4),

$$\alpha_1 = |S_{11} \pm jTS_{12}| \quad . \tag{6.2-26}$$

Thus

$$\alpha_1^2 = S_{11}^2 + |T|^2 S_{12}^2 \mp 2\mathrm{Im}\left\langle TS_{11}S_{12}\right\rangle \quad , \text{ and} \tag{6.2-27}$$

$$E\{\alpha_1^2\} = E\{S_{11}^2\} + |T|^2 E\{S_{12}^2\} \mp 2\mathrm{Im}\left\langle E\{TS_{11}S_{12}\}\right\rangle \quad . \tag{6.2-28}$$

Consideration is now given to the second term,

$$\mathrm{Re}\left\langle E\{e_1^*(k)\, e_2(k)\, G'(k)\}\right\rangle \quad , \tag{6.2-29}$$

in equation (6.2-19). Application of condition five in section 6.1 in conjunction with the development in appendix D permits the preceeding term to be expressed as

$$\mathrm{Re}\left\langle E\{e_1^*(k)\, e_2(k)\}\, E\{G'(k)\}\right\rangle \quad . \tag{6.2-30}$$

Equations (6.2-1) and (6.2-2) may be used to obtain an expression for $e_1^*(k)e_2(k)$.

$$e_1^*(k)\, e_2(k) = \frac{\mp|A|^2}{2} \left[\mathrm{Im}(T) \left(X_1(k)X_2(k) + Y_1(k)Y_2(k)\right)\right.$$

$$\left. + \mathrm{Re}(T) \left(X_1(k)Y_2(k) - X_2(k)Y_1(k)\right)\right]$$

$$\pm j\frac{|A|^2}{2} \left[\mathrm{Re}(T) \left(X_1(k)X_2(k) + Y_1(k)Y_2(k)\right)\right.$$

$$\left. - \mathrm{Im}(T) \left(X_1(k)Y_2(k) - X_2(k)Y_1(k)\right)\right] \qquad (6.2\text{-}31)$$

$$E\{e_1^*(k)e_2(k)\} = \frac{\mp|A|^2}{2} \left[\mathrm{Im}(T) \left(E\{X_1(k)X_2(k)\} + E\{Y_1(k)Y_2(k)\}\right)\right.$$

$$\left. + \mathrm{Re}(T) \left(E\{X_1(k)Y_2(k)\} - E\{X_2(k)Y_1(k)\}\right)\right]$$

$$\pm j\frac{|A|^2}{2} \left[\mathrm{Re}(T) \left(E\{X_1(k)X_2(k)\} + E\{Y_1(k)Y_2(k)\}\right)\right.$$

$$\left. - \mathrm{Im}(T) \left(E\{X_1(k)Y_2(k)\} - E\{X_2(k)Y_1(k)\}\right)\right] \qquad (6.2\text{-}32)$$

The cross correlation terms in the preceeding equation are evaluated in appendix E.

Now attention must be given to the evaluation of $E\{G'(k)\}$. From equation (6.2-3),

$$G'(k) = \sum_{\substack{\ell=k-M \\ \ell\neq k}}^{k+M} \frac{e_1(\ell)}{e_2(\ell)} \qquad (6.2\text{-}33)$$

$$= \sum_{\substack{\ell=k-M \\ \ell\neq k}}^{k+M} \left[\frac{X_1(\ell) + jY_1(\ell)}{\pm jT\left(X_2(\ell) + jY_2(\ell)\right)}\right] \qquad (6.2\text{-}34)$$

$$= \mp \sum_{\substack{\ell=k-M \\ \ell\neq k}}^{k+M} \left[\frac{[X_1(\ell)Y_2(\ell) - X_2(\ell)Y_1(\ell)]\mathrm{Re}(T) + [X_1(\ell)X_2(\ell) + Y_1(\ell)Y_2(\ell)]\mathrm{Im}(T)}{|T|^2\,[X_2^2(\ell) + Y_2^2(\ell)]} \right]$$

$$\mp j \sum_{\substack{\ell=k-M \\ \ell\neq k}}^{k+M} \left[\frac{[X_1(\ell)X_2(\ell) + Y_1(\ell)Y_2(\ell)]\mathrm{Re}(T) - [X_1(\ell)Y_2(\ell) - X_2(\ell)Y_1(\ell)]\mathrm{Im}(T)}{|T|^2\,[X_2^2(\ell) + Y_2^2(\ell)]} \right].$$

(6.2-35)

The assumed uniformity in space and time of the statistical distributions allows the the expectation of $G'(k)$ to be expressed in the following form.

$$E\{G'(k)\} = \frac{\mp 2M}{|T|^2}\; E\left\{ \frac{[X_1(\ell)Y_2(\ell) - X_2(\ell)Y_1(\ell)]\mathrm{Re}(T) + [X_1(\ell)X_2(\ell)+Y_1(\ell)Y_2(1)]\mathrm{Im}(T)}{[X_2^2(\ell) + Y_2^2(\ell)]} \right\}$$

$$\frac{\mp j 2M}{|T|^2}\; E\left\{ \frac{[X_1(\ell)X_2(\ell)+Y_1(\ell)Y_2(\ell)]\mathrm{Re}(T) - [X_1(\ell)Y_2(\ell)-X_2(\ell)Y_1(\ell)]\mathrm{Im}(T)}{[X_2^2(\ell) + Y_2^2(\ell)]} \right\}$$

(6.2-36)

Evaluation of $E\{G'(k)\}$ requires that the expectation of the quantities

$$\frac{X_1(\ell)Y_2(\ell)}{X_2^2(\ell) + Y_2^2(\ell)}\,,\quad \frac{X_2(\ell)Y_1(\ell)}{X_2^2(\ell) + Y_2^2(\ell)}\,,\quad \frac{X_1(\ell)X_2(\ell)}{X_2^2(\ell) + Y_2^2(\ell)}\,,\ \text{and}\ \frac{Y_1(\ell)Y_2(\ell)}{X_2^2(\ell) + Y_2^2(\ell)}$$

be determined. The required expectations are in the form of three dimensional integrals, and appendix G shows how the integrals may be reduced to two dimensional forms.

The third term of equation (6.2-19) may now be expressed as

$$\frac{1}{(2M+1)^2} E\{|G'(k)|^2\} \cdot E\{|e_2(k)|^2\}$$

as a result of the work culminating in equation (6.2-30). $E\{|e_2(k)|^2\}$ is evaluated in the same manner as was $E\{|e(k)|^2\}$.

$$E\{|e_2(k)|^2\} = \frac{|T|^2 |A|^2}{2} [E\{X_2^2(k)\} + E\{Y_2^2(k)\}] \qquad (6.2\text{-}37)$$

From appendix A,

$$E\{X_2^2(k)\} = E\{N_k\} E\left\{\frac{G^4(\alpha,\beta)}{2}\right\} E\{\alpha_2^2\} \quad , \text{and} \qquad (6.2\text{-}38)$$

$$E\{Y_2^2(k)\} = E\{N_k\} E\left\{\frac{G^4(\alpha,\beta)}{2}\right\} E\{\alpha_2^2\} \; . \qquad (6.2\text{-}39)$$

Equation (6.2-5) may be used to show that

$$|\alpha_2|^2 = S_{21}^2 + |T|^2 S_{22}^2 \mp 2\mathrm{Im}(TS_{21}S_{22}) \; . \qquad (6.2\text{-}40)$$

Thus,

$$E\{|\alpha_2|^2\} = E\{S_{21}^2\} + |T|^2 E\{S_{22}^2\} \mp 2\mathrm{Im}(T)\, E\{S_{21}S_{22}\} \; . \qquad (6.2\text{-}41)$$

$|G'(k)|^2$ is indicated in equation (6.2-17) as being the sum of two squared quantities. Each of the two squared quantities may, through application of equation (6.2-18), be shown to be as indicated in the following.

$$\sum_{\substack{\ell=k-M \\ \ell\neq k}}^{\ell+M}\left[\frac{\mathrm{Re}(T)\left(X_2(\ell)Y_1(\ell)-X_1(\ell)Y_2(\ell)\right)+\mathrm{Im}(T)\left(X_2(\ell)Y_1(\ell)-X_1(\ell)Y_2(\ell)\right)}{|T|^2\left(X_2^2(\ell)+Y_2^2(\ell)\right)}\right]^2 +$$

$$\sum_{\substack{\ell=k-M \\ \ell\neq k}}^{k+M}\sum_{\substack{j=k-M \\ j\neq k \\ \ell\neq j}}^{k+M}\frac{\mathrm{Re}(T)\left(X_2(\ell)Y_1(\ell)-X_1(\ell)Y_2(\ell)\right)+\mathrm{Im}(T)\left(X_2(\ell)Y_1(\ell)-X_1(\ell)Y_2(\ell)\right)}{|T|^2\left(X_2^2(\ell)+Y_2^2(\ell)\right)} \cdot$$

$$\frac{\mathrm{Re}(T)\left(X_2(j)Y_1(j)-X_1(j)Y_2(j)\right)+\mathrm{Im}(T)\left(X_2(j)Y_1(j)-X_1(j)Y_2(j)\right)}{|T|^2\left(X_2^2(j)+Y_2^2(j)\right)} \qquad (6.2\text{-}42)$$

The above represents the first term of equation (6.2-17), and the following is another form for the second term in the same equation.

$$\sum_{\substack{\ell=k-M \\ \ell\neq k}}^{k+M}\left[\frac{\mathrm{Re}(T)\left(X_1(\ell)X_2(\ell)+Y_1(\ell)Y_2(\ell)\right)+\mathrm{Im}(T)\left(X_2(\ell)Y_1(\ell)-X_1(\ell)Y_2(\ell)\right)}{|T|^2\left(X_2^2(\ell)+Y_2^2(\ell)\right)}\right]^2 +$$

$$\sum_{\substack{\ell=k-M \\ \ell\neq k}}^{k+M}\sum_{\substack{j=k-M \\ j\neq k \\ \ell\neq j}}^{k+M}\left[\frac{\mathrm{Re}(T)\left(X_1(\ell)X_2(\ell)+Y_1(\ell)Y_2(\ell)\right)+\mathrm{Im}(T)\left(X_2(\ell)Y_1(\ell)-X_1(\ell)Y_2(\ell)\right)}{|T|^2\left(X_2^2(\ell)+Y_2^2(\ell)\right)}\right] \cdot$$

$$\left[\frac{\mathrm{Re}(T)\left(X_1(j)X_2(j)+Y_1(j)Y_2(j)\right)+\mathrm{Im}(T)\left(X_2(j)Y_1(j)-X_1(j)Y_2(j)\right)}{|T|^2\left(X_2^2(j)+Y_2^2(j)\right)}\right] \qquad (6.2\text{-}43)$$

Note that when T is real the following simplified form results for $|G'(k)|^2$.

$$|G'(k)|^2 = \sum_{\substack{\ell=k-M \\ \ell\neq k}}^{k+M}\left[\frac{X_2(\ell)Y_1(\ell)-X_1(\ell)Y_2(\ell)}{T\left(X_2^2(\ell)+Y_2^2(\ell)\right)}\right]^2 +$$

$$\sum_{\substack{\ell=k-M \\ \ell\neq k}}^{k+M} \sum_{\substack{j=k-M \\ j\neq k \\ \ell\neq j}}^{k+M} \left[\frac{X_2(\ell)Y_1(\ell)-X_1(\ell)Y_2(\ell)}{T\left(X_2^2(\ell)+Y_2^2(\ell)\right)}\right]\left[\frac{X_2(j)Y_1(j)-X_1(j)Y_2(j)}{T\left(X_2^2(j)+Y_2^2(j)\right)}\right] +$$

$$\sum_{\substack{\ell=k-M \\ \ell\neq k}}^{k+M} \left[\frac{X_1(\ell)X_2(\ell)+Y_1(\ell)Y_2(\ell)}{T\left(X_2^2(\ell)+Y_2^2(\ell)\right)}\right]^2 +$$

$$\sum_{\substack{\ell=k-M \\ \ell\neq k}}^{k+M} \sum_{\substack{j=k-M \\ j\neq k \\ \ell\neq j}}^{k+M} \left[\frac{X_1(j)X_2(j)+Y_1(j)Y_2(j)}{T\left(X_2^2(j)+Y_2^2(j)\right)}\right]\left[\frac{X_1(\ell)X_2(\ell)+Y_1(\ell)Y_2(\ell)}{T\left(X_2^2(\ell)+Y_2^2(\ell)\right)}\right] \qquad (6.2\text{-}44)$$

$$E\{|G'(k)|^2\} = 2M\,E\left\{\frac{[X_2(\ell)Y_1(\ell)]^2 - 2[X_1(\ell)X_2(\ell)Y_1(\ell)Y_2(\ell)] + [X_1(\ell)Y_2(\ell)]^2}{T^2\left(X_2^2(\ell)+Y_2^2(\ell)\right)^2}\right\}$$

$$+ 2M\,E\left\{\frac{[X_1(\ell)X_2(\ell)]^2 + 2[X_1(\ell)X_2(\ell)Y_1(\ell)Y_2(\ell)] + [Y_1(\ell)Y_2(\ell)]^2}{T^2\left(X_2^2(\ell)+Y_2^2(\ell)\right)^2}\right\}$$

$$+ (4M^2-2M)\left[E\left\{\frac{X_2(\ell)Y_1(\ell) - X_1(\ell)Y_2(\ell)}{T\left(X_2^2(\ell)+Y_2^2(\ell)\right)}\right\}\right]^2$$

$$+ (4M^2-2M)\left[E\left\{\frac{X_1(\ell)X_2(\ell) + Y_1(\ell)Y_2(\ell)}{T\left(X_2^2(\ell)+Y_2^2(\ell)\right)}\right\}\right]^2 \qquad (6.2\text{-}45)$$

Effectively, the last two terms of equation (6.2-45) were evaluated in the discussion of $E\{G'(k)\}$. Evaluation of the first two terms of equation (6.2-45) requires knowledge of

$$E\left\{\frac{\left(X_2(\ell)Y_1(\ell)\right)^2}{T^2[X_2^2(\ell)+Y_2^2(\ell)]^2}\right\}, \quad E\left\{\frac{\left(X_1(\ell)Y_2(\ell)\right)^2}{T^2[X_2^2(\ell)+Y_2^2(\ell)]^2}\right\},$$

$$E\left\{\frac{\left(X_1(\ell)X_2(\ell)\right)^2}{T^2\left[X_2^2(\ell)+Y_2^2(\ell)\right]^2}\right\} \quad \text{, and} \quad E\left\{\frac{\left(Y_1(\ell)Y_2(\ell)\right)^2}{T^2\left[X_2^2(\ell)+Y_2^2(\ell)\right]^2}\right\} \quad .$$

A technique is presented in appendix F whereby the above expectations may be reduced to two dimensional integrals.

6.3 Lower Bound on Performance

Conditions were specified in chapter 4 under which the lower bound of performance resulted for the ordinary system. Those same conditions will be applied here to the cancellation system equations for the purpose of comparing the performance of the cancellation system with the known lower bound of performance of the ordinary system. The conditions described in chapter 4 require that

$$\cos^2(\psi) \approx \left(\frac{V_\infty}{V_r}\right)^2 \quad , \tag{6.3-1}$$

$$\sin^2(\psi) \approx 1 - \left(\frac{V_\infty}{V_r}\right)^2 \quad , \tag{6.3-2}$$

$$\sin(\zeta) = 1 \quad \text{, and} \tag{6.3-3}$$

$$\cos(\zeta) = 0 \quad . \tag{6.3-4}$$

Under these conditons, the S matrix elements become

$$S_{11} \approx g_x - (g_x - g_y)\,(V_\infty/V_r)^2 \tag{6.3-5}$$

$$S_{12} \approx (g_x - g_y)\,(V_\infty/V_r)\sqrt{1-(V_\infty/V_r)^2} \tag{6.3-6}$$

$$S_{22} \approx (g_x - g_y)\,(V_\infty/V_r)^2 + g_y \quad . \tag{6.3-7}$$

Other results from chapter four which will be used here are

$$g_x^2 = \left[\frac{\pi\varepsilon_1}{6 \times 10^9}\right]^2 d_0^6 \left[8.25 - 0.244d_0^2 + 0.023d_0^3\right] , \qquad (6.3\text{-}8)$$

$$g_y^2 = \left[\frac{\pi\varepsilon_1}{6 \times 10^9}\right]^2 d_0^6 \left[8.33 + 0.112d_0^2\right] , \qquad (6.3\text{-}9)$$

$$(g_x - g_y)^2 = \left[\frac{\pi\varepsilon_1}{6 \times 10^9}\right]^2 d_0^8 \left[0.0024 + 0.00415d_0^2\right] , \qquad (6.3\text{-}10)$$

$$g_x g_y = \left[\frac{\pi\varepsilon_1}{6 \times 10^9}\right]^2 d_0^6 \left[8.29 - 0.0672d_0^2 + 0.0115d_0^3 - 0.002075d_0^4\right] , \qquad (6.3\text{-}11)$$

$$V_\infty = 10.105 \left[1 - e^{-d_0/2}\right] , \qquad (6.3\text{-}12)$$

and the drop size distribution is

$$P(d_0) = \frac{\gamma^3}{2} d_0^2 e^{-\gamma d_0} . \qquad (6.3\text{-}13)$$

Evaluation of the cancellation system's output equation requires knowledge of various moments of the S matrix elements. The required moments are given below.

$$E\{S_{11}^2\} = E\{g_x^2\} - 2E\{g_x(g_x - g_y)(V_\infty/V_r)^2\} + E\{(g_x - g_y)^2(V_\infty/V_r)^4\} \qquad (6.3\text{-}14)$$

$$E\{S_{12}^2\} = E\{(g_x - g_y)^2 (V_\infty/V_r)^2\} - E\{(g_x - g_y)^2 (V_\infty/V_r)^4\} \qquad (6.3\text{-}15)$$

$$E\{S_{22}^2\} = E\{(g_x-g_y)^2\ (V_\infty/V_r)^4\} + 2E\{g_y(g_x-g_y)\ (V_\infty/V_r)^2\} + E\{g_y^2\} \quad (6.3\text{-}16)$$

$$E\{S_{11}S_{12}\} = E\{g_x(g_x-g_y)\ (V_\infty/V_r)\} - (\tfrac{1}{2})\ E\{g_x(g_x-g_y)\ (V_\infty/V_r)^3\}$$

$$- E\{(g_x-g_y)^2\ (V_\infty/V_r)^3\} + (\tfrac{1}{2})\ E\{(g_x-g_y)^2\ (V_\infty/V_r)^5\} \quad (6.3\text{-}17)$$

$$E\{S_{11}S_{22}\} = E\{g_x(g_x-g_y)\ (V_\infty/V_r)^2\} - E\{(g_x-g_y)^2\ (V_\infty/V_r)^4\}$$

$$+ E\{g_xg_y)\} - E\{g_y(g_x-g_y)\ (V_\infty/V_r)^2\} \quad (6.3\text{-}18)$$

Evaluation of equations (6.3-14) through (6.3-18) is accomplished in appendix G, and the following material shows how to apply the results obtained to determine the output noise for the cancellation system. The following assumes that T is real.

$$E\{|e_1(k)|^2\} = |A|^2\ E\{N_k\}\ E\{\frac{G^4(\alpha,\beta)}{2}\} \cdot \left[E\{S_{11}^2\} + T^2\ E\{S_{12}^2\}\right] \quad (6.3\text{-}19)$$

$$E\{e_1^*(k)e_2(k)\} = \frac{\mp|A|^2T}{2}\ \Big[\Big(E\{X_1(k)Y_2(k)\} - E\{X_2(k)Y_1(k)\}\Big)$$

$$-j\left(E\{X_1(k)X_2(k)\} + E\{Y_1(k)Y_2(k)\}\right)\Big] \quad (6.3\text{-}20)$$

$$= \frac{\mp|A|^2}{2}\ TE\{N_k\}\ E\{G^4(\alpha,\beta)\}\ \Big[\pm(T)E\{S_{11}S_{22}-S_{12}^2\}$$

$$-j\ E\{S_{11}S_{21} + S_{12}S_{22}T^2\}\Big] \quad (6.3\text{-}21)$$

$$E\{|e_2(k)|^2\} = T^2\ |A|^2\ E\{N_k\}\ E\{\frac{G^4(\alpha,\beta)}{2}\} \cdot \left[E\{S_{21}^2\} + T^2E\{S_{22}^2\}\right] \quad (6.3\text{-}22)$$

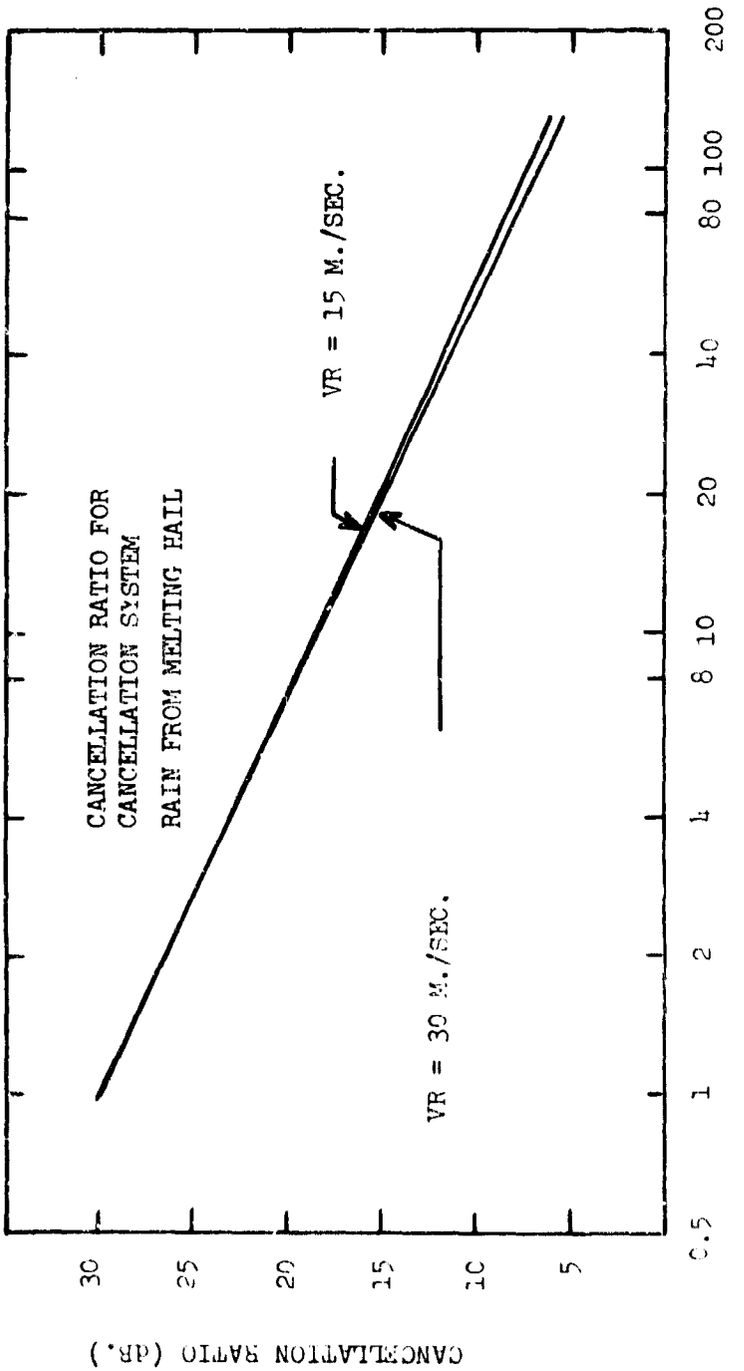
CANCELLATION RATIO FOR
CANCELLATION SYSTEM
RAIN FROM MELTING HAIL
VR = 15 M./SEC.
VR = 30 M./SEC.
CANCELLATION RATIO (dB.)
RAIN INTENSITY (MM./HR.)
0.5
1
2
4
8
10
20
40
80
100
200
5
10
15
20
25
30

Fig. 6.3-1.

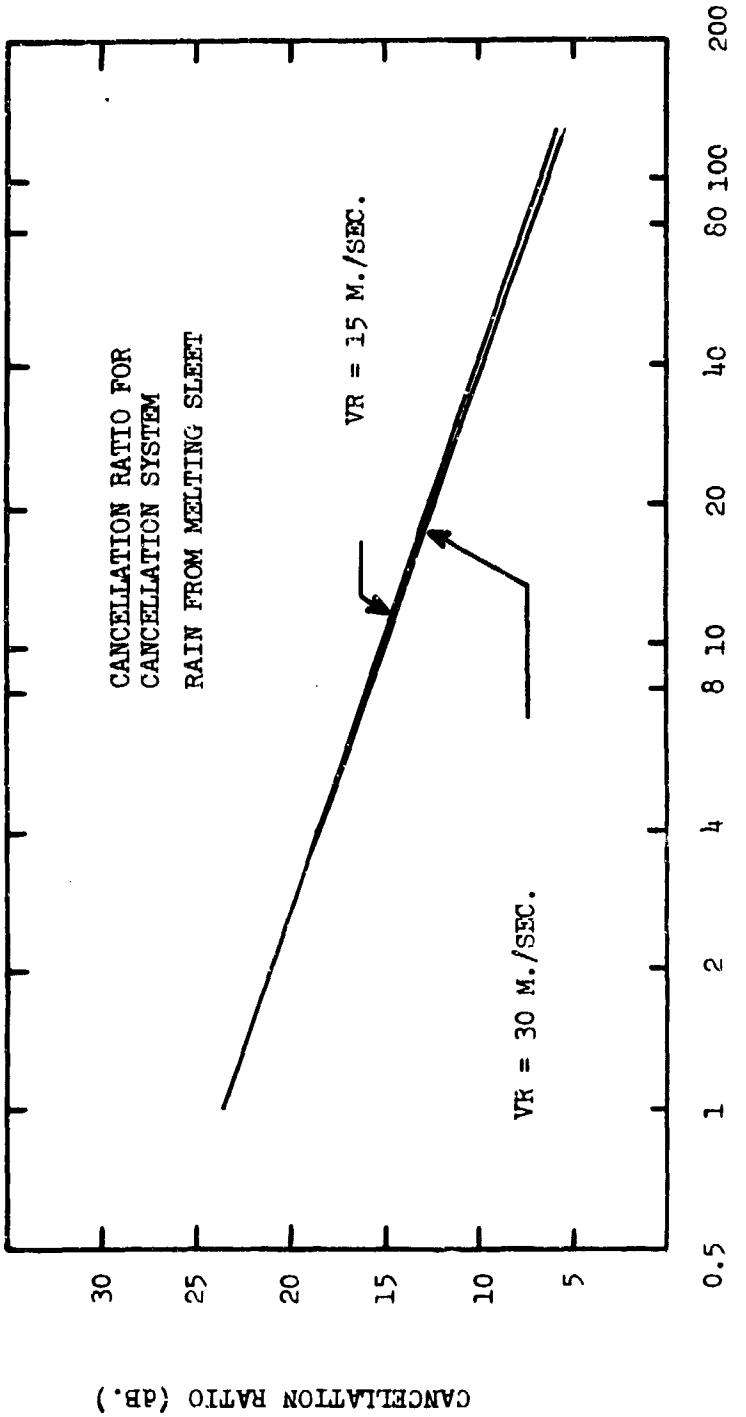
CANCELLATION RATIO FOR
CANCELLATION SYSTEM
RAIN FROM MELTING SLEET
VR = 15 M./SEC.
VR = 30 M./SEC.
CANCELLATION RATIO (dB.)
30
25
20
15
10
5
0.5
1
2
4
8 10
20
40
60 100
200
RAIN INTENSITY (MM./HR.)

Fig. 6.3-2.

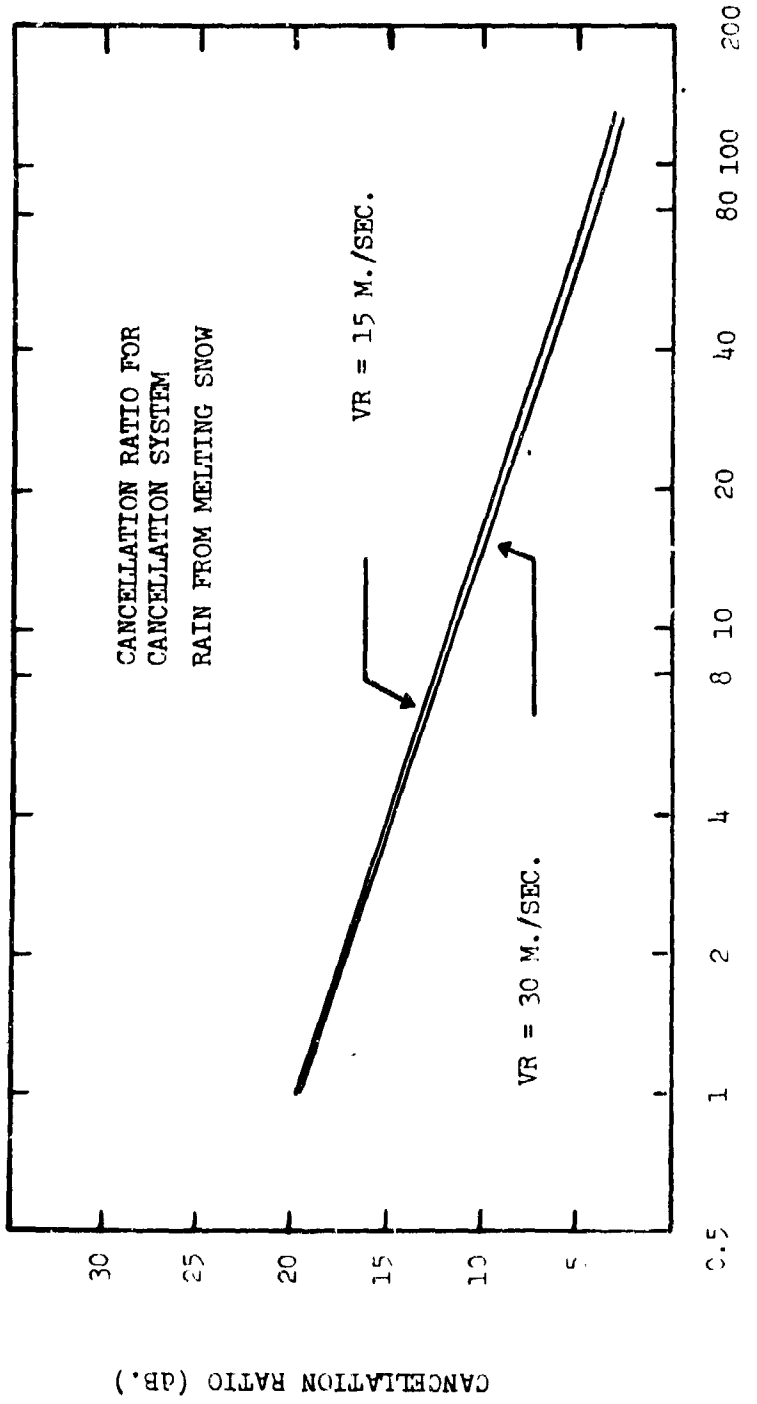
CANCELLATION RATIO FOR
CANCELLATION SYSTEM
RAIN FROM MELTING SNOW
VR = 15 M./SEC.
VR = 30 M./SEC.
CANCELLATION RATIO (dB.)
RAIN INTENSITY (MM./HR.)
30
25
20
15
10
0.5
1
2
4
8
10
20
40
80
100
200

Fig. 6.3-3.

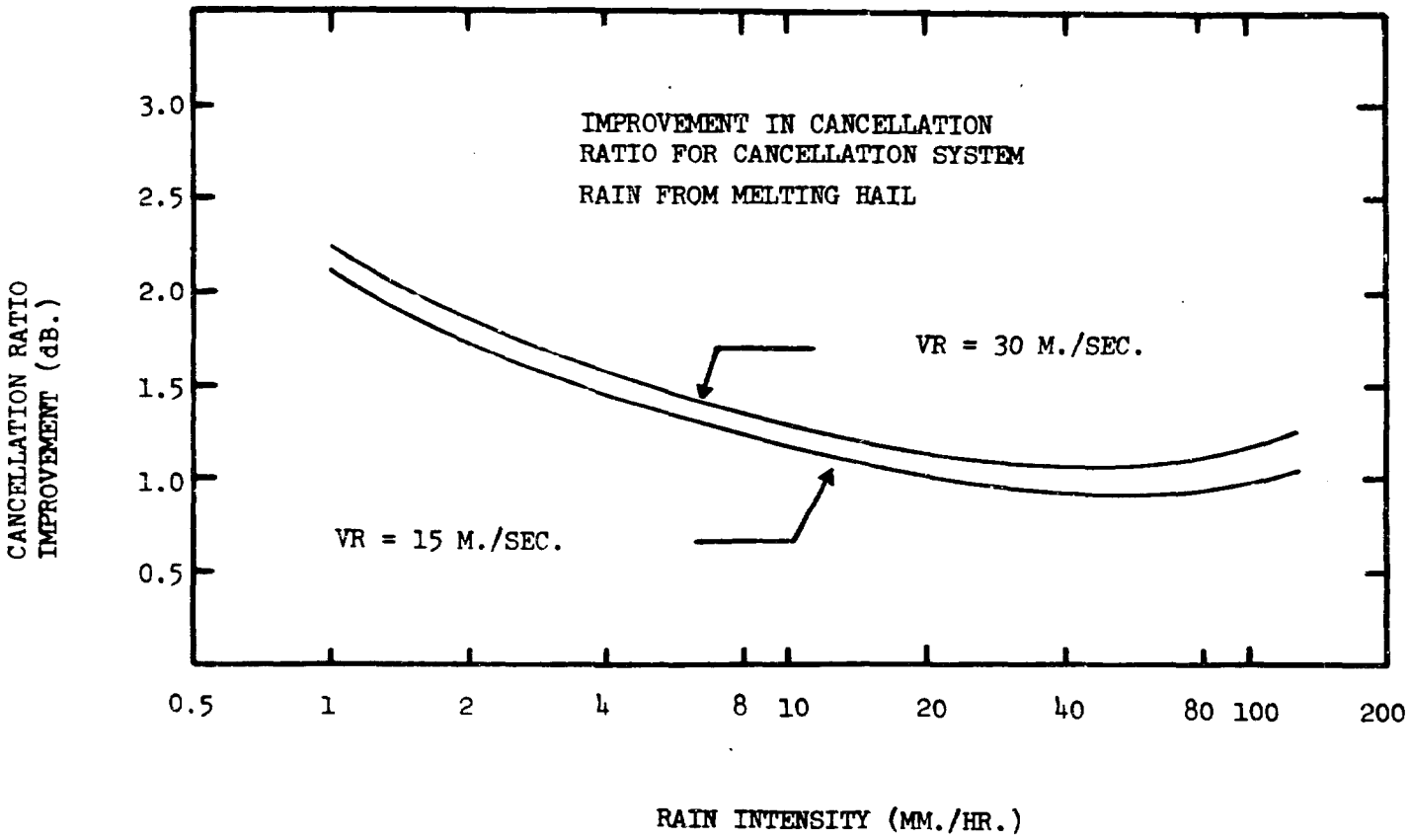

Fig. 6.3-4.
Lower Bound on Cancellation Improvement
Cancellation System vs. Ordinary C.P.System

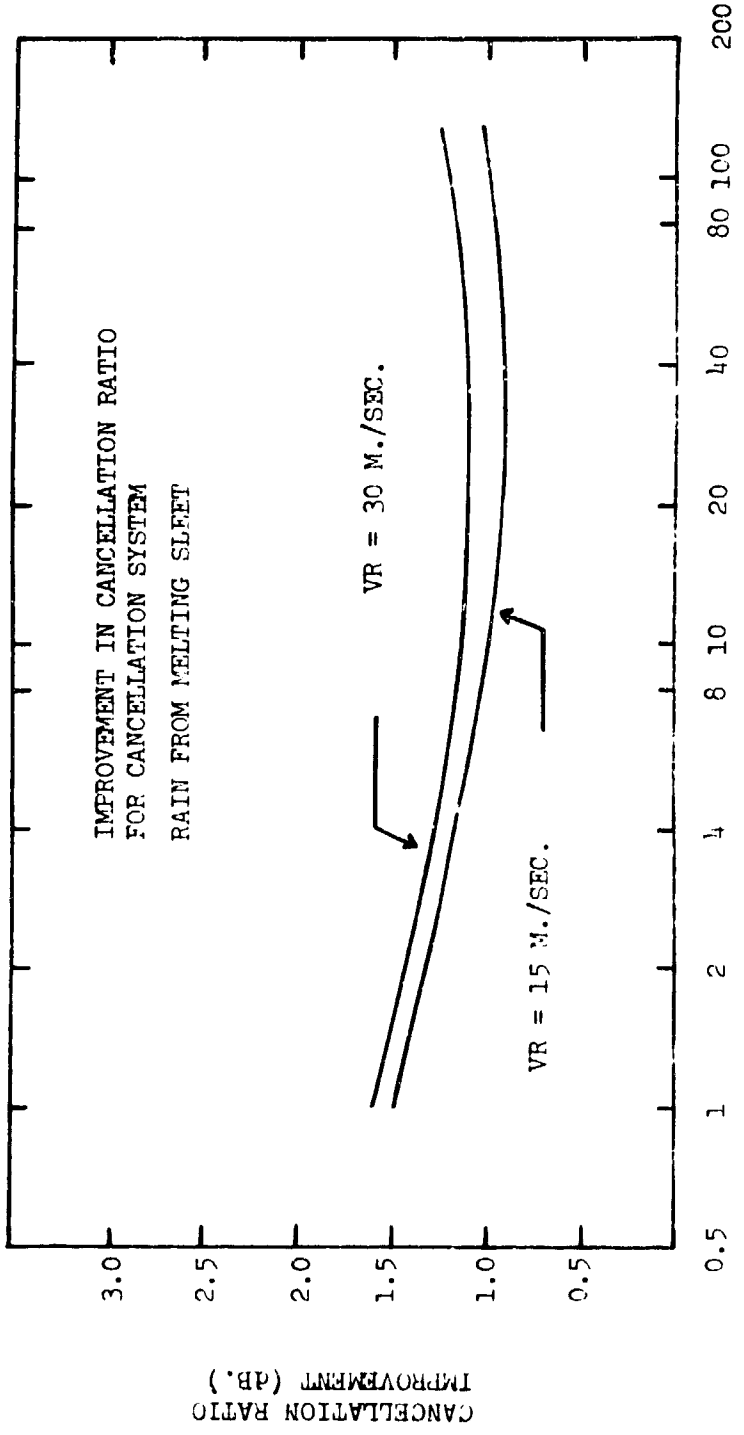

Fig. 6.3-5.
Lower Bound on Cancellation Improvement
Cancellation System vs. Ordinary C.P. System

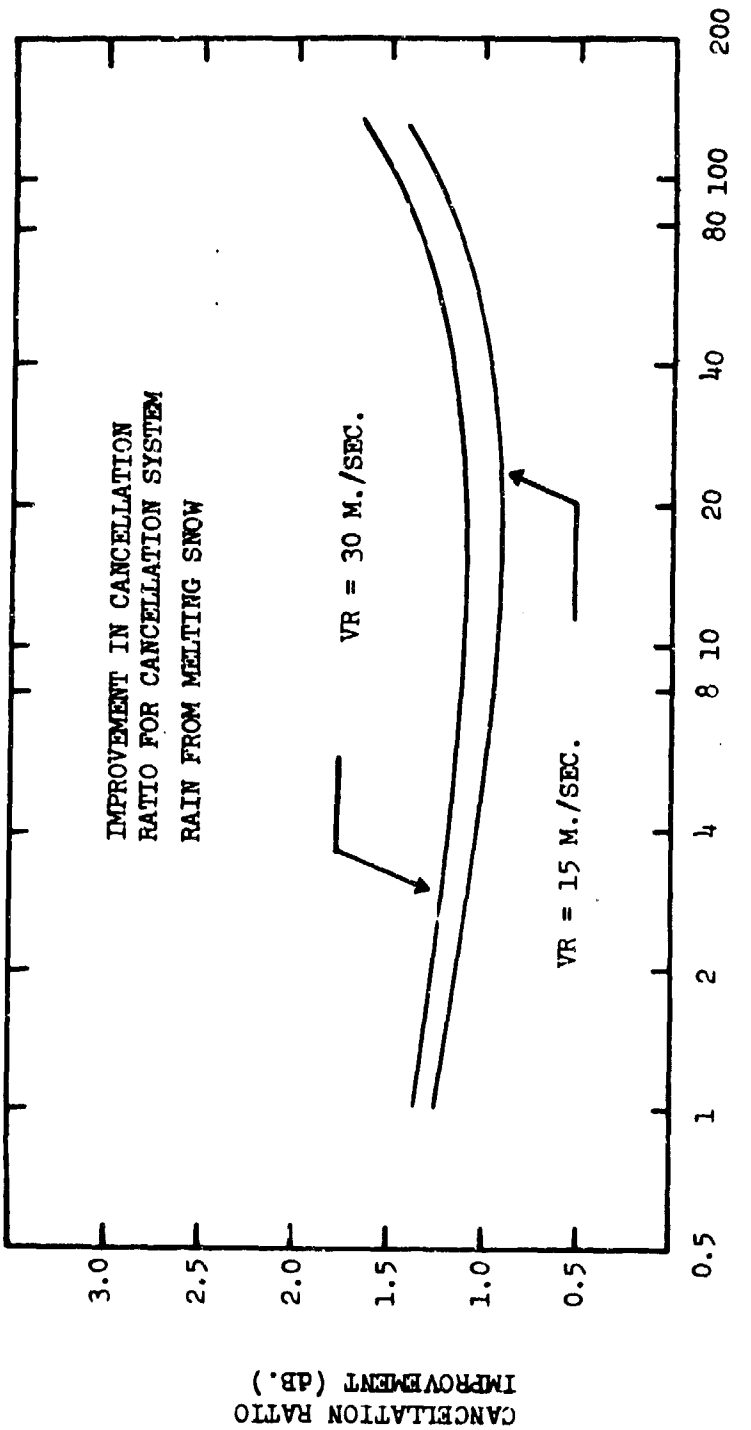

Fig. 6.3-6.
Lower Bound on Cancellation Improvement
Cancellation System vs. Ordinary C.P. System

The terms presented in equations (6.3-19), (6.3-21), and (6.3-22) may be reduced to simple algebraic expression by the techniques presented in appendix G, but no means has as yet been found that accomplishes the same reduction for the moments of $G'(k)$. Thus, the moments of $G'(k)$ have been evaluated by numerical integration techniques presented in appendix H.

When the numerical values of equations (6.3-19), (6.3-21), and (6.3-22) are combined with the evaluated moments of $G'(k)$ according to equation (6.2-19) the result is an expression for the output noise power of the cancellation system. The value for noise power thus obtained may be taken in ratio, according to equation (5.4-5), with the output power of the reference system to obtain the cancellation ratio. Note that the reference system output power is

$$E\{|e_r(k)_{REF}|^2\} = |A|^2 \, E\{N_k\} \, E\{G^4(\alpha,\beta)\} \, E\{S_{11}^2\} \quad . \tag{6.3-23}$$

Numerical data are presented in the following figures which describe the performance of the cancellation system relative to the reference system for various rain sources over a wide range of rain intensity.

6.4 Upper Bound on Performance

As indicated in chapter four, the conditions which lead to the upper bound of performance for the ordinary system are

$$\sin^2(\zeta) = 0 \quad , \tag{6.4-1}$$

$$\cos^2(\zeta) = 1 \quad , \tag{6.4-2}$$

$$\cos^2(\psi) = \left(\frac{V_\infty}{V_r}\right)^2 \quad , \text{ and} \tag{6.4-3}$$

$$\sin^2(\psi) = 1 - \left(\frac{V_\infty}{V_r}\right)^2 \quad . \tag{6.4-4}$$

The S matrix elements are defined to be

$$S_{11} = g_y \quad , \tag{6.4-5}$$

$$S_{12} = 0 \quad , \text{ and} \tag{6.4-6}$$

$$S_{22} = g_y + (g_x - g_y) \left(\frac{V_\infty}{V_r}\right)^2 \tag{6.4-7}$$

under these constraints. Evaluation of the cancellation system output equation is carried out in the same manner as was used in the analysis of the lower bound case with the exception that the above expressions for the S matrix elements are used rather than those given in section 6.3.

Numerical data in the form of the cancellation ratio is shown in the following figures. Again various rain sources are considered, and the variation in performance with rain intensity is also shown.

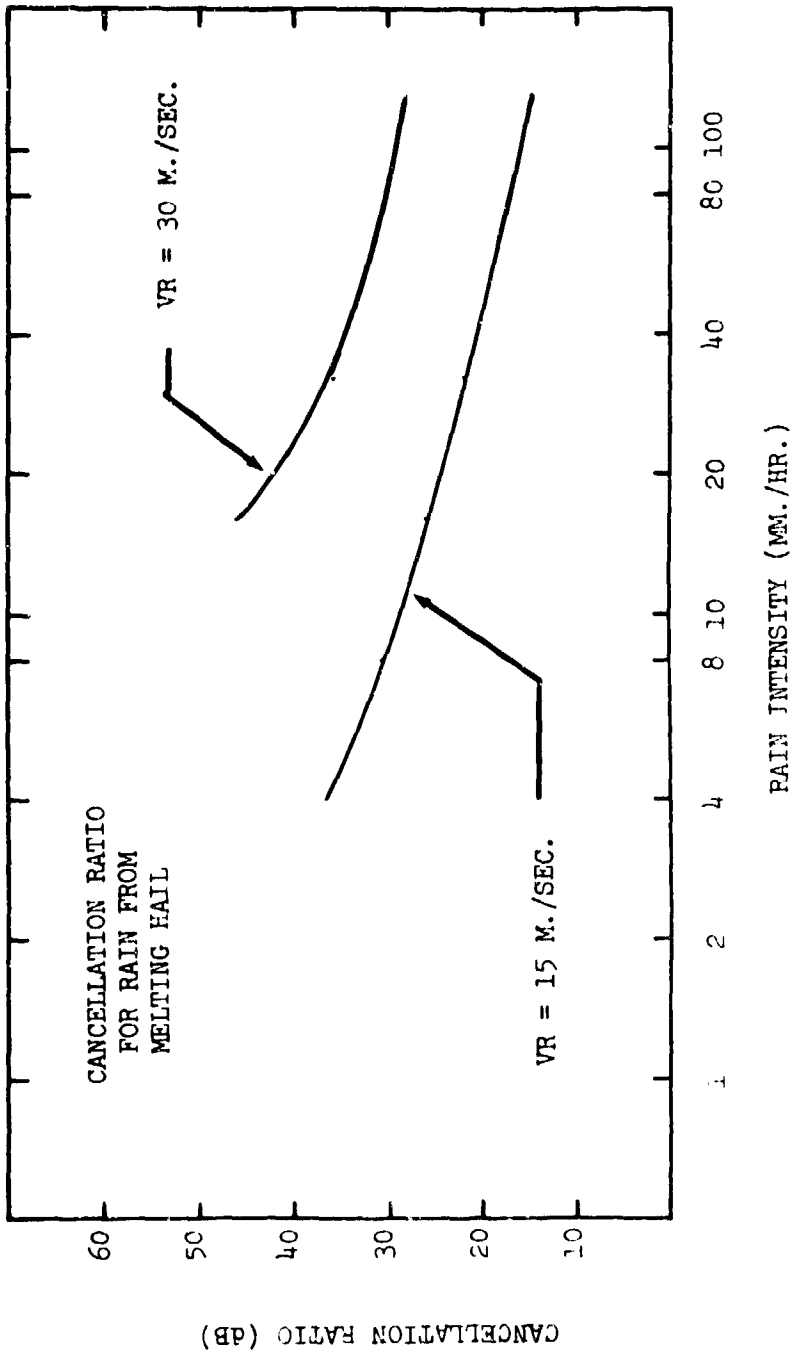

Fig. 6.4-1. Upper bound of cancellation.

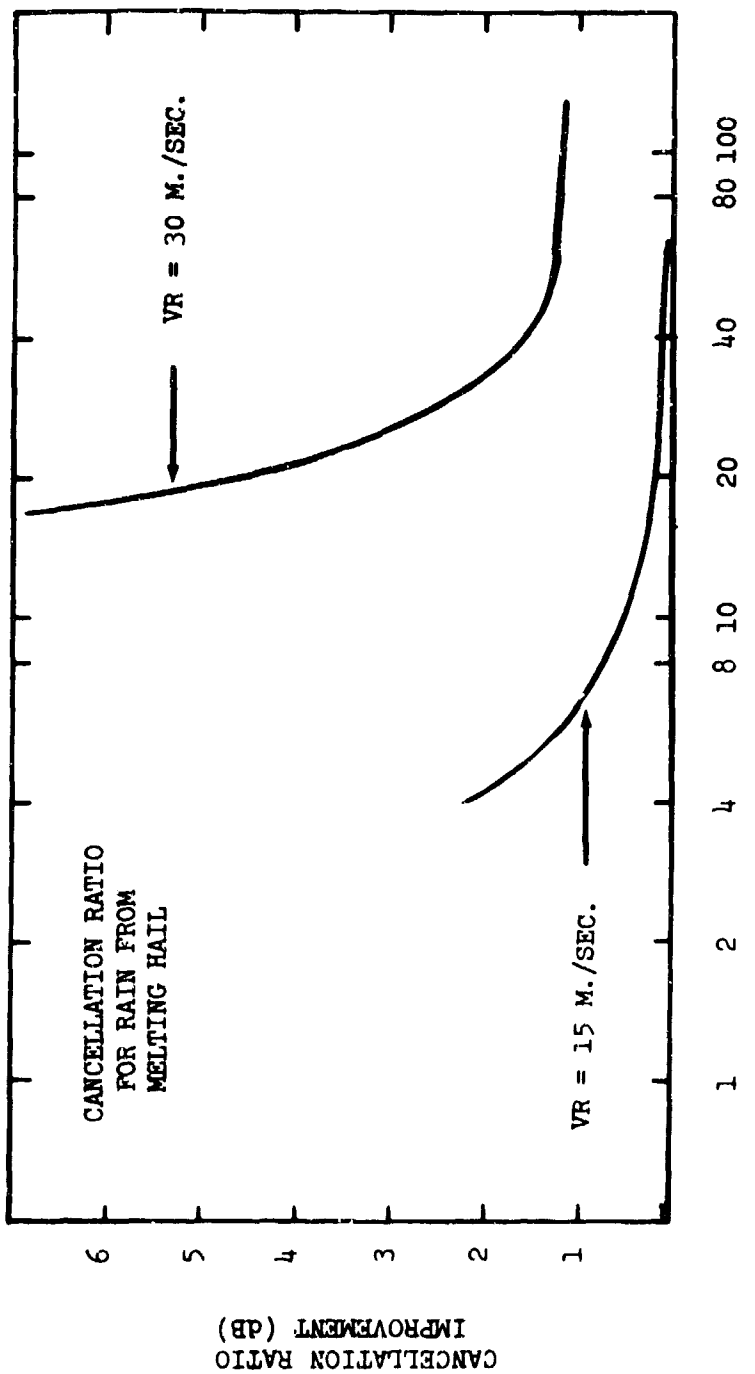

Fig. 6.4-2. Upper Bound on Cancellation Improvement
Cancellation System vs. Ordinary C.P.System

7.0 CONCLUSIONS

Based on the computer simulations and the rain model described in paragraph 6.1 of this report, rain cancellation improvement of 1 dB to over 8 dB can be achieved over that of circular polarization when a rain polarization estimater is used to determine the proper null polarization. These results are illustrated in Figures 6.3-4 through 6.3-6 and 6.4-2 and represent rain of certain origins.

A study of this type must be followed by an experimental program in order to subject the technique to real world environments.

REFERENCES

[1] Ridenour, L.N., Radar System Engineering, McGraw-Hill Book Co., 1947.

[2] White, W.D., Circular Polarization Cuts Rain Clutter, Electronics, vol. 27 (March, 1954), pp. 158-160.

[3] Hunter, I.M., Polarization of Radar Echos from Meteorological Precipitation, Nature, vol. 173 (1954), pp. 165-166.

[4] Pruppacher, H.R. and Beard, K.V., "A Wind Tunnel Investigation of the Internal Circulation and Shape of Water Drops Falling at Terminal Velocity in Air," Quart. J.R. Met. Soc., v. 96 (1970), pp.247-256.

[5] Pruppacher, H.R. and Pitter, R.L., A Semi-Empirical Determination of the Shape of Cloud and Rain Drops, J. of the Atmospheric Sciences, v. 28 (1971), pp. 86-94.

[6] Logan, N.A., Survey of Some Early Studies of the Scattering of Plane Waves by a Sphere, Proceedings of the IEEE, August, 1965, pp. 773-785.

[7] Corriher, H.A., Pyron, B.O., A Bibliography of Articles on Radar Reflectivity and Related Subjects: 1957-1964, Proceedings of the IEEE, August, 1965, pp. 1025-1058.

[8] Labrum, N.R., The Scattering of Radio Waves by Meteorological Particles, Jour. of Applied Physics, v. 23, No. 12 (Dec. 1952), pp. 1324-1330.

[9] Atlas, D., Kerker, M., and Hitschfeld, Scattering and Attenuation by Non-spherical Atmoshperic Particles, Journal of Atmospheric and Terrestial Physics, vol. 3 (1953), pp. 108-119.

[10] Stratton, J.A., Electromagnetic Thecry, McGraw-Hill Book Co., 1941.

[11] Rice, R.W., and Peebles, P.Z., Jr., Rain Clutter Cancellation Using a Polarization Technique, Proceedings of the 10th Annual IEEE Region 3 Convention, 1972, pp. G2-1-G2-4.

[12] Popović, B.D., Introductory Engineering Electromagnetics, Addison-Wesley Publishing Co., 1971.

[13] Koenig, R., Drop Freezing through Drop Breakup, J. of the Atmospheric Sciences, v. 22, pp. 448-451.

[14] Gunn, K.L.S. and East, T.W.R., The Microwave Properties of Precipitation Particles, Quarterly J. of the Royal Meteorological Soc., v. 80 (1954), pp. 522-545.

[15] Beard, K. and Pruppacher, H., A Determination of the Terminal Velocity and Drag of Small Water Drops by Means of a Wind Tunnel, J. Atmos. Sci., v. 26 (1969), pp. 1066-1072.

[16] Blanchard, D.C., The Behavior of Water Drops at Terminal Velocity in Air, Trans. Amer. Geophysical Union, v. 31, No. 6, (Dec. 1950), pp. 836-842.

[17] Savid, P., Circulation and Distortion of Liquid Drops Falling Through a Viscous Medium, Nati'l Res. Council, Canada, Rept. NCR-'TT-22.

[18] International Telephone and Telegraph, Reference Data for Radio Enigneers, Howard Sams, Inc., 1970 (Fifth Edition).

[19] Jahnke, E.and Emde, F., Tables of Functions with Formalae and Curves, Dover Publications, New York, 1945.

[20] Magono, C., "On the Shape of Water Drops Falling in Stagnant Air," J. of Atmospheric Science, v. 11 (1954), pp. 77-79.

[21] Laws, J.O. and Parsons, D.A., "The Relation of Raindrop-Size to Intensity," Trans. Amer. Geophys. Union, vol. 24, part II, 1943, pp. 452-460.

[22] Marshall, J.S. and Palmer, W. Mck., "The Distribution of Raindrops with size," Jour. of Meteorology, v. 5, 1948, pp. 165-166.

[23] Marshall, J.S., Langille, R.C. and Palmer, W. Mck., "Measurement of Rainfall by Radar," Jour. of Meteorology, v. 4, 1947, pp. 186-192.

[24] Blanchard, D.C., "Raindrop Size-Distribution in Hawaiian Rins," Jour. of Meteorology, vol. 10, December, 1953, pp. 457-473.

[25] Mason, B.J. and Ramanadham, R., "Modification of the Size Distribution of Falling Raindrops by Coalescence," Quart. Jour. Royal Meteorological Soc., v. 80, 1954, pp. 388-394.

[26] Ramana Murty, Bh.V., and Gupta, S.C., "Precipitation Characteristics Based on Raindrop Size Measurements at Delhi and Khandala During South-west Monsoon," Jour. Scientific and Industr. Research, vol. 18A, 1959, pp. 352-371.

[27] Fujiwara, M., "Raindrop Size Distributions with Rainfall Types and Weather Conditions," Research Report No. 8, Illinois State Water Survey Meteorology Lab., Univ. of Ill., Urbana, Ill., 1961.

[28] Fujiwara, M., "Raindrop-size Distribution from Individual Storms," Jour. of the Atmospheric Sciences, vol. 22, Sept., 1965, pp. 585-591.

[29] Sivaramakrishran, M.V., "Studies of Raindrop Size Characteristics in Different Types of Tropical Rain Using a Simple Raindrop Recorder," Indian Jour. of Meteorology and Geophysics, vol. 12, 1961, pp. 189-216.

[30] Hardy, K.R., "The Development of Raindrop-size Distributions and Implications Related to the Physics of Precipitation," Jour. of the Atmospheric Sciences, vol. 20, July, 1963, pp. 299-312.

[31] Dingle, A.N., "Raindrop-Size Studies," Final report by College of Engineering, the Univ. of Michigan, on Contract No. AF 19(628)-281, Project 8620, Task 862002, October, 1963. Also Def. Doc. Cent. No. AD 426171.

[32] Caton, P.G.F., "A Study of Raindrop-size Distributions in the Tree Atmosphere," Quart. Jour. of the Royal Meteorological Soc., vol. 92, 1966, pp. 15-30.

[33] Blanchard, D.C. and Spencer, A.T., "Experiments on the Generation of Raindrop-size Distributions by Drop Breakup," Jour. of the Atmospheric Sciences, vol. 27, January, 1970, pp. 101-108.

[34] Mueller, E.A. and Sims, A.L., "investigation of the Quantitative Determination of Point and Areal Precipitation by Radar Echo Measurements," Tech. Rept. ECOM-00032-F, Ill. State Water Survey, Contract DA-28-043AMC-00032(E), 1966. Much of the report also appears in "Rada Cross Sections from Drop Size Spectra," Ph.D. Diss. of E.A. Mueller, 1966, the Univ. of Ill.

[35] Hudson, N.W., "Raindrop Size Distribution in High Intensity Storms," Rhodesian Jour. Agric. Res., vol. 1, 1963, pp. 299-312.

[36] Dyer, R., Sect. 5.2 of "Precipitation and Clouds," a revision of Ch. 5, Handbook of Geophysics and Space Environments, A.E. Cole, R.J. Donaldson, R. Dyer, A.J. Kantor and R.A. Skrivanek, AFCRL-69-0487, Nov. 1969, Air Force Surveys in Geophysics, No. 212 (Also AD 703288).

[37] Best, A.C., "The Size Distribution of Raindrops," Quart. Jour. Roy. Met. Soc., vol. 76, 1950, pp. 16-36.

[38] Litvinov, I.V., "On the Distribution Function of Particles of Rainfall," Izvestia AN SSSR, Geophysical Series, No. 5, 1956.

[39] Litvinov, I.V., "On the Distribution Function of Particles of Rainfall," Izvestia AN SSSR, Geophysical Series, No. 6., 1957, pp. 838-839.

[40] Litvinov, I.V., "Size Distribution of Raindrops from Melting Hail," Ivestia Geophys. Ser. 1958, pp. 903-912.

[41] Krasywk, N.P., Rozenberg, V.I. and Chistyakov, D.A., "Attenuation and Scattering of Radar Signals by Rains with Shifrin and Marshall-Palmer Drop Size Distributions," Trans. Russian Jour., Radio Engineering and Electronic Physics, vol. 13, No. 10, 1968, pp. 1638-1640.

[42] Levine, L.M., "On the Size Distribution Function of Cloud and Shower Drops," Proc. (Dokl.) Acad. Sci. USSR, v. 94, No. 6, 1954.

[43] Hayt, W.H., and Kemmerly, J.E., Engineering Circuit Analysis, McGraw-Hill Book Co., 1962.

[44] Taub, H., and Shilling, D.L., Principles of Communication Systems, McGraw-Hill Book Co., 1971.

[45] Thomas, J.B., An Introduction to Statistical Communication Theory, John Wiley and Sons, Inc., 1969.

[46] Beckmann, P., Probability in Communication Enigneering, Harcourt, Brace & World, 1967.

[47] Mathews, J., and Walker, R.L., Mathematical Methods of Physics, W.A. Benjamin & Co., 1970.

[48] Weeg, G.P., and Reed, G.B., Introduction to Numerical Integration, Blaisdell Publishing Co., 1966.

[49] Wilks, S.S., Mathematical Statistics, John Wiley & Sons, Inc., 1962.

[50] Kreyszig, E., Advanced Engineering Mathematics, John Wiley & Sons, Inc., 1967.

[51] Davis, P.J., and Rabinowitz, P., Numerical Integration, Blaisdell Publishing Co., 1967.

APPENDIX A: ANALYSIS OF MOMENTS FOR RANDOM SUMS

Asssume that it is desired to find the statistical moments of the random quantity

$$X = \sum_{i=1}^{n} U_i \tag{A-1}$$

where n and U_i are both random in nature. Beckmann [46] has shown that the density function for the variable X is

$$f(x) = \sum_{n=0}^{\infty} P(n)\ p(X^{(n)}) \tag{A-2}$$

where P(n) is the discrete density function of n and $p(X^{(n)})$ is the conditional density function of X given a specific value of n.

The mean value of X is calculated as follows.

$$E\{X\} = \int_{-\infty}^{\infty} x\ f(x)\ dx \tag{A-3}$$

$$= \int_{-\infty}^{\infty} x \sum_{n=0}^{\infty} P(n)\ p(X^{(n)})\ dx \tag{A-4}$$

$$= \sum_{n=0}^{\infty} P(n) \int_{-\infty}^{\infty} X^{(n)}\ p(X^{(n)})\ dx^{(n)} \tag{A-5}$$

If $X^{(n)}$ is Gaussian then

$$p(X^{(n)}) = \frac{1}{\sigma\sqrt{2\pi n}} \exp\left[\frac{-(X^{(n)} - na)^2}{2n\sigma^2}\right] \tag{A-6}$$

where $a = E\{U_i\}$ (A-7)

and $\sigma^2 = E\{(U_i - a)^2\}$ (A-8)

Returning to the mean value calculation,

$$E\{x\} = \sum_{n=0}^{\infty} P(n) \cdot n \cdot E\{U_i\} \tag{A-9}$$

$$= E\{U_i\} \cdot E\{n\} \tag{A-10}$$

The mean squared value of x is

$$E\{x^2\} = \int_{-\infty}^{\infty} x^2 f(x)\, dx \tag{A-11}$$

$$= \int_{\infty}^{\infty} x^2 \sum_{n=0}^{\infty} P(n)\, p(x^{(n)})\, dx \tag{A-12}$$

$$= \sum_{n=0}^{\infty} P(n) \int_{-\infty}^{\infty} x^{(n)^2}\, p(x^{(n)})\, dx^{(n)} \tag{A-13}$$

Again, if $x^{(n)}$ is Gaussian then

$$E\{x^2\} = \sum_{n=0}^{\infty} P(n) \cdot n\sigma^2 \tag{A-14}$$

$$= E\{n\} \cdot \sigma^2 \tag{A-15}$$

The foregoing analysis may be applied to the evaluation of moments of $x_1(k)$, $x_2(k)$, $y_1(k)$, and $y_2(k)$. All four quantities are the result of a summation of random terms, and the number of terms in the summation is also

random. Beckmann [46] observes that terms having the form exhibited by $x_1(k)$, $y_1(k)$, $x_2(k)$, and $y_2(k)$ tend to be Gaussian in nature if the number of terms in the appropriate summations is large. The number of terms in the summations corresponds to the number of rain particles in a range cell, and the material of Chapter 3 indicates that the number of particles in a range cell is generally very large. Thus, the density function for $x_1(k)$ is

$$p(x_1^{(n)}(k)) = \frac{1}{\sigma\sqrt{2\pi n}} \exp \frac{-(x_1^{(n)}(k) - na)^2}{2n\sigma^2} \tag{A-16}$$

where

$$a = E\left\{G^2(\alpha_i, \beta_i)\alpha_{1i}(k) \cos(\gamma_{1i}(k) - \theta_i)\right\} \tag{A-17}$$

$$= E\left\{G^2(\alpha_i, \beta_i)\alpha_{1i}(k) \cos(\gamma_{1i}(k))\cos(\theta_i)\right\}$$

$$+ E\left\{G^2(\alpha_i, \beta_i)\alpha_{1i}(k) \sin(\gamma_{1i}(k))\sin(\theta_i)\right\} \tag{A-18}$$

and

$$\sigma^2 = E\{(U_i - a)^2\} \tag{A-19}$$

The condition of uniform particle distribution means that θ_i, as defined in equation (5.2-6), is uniformly distributed between the symmetric extremes $+\theta_M$ and $-\theta_M$ where

$$\theta_M = 2\beta_0 \Delta z_M \, . \tag{A-20}$$

Thus, the density function for θ_i is

$$p(\theta_i) = \frac{1}{2\theta_M} \, . \tag{A-21}$$

If

$$\theta_M = \pm m\pi \ , \ m = 1, 2, 3, \ldots \tag{A-22}$$

then a in equation (A-17) equals zero, but another statement of the condition given in equation (A-22) is

$$2\,\Delta z_M = \frac{ct_p}{2} = \frac{\vartheta_M}{\beta_0} \tag{A-23}$$

where tp is the transmitter pulse length and c is the speed of light. Equation (A-23) may be rearranged to obtain

$$t_p = \pm m/f_0 \tag{A-24}$$

where f_0 is the carrier frequency of the transmitter. In the following work it will be assumed that the condition of equation (A-24) is satisfied.

Application of conditions one and two as stated in section 6.1 to equation (A-18) and (A-19) gives the following.

$$a = E\{G^2(\alpha, \beta)\alpha_1 \cos\gamma\}\, E\{\cos\theta\}$$

$$+ E\{G^2(\alpha, \beta)\alpha_1 \sin\gamma\}\, E\{\sin\theta\} \ . \tag{A-25}$$

$$= 0 \tag{A-26}$$

$$\sigma^2 = E\{U_i^2\} \tag{A-27}$$

$$= E\{G^4(\alpha, \beta)\alpha_1^2 \cos^2(\gamma_1 - \theta)\} \tag{A-28}$$

$$= (\tfrac{1}{2})[E\{G^4(\alpha, \beta)\alpha_1^2\}$$

$$+ E\{G^4(\alpha, \beta)\alpha_1^2 \cos(2\gamma_1 - 2\theta)\}] \tag{A-29}$$

$$= (\tfrac{1}{2})E\{G^4(\alpha, \beta)\}\, E\{\alpha_1^2\} \tag{A-30}$$

Thus, from equations (A-10) and (A-15)

$$E\{x_1(k)\} = 0 \tag{A-31}$$

$$E\{x_1^2(k)\} = E\{N_k\}\ E\{\frac{G^4(\alpha, \beta)}{2}\}\ \ E\{\alpha_1^2\} \tag{A-32}$$

The moments for $x_2(k)$, $y_1(k)$, and $y_2(k)$ are evaluated in a manner similar to that used above for $x_1(k)$, and the results are presented below.

$$E\{x_2(k)\} = 0 \tag{A-33}$$

$$E\{x_2^2(k)\} = E\{N_k\}\ E\{\frac{G^4(\alpha, \beta)}{2}\}\ \ E\{\alpha_2^2\} \tag{A-34}$$

$$E\{y_1(k)\} = 0 \tag{A-35}$$

$$E\{y_1^2(k)\} = E\{N_k\}\ E\{\frac{G^4(\alpha, \beta)}{2}\}\ E\{\alpha_1^2\} \tag{A-36}$$

$$E\{y_2(k)\} = 0 \tag{A-37}$$

$$E\{y_2^2(k)\} = E\{N_k\}\ E\{\frac{G^4(\alpha, \beta)}{2}\}\ \ E\{\alpha_2^2\} \tag{A-38}$$

APPENDIX B: THE MEAN VALUE OF N_k

The material in Chapter 3 indicates that the volumetric particle density is of the form

$$PD = K_1 I^{K_2} \tag{B-1}$$

where I is the rain intensity, and K_1 and K_2 are constants determined by the type of rain. Additionally, I may be represented as

$$I = I_0 + \delta I \tag{B-2}$$

where I_0 is the mean value of the rain intensity, and δI is the random component of the rain intensity.

Calculation of the total number of particles is accomplished by forming a product of the cell volume, V_k, and the particle density, PD.

$$N_k = PD \cdot V_k \tag{B-3}$$

$$= K_1 (I_0 + \delta I)^{K_2} V_k \tag{B-4}$$

$$= K_1 V_k I_0^{K_2} \left[1 + \left(\frac{\delta I}{I_0}\right)\right]^{K_2} \tag{B-5}$$

It will be assumed that δI is a zero mean Gaussian variate and that most of the time

$$\left(\frac{\delta I}{I_0}\right) << 1. \tag{B-6}$$

Thus

$$N_k \simeq K_1 V_k I_0^{K_2} \left[1 + \frac{K_2 \delta I}{I_0}\right], \text{ and} \tag{B-7}$$

$$E\{N_k\} = K_1 V_k I_0^{K_2} \tag{B-8}$$

The values of K_1 and K_2 are provided in Table B.1.

Table B.1. Parameters K_1 and K for several rain sources.

SOURCE OF RAIN	K_1	K_2
MELTING HAIL	384	0.31
MELTING SLEET	203	0.31
MELTING SNOW	87.5	0.39

APPENDIX C: EVALUATION OF THE FOURTH MOMENT OF THE RADIATION CHARACTERISTIC

The radiation characteristic assumed for this work is in any plane passing through the axis of propagation

$$G(\chi,\Omega) = \frac{2J_1(\chi)}{\chi} \qquad ,0 \leq \chi \leq \chi_u = 3.83 \ (18) \tag{C-1}$$

where $J_1(\chi)$ is the Bessel function of the first kind and first order, and where χ and Ω are defined in FIG. C-1. It is assumed that the particle position parameters, χ and Ω, are statistically independent of one another and that the distributions of these variables are uniform.

$$p(\chi,\Omega) = \frac{1}{2\pi\chi_u} \tag{C-2}$$

The fourth moment of $G(\chi,\Omega)$ which is required for the analysis in chapter 5 is of the form

$$E\{G^4(\chi,\Omega)\} = \int_0^{\chi_u} \int_0^{2\pi} \left[\frac{2J_1(\chi)}{\chi}\right] \left[\frac{1}{2\pi\chi_u}\right] d\Omega \, d\chi \tag{C-3}$$

$$= \int_0^{\chi_u} \frac{16J_1^4(\chi)}{\chi^4} \left[\frac{1}{\chi_u}\right] d\chi \tag{C-4}$$

$$= \frac{16}{\chi_u} \int_0^{\chi_u} \frac{J_1^4(\chi)}{\chi^4} \, d\chi \tag{C-5}$$

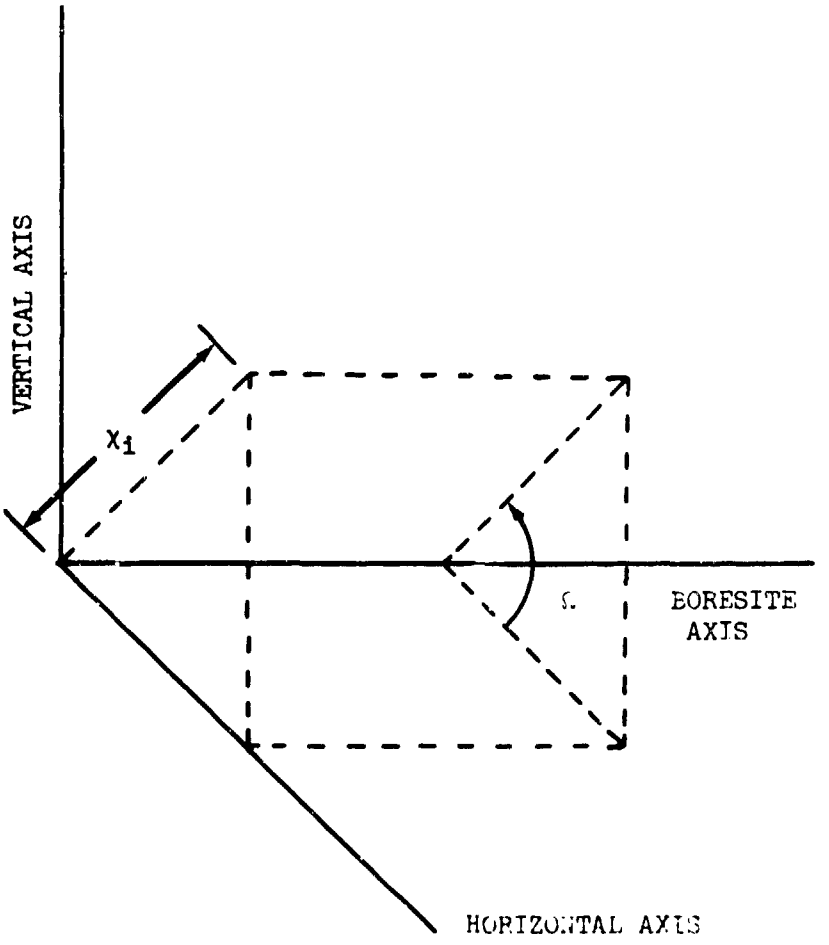

Fig. C-1. Definition of antenna pattern parameters.

Attempts at evaluating equation (C-5) analytically in closed form have thus far been unproductive, and therefore, an evaluation was affected by means of numerical integration. The numerical method used was a Newton-Cotes five point formula as suggested by Weeg and Reed [48] with an increment in the independent variable, χ, of 0.01.

$$E\{G^4(\chi,\Omega)\} = 0.70808 \qquad (C-7)$$

APPENDIX D: STATISTICAL CONSIDERATIONS OF A PRODUCT

It is assumed that several random processes exist and may be divided into two groups, x and y, such that the members of the groups exhibit the characteristics that x_i and x_j are statistically independent if $i \neq j$, that y_i and y_j are statistically independent if $i \neq j$, and that x_i and y_j are statistically independent if $i \neq j$. Under the stated conditions, one may represent the joint density function of elements of the two sets as follows by application of the concept of conditional probability.

$$p(x_1, \ldots, x_n, y_1, \ldots y_n) =$$

$$p(x_1,y_1)p(x_2, \ldots x_n, y_2, \ldots y_n \,|x_1, y_1) \tag{D-1}$$

The assumed independence requires that the individual or joint outcomes of x_1 and y_1 in no way influence the realizations observed for the other x and y elements. Thus

$$p(x_2, \ldots, x_n, y_2, \ldots, y_n \,|x_1, y_1) =$$

$$p(x_2, \ldots, x_n, y_2, \ldots y_n), \text{ and} \tag{D-2}$$

$$p(x_1, \ldots, x_n, y_1, \ldots, y_n) =$$

$$p(x_1, y_1)p(x_2, \ldots, x_n, y_2, \ldots, y_n). \tag{D-3}$$

Let a function f exist such that

$$f = x_1 \cdot y_1 \cdot g \quad \text{where} \tag{D-4}$$

$$g = g(x_2, \ldots, x_n, y_2, \ldots, y_n). \tag{D-5}$$

Then

$$E\{f\} = \int_{2n} \ldots \int x_1 y_1 g(x_2, \ldots, y_n) p(x_1, x_2).$$

$$p(x_2, \ldots, y_n) dx_1 \ldots dy_n \tag{D-6}$$

$$= \int_{2(n-1)} \cdots \int g(x_2, \ldots, y_n) p(x_2, \ldots, y_n) dx_2 \ldots dx_n dy_2 \ldots dy_n$$

$$\cdot \iint x_1 y_1 \, p(x_1, y_1) dx_1 dy_1 \qquad \text{(D-7)}$$

$$= E\{g\} \cdot E\{x_1 y_1\} \qquad \text{(D-8)}$$

APPENDIX E: THE CROSS CORRELATION OF $X_1(k)$, $X_2(k)$, $Y_1(k)$, AND $Y_2(k)$.

The cross correlation of the four parameters $x_1(k)$, $x_2(k)$, $y_1(k)$, and $Y_2(k)$ is full described by the six quantities $E\{X_1(k)\ T_1(k)\}$, $E\{x_2(k)\ Y_2(k)\}$, $E\{x_1(k)\ x_2(1)\}$, $E\{Y_1(k)\ Y_2(k)\}$, $E\{x_1(k)\ Y_2(k)\}$, and $E\{x_2(k)\ Y_1(k)\}$. These quantities will be evaluated in the stated order, and it should be noted that all conditions imposed or assumed in section 6.1 are applied to the following calculations.

$$x_1(k)y_1(k) = \sum_{i=1}^{N_k} G^2(\alpha_i, \beta_i)\ \alpha_{1i}(k)\ \cos\left(\gamma_{1i}(k) - \theta_i\right)$$

$$\cdot \sum_{i=1}^{N_k} G^2(\alpha_i, \beta_i)\ \alpha_{1i}(k)\ \sin\left(\gamma_{1i}(k) - \theta_i\right) \qquad \text{(E-1)}$$

$$= \sum_{i=1}^{N_k} G^4(\alpha_i, \beta_i)\ \alpha_{1i}^2(k)\ \sin\left(\gamma_{1i}(k) - \theta_i\right)\cos\left(\gamma_{1i}(k) - \theta_i\right)$$

$$+ \sum_{\substack{i=1 \\ i\neq\ell}}^{N_k} \sum_{\ell=1}^{N_k} G^2(\alpha_i, \beta_i)\ G^2(\alpha_\ell, \beta_\ell)\alpha_{1i}(k)\alpha_{1\ell}(k)\ \cos\left(\gamma_{1i}(k) - \theta_i\right)$$

$$\cdot \sin\left(\gamma_{1\ell}(k) - \theta_\ell\right) \qquad \text{(E-2)}$$

$$E\{X_1(k)y_1(k)\} = E\{N_k\}\ E\{G^4(\alpha,\beta)\}\ \left[E\left\{\frac{\alpha_1^2}{2}\sin 2\gamma_1\right\}\ \cdot E\{\cos 2\theta\}\right.$$

$$\left. + E\left\{\frac{\alpha_1^2}{2}\cos 2\gamma_1\right\}\ \cdot E\{\sin 2\theta\}\right] \qquad \text{(F-3)}$$

$$= 0 \qquad \text{(F-4)}$$

$$x_2(k)Y_2(k) = \sum_{i=1}^{N_k} G^2(\alpha_i,\beta_i)\alpha_{2i}(k)\cos\left(\gamma_{2i}(k) - \theta_i\right)$$

$$\cdot \sum_{i=1}^{N_k} G^2(\alpha_i,\beta_i)\alpha_{2i}(k)\sin\left(\gamma_{2i}(k) - \theta_i\right) \qquad \text{(E-5)}$$

$$= \sum_{i=1}^{N_k} G^4(\alpha_i,\beta_i)\alpha_{2i}^2(k)\cos\left(\gamma_{2i}(k) - \theta_i\right)\sin\left(\gamma_{2i}(k) - \theta_i\right) +$$

$$\sum_{i=1}^{N_k}\sum_{\substack{\ell=1 \\ \ell\neq i}}^{N_k} G^2(\alpha_i,\beta_i)G^2(\alpha_\ell,\beta_\ell)\gamma_{2i}(k)\alpha_{2\ell}(k)\cos\left(\gamma_{2i}(k)-\theta_i\right)\sin\left(\gamma_{2\ell}(k)-\theta_\ell\right) \qquad \text{(E-6)}$$

$$E\{x_2(k)Y_2(k)\} = E\{N_k\}\, E\{G^4(\alpha,\beta)\}\left[E\left\{\frac{\alpha_2^2}{2}\sin 2\gamma_2\right\} \cdot E\{\cos 2\theta\}\right.$$

$$\left. + E\left\{\frac{\alpha_2^2}{2}\cos 2\gamma_2\right\} \cdot E\{\sin 2\theta\}\right] \qquad \text{(E-7)}$$

$$= 0 \qquad \text{(E-8)}$$

$$X_1(k)X_2(k) = \sum_{i=1}^{N_k} G^2(\alpha_i,\beta_i)\alpha_{1i}(k)\cos\left(\gamma_{1i}(k) - \theta_i\right)$$

$$\sum_{i=1}^{N_k} G^2(\alpha_i,\beta_i)\alpha_{2i}(k)\cos\left(\gamma_{2i}(k)-\theta_i\right) \qquad \text{(E-9)}$$

$$= \sum_{i=1}^{N_k} G^4(\alpha_i,\beta_i)\frac{\alpha_{1i}(k)\alpha_{2i}(k)}{2}\left[\cos\left(\gamma_{1i}(k)+\gamma_{2i}(k)-2\theta_i\right)\right.$$

$$+ \cos\left(\gamma_{1i}(k) - \gamma_{2i}(k)\right)\Big] +$$

$$\sum_{i=1}^{N_k} \sum_{\substack{\ell=1 \\ i\neq\ell}}^{N_k} G^2(\alpha_i,\beta_i)G^2(\alpha_\ell,\beta_\ell)\alpha_{1i}(k)\alpha_{2\ell}(k)\cos\left(\gamma_{\ell}(k)-\theta_\ell\right)\cos\left(\gamma_{2\ell}(k)-\theta_\ell\right) \qquad \text{(E-10)}$$

$$E\{x_1(k)x_2(k)\} = E\{N_k\}\, E\{G^4(\alpha,\beta)\} \left[E\left\{\frac{\alpha_1\alpha_2}{2}\cos(\gamma_1+\gamma_2)\right\} E\{\cos 2\theta\}\right.$$

$$\left. + E\left\{\frac{\alpha_1\alpha_2}{2}\sin(\gamma_1+\gamma_2)\right\} E\{\sin 2\theta\} + E\left\{\frac{\alpha_1\alpha_2}{2}\cos(\gamma_1-\gamma_2)\right\}\right] \qquad \text{(E-11)}$$

$$= E\{N_k\}\, E\{G^4(\alpha,\beta)\}\, E\left\{\frac{\alpha_1\alpha_2}{2}\cos(\gamma_1-\gamma_2)\right\} \qquad \text{(E-12)}$$

The following expressions, obtained from equations (6.2-4) and (6.2-5), may be applied to equation (E-12).

$$\cos\gamma_1 = \frac{S_{11} \pm S_{12}\,\mathrm{Im}(T)}{\alpha_1} \qquad \text{(E-13)}$$

$$\sin\gamma_1 = \frac{\pm S_{12}\,R_e(T)}{\alpha_1} \qquad \text{(E-14)}$$

$$\cos\gamma_2 = \frac{S_{21} \pm S_{22}\,\mathrm{Im}(T)}{\alpha_2} \qquad \text{(E-15)}$$

$$\sin\gamma_2 = \frac{\pm S_{22}R_e(T)}{\alpha_2} \qquad \text{(E-16)}$$

Thus equation (E-12) may be rewritten as

$$E\{x_1(k)x_2(k)\} = E\{N_k\}\, E\{G^4(\alpha,\beta)\} \left[E\left\{\frac{\alpha_1\alpha_2}{2}\cos\gamma_1\cos\gamma_2\right\}\right.$$

$$\left. + E\left\{\frac{\alpha_1\alpha_2}{2}\sin\gamma_1\sin\gamma_2\right\}\right. \qquad \text{(E-17)}$$

$$= E\{N_k\}\, E\{G^4(\alpha,\beta)\} \left[\left(\frac{1}{2}\right) E\left\{\left(S_{11} \pm S_{12}\mathrm{Im}(T)\right)\left(S_{21} \pm S_{22}\mathrm{Im}(T)\right)\right.\right.$$

$$\left.\left. + S_{12}S_{22}R_e^2(T)\right\}\right] \quad . \tag{E-18}$$

The fourth term to be evaluated is $E\{Y_1(k)Y_2(k)\}$.

$$Y_1(k)Y_2(k) = \sum G^2(\alpha_i, \beta_i)\alpha_{1i}(k)\sin\left(\gamma_{1i}(k)-\theta_i\right)$$

$$\cdot \sum G^2(\alpha_i,\beta_i)\alpha_{2i}(k)\sin\left(\gamma_{2i}(k)-\theta_i\right) \tag{E-19}$$

$$= \sum G^4(\alpha_i,\beta_i)\frac{\alpha_{1i}(k)\alpha_{2i}(k)}{2}\left[\cos\left(\gamma_1(k)-\gamma_2(k)\right)\right.$$

$$\left.-\cos\left(\gamma_1(k)-\gamma_2(k)-2\theta_i\right)\right] \quad +$$

$$\sum \sum G^2(\alpha_i,\beta_i)G^2(\alpha_\ell,\beta_\ell)\,\frac{\alpha_{1i}(k)\alpha_{2\ell}(k)}{2}\left[\cos\left(\gamma_{1i}(k)-\theta_i-\gamma_{2\ell}(k)-\theta_\ell\right)\right.$$

$$\left.- \cos\left(\gamma_{1i}(k)-\theta_i+\gamma_{2\ell}(k)-\theta_\ell\right)\right] \tag{E-20}$$

$$E\{Y_1(k)Y_2(k)\} = E\{N_k\}\, E\{G^4(\alpha,\beta)\}\, E\left\{\frac{\alpha_1\alpha_2}{2}\cos(\gamma_1-\gamma_2)\right\}$$

$$= E\{x_1(k)x_2(k)\} \tag{E-21}$$

$$x_1(k)Y_2(k) = \sum G^2(\alpha_i,\beta_i)\alpha_{1i}(k)\cos\left(\gamma_{1i}(k)-\theta_i\right)$$

$$\sum_{i=1}^{N_k} G^2(\alpha_i,\beta_i)\alpha_{2i}(k)\sin\left(\gamma_{2i}(k)-\theta_i\right) \tag{E-22}$$

$$= \sum_{i=1}^{N_k} G^4(\alpha_i,\beta_i)\frac{\alpha_{1i}(k)\alpha_{2i}(k)}{2}\left[\sin\left(\gamma_{1i}(k)+\gamma_{2i}(k)-2\theta_i\right)\right.$$

$$\left. + \sin\left(\gamma_{2i}(k)-\gamma_{1i}(k)\right)\right] +$$

$$\sum_{\substack{i=1\\ i\neq\ell}}^{N_k}\sum_{\ell=1}^{N_k} G^2(\alpha_i,\beta_i)G^2(\alpha_\ell,\beta_\ell)\frac{\alpha_{1i}(k)\alpha_{2\ell}(k)}{2}\left[\sin\left(\gamma_{1i}(k)+\gamma_{2\ell}(k)-\theta_i-\theta_\ell\right)\right.$$

$$\left. + \sin\left(\gamma_{2\ell}(k)-\gamma_{1i}(k)-\theta_\ell+\theta_i\right)\right] \tag{E-23}$$

$$E\{x_1(k)y_2(k)\} = E\{N_k\}\ E\{G^4(\alpha,\beta)\}\ E\left\{\frac{\alpha_1\alpha_2}{2}\sin(\gamma_2-\gamma_1)\right\} \tag{F-24}$$

$$= \pm\ E\{N_k\}\ E\{G^4(\alpha,\beta)\}\ \left(\tfrac{1}{2}\right)\ E\left\{S_{22}\left(S_{11} \pm S_{12}\mathrm{Im}(T)\right)\right.$$

$$\left.\cdot\ R_e(T) - S_{12}\left(S_{21} \pm S_{22}\mathrm{Im}(T)\right)\ R_e(T)\right\} \tag{E-25}$$

$$= \pm\ E\{N_k\}\cdot E\{G^4(\alpha,\beta)\}\cdot\frac{\mathrm{Re}(T)}{2}\ E\{S_{22}[S_{11} \mp S_{12}\mathrm{Im}(T)]$$

$$- S_{12}[S_{21} \mp S_{22}\mathrm{Im}(T)]\} \tag{E-26}$$

$$Y_2(k)Y_1(k) = \sum_{i=1}^{N_k} G^2(\alpha_i,\beta_i)\alpha_{2i}(k)\cos\left(\gamma_{2i}(k)-\theta_i\right)$$

$$\cdot\sum_{i=1}^{N_k} G^2(\alpha_i,\beta_i)\alpha_{1i}(k)\sin\left(\gamma_{1i}(k)-\theta_i\right) \tag{E-27}$$

$$= \sum_{i=1}^{N_k} G^4(\alpha_i,\beta_i)\,\frac{\alpha_{1i}(k)\alpha_{2i}(k)}{2}\left[\sin\left(\gamma_{1i}(k)+\gamma_{2i}(k)-2\theta_i\right)\right.$$

$$\left. + \sin\left(\gamma_{1i}(k)-\gamma_{2i}(k)\right)\right] +$$

$$\sum_{i=1}^{N_k}\sum_{\substack{\ell=1\\ i\neq\ell}}^{N_k} G^2(\alpha_i,\beta_i)G^2(\alpha_\ell\ \beta_\ell)\,\frac{\alpha_{2i}(k)\alpha_{1\ell}(k)}{2}\left[\sin\left(\gamma_{1\ell}(k)+\gamma_{2i}(k)-\theta_i-\theta_\ell\right)\right.$$

$$\left. + \sin\left(\gamma_{1\ell}(k)-\gamma_{2i}(k)-\theta_\ell+\theta_i\right)\right] \qquad \text{(E-28)}$$

$$E\{x_2(k)Y_1(k)\} = E\{N_k\}\ E\{G^4(\alpha,\beta)\}\ E\left\{\frac{\alpha_1\alpha_2}{2}\sin(\gamma_1-\gamma_2)\right\} \qquad \text{(E-24)}$$

$$= -E\{N_k\}\ E\{G^4(\alpha,\beta)\}\ E\left\{\frac{\alpha_1\alpha_2}{2}\sin(\gamma_2-\gamma_1)\right\} \qquad \text{(E-25)}$$

$$= -E\{x_1(k)Y_2(k)\} \qquad \text{(E-26)}$$

APPENDIX F: THE REDUCTION IN DIMENSION OF INTEGRALS USED TO EVALUATE THE EXPECTATION OF $G'(k)$ AND $|G'(k)|^2$

Evaluation of $E\{G'(k)\}$ requires the determination of

$$E\left\{\frac{X_1(\ell)X_2(\ell)}{X_2^2(\ell)+Y_2^2(\ell)}\right\},\quad E\left\{\frac{Y_1(\ell)Y_2(\ell)}{X_2^2(\ell)+Y_2^2(\ell)}\right\},\quad E\left\{\frac{X_1(\ell)Y_2(\ell)}{X_2^2(\ell)+Y_2^2(\ell)}\right\},\text{ and } E\left\{\frac{X_2(\ell)Y_1(\ell)}{X_2^2(\ell)+Y_2^2(\ell)}\right\}$$

$$E\left\{\frac{X_1(\ell)X_2(\ell)}{X_2^2(\ell)+T_2^2(\ell)}\right\} = \iiiint \frac{X_1(\ell)X_2(\ell)}{X_2^2(\ell)+Y_2^2(\ell)}\, p\Big(X_1(\ell),X_2(\ell),Y_1(\ell),Y_2(\ell)\Big)dX_1(\ell)\ldots dY_2(\ell) \tag{F-1}$$

Wilks [20] indicates that integration of the density function, $p(\cdot)$, with respect to $Y_1(\ell)$ will result in a marginal density function of three variables with the same means and variances. Thus,

$$E\left\{\frac{X_1(\ell)X_2(\ell)}{X_2^2(\ell)+Y_2^2(\ell)}\right\} = \iiint \frac{X_1(\ell)X_2(\ell)}{X_2^2(\ell)+Y_2^2(\ell)}\, p\Big(X_1(\ell),X_2(\ell),Y_2(\ell)\Big)dX_1(\ell)\ldots dY_2(\ell) \tag{F-2}$$

Appendix A points out that the X and Y parameters are zero mean Gaussian variates, and thus the joint density function may be expressed in the form

$$p\Big(X_1(\ell),X_2(\ell),Y_2(\ell)\Big) = K_1 e^{-[C_1X_1^2 + C_2X_1 + C_3]} \tag{F-3}$$

The quadratic form appearing in the exponential is known to be positive definite [47], and thus C_1 is known to be positive [50]. Therefore,

$$E\left\{\frac{X_1(\ell)X_2(\ell)}{X_2^2(\ell)+Y_2^2(\ell)}\right\} = \int_{-\infty}^{+\infty}\int_{-\infty}^{+\infty}\left(\frac{-K_1C_2\sqrt{\pi}}{2C_1\sqrt{C_1}}\right)\left(\frac{X_2(\ell)}{X_2^2(\ell)+Y_2^2(\ell)}\right) e^{-[C_3-\frac{C_2^2}{4C_1}]}\, dX_2(\ell)dY_2(\ell) \tag{F-4}$$

where the inverse of the covariance matrix of the variables $X_1(\ell)$, $X_2(\ell)$, and $Y_2(\ell)$ is

$$\Lambda_B^{-1} = \begin{bmatrix} a & b & c \\ d & e & f \\ g & h & i \end{bmatrix} \tag{F-5}$$

and

$$c_1 = a/2 \tag{F-6}$$

$$c_2 = [(b+d)X_2(\ell)+(c+g)Y_2(\ell)]/2 \tag{F-7}$$

$$c_3 = [eX_2^2(\ell)+(f+h)X_2(\ell)Y_2(\ell)+iY_2^2(\ell)]/2 \tag{F-8}$$

$$K_1 = \frac{1}{(2\pi)^{3/2}\cdot\sqrt{\det(\Lambda_B)}} \quad . \tag{F-9}$$

A similar approach is used in evaluating the other expectation terms. The results are presented below.

$$E\left\{\frac{Y_1(\ell)Y_2(\ell)}{X_2^2(\ell)+Y_2^2(\ell)}\right\} = \int_{-\infty}^{+\infty}\int_{-\infty}^{+\infty}\left(\frac{-K_2C_5\sqrt{\pi}}{2C_4\sqrt{C_4}}\right) e^{-[C_6-\frac{C_5^2}{4C_4}]}\, dX_2(\ell)dY_2(\ell) \tag{F-10}$$

where the inverse of the covariance matrix of the variables $Y_1(\ell)$, $Y_2(\ell)$, and $X_2(\ell)$ is

$$\Lambda_F^{-1} = \begin{bmatrix} a & b & c \\ d & e & f \\ g & h & i \end{bmatrix} \tag{F-11}$$

and

$$C_4 = a/2 \tag{F-12}$$

$$C_5 = [(b+d)Y_2(\ell) + (C+g)X_2(\ell)]/2 \tag{F-13}$$

$$C_6 = [eY_2^2(\ell) + (f+h)X_2(\ell)Y_2(\ell) + iX_2^2(\ell)]/2 \tag{F-14}$$

$$K_2 = \frac{1}{(2\pi)^{3/2} \cdot \sqrt{\det(\Lambda_F)}} \quad . \tag{F-15}$$

$$E\left\{\frac{X_1(\ell)Y_2(\ell)}{X_2^2(\ell)+Y_2^2(\ell)}\right\} = \int_{-\infty}^{+\infty}\int \left(\frac{-K_1 C_2\sqrt{\pi}}{2C_1\sqrt{C_1}}\right)\left(\frac{Y_2(\ell)}{X_2^2(\ell)+Y_2^2(\ell)}\right) e^{-[C_3 - \frac{C_2^2}{4C_1}]}\, dX_2(\ell)dY_2(\ell) \tag{F-16}$$

$$E\left\{\frac{X_2(\ell)Y_1(\ell)}{X_2^2(\ell)+Y_2^2(\ell)}\right\} = \int_{-\infty}^{+\infty}\int \left(\frac{-K_2 C_5\sqrt{\pi}}{2C_2\sqrt{C_2}}\right)\left(\frac{X_2(\ell)}{X_2^2(\ell)+Y_2^2(\ell)}\right) e^{-[C_6 - \frac{C_5^2}{4C_4}]}\, dX_2(\ell)dY_2(\ell) \tag{F-17}$$

The following expressions are derived for use in evaluating $E\{|G'(k)|^2\}$.

$$E\left\{\frac{\left(X_1(\ell)X_2(\ell)\right)^2}{[X_2^2(\ell)+Y_2^2(\ell)]^2}\right\} = \iiint \frac{X_1^2(\ell)X_2^2(\ell)}{[X_2^2(\ell)+Y_2^2(\ell)]^2}\, p\left(X_1(\ell),X_2(\ell),Y_2(\ell)\right) dX_1(\ell)\ldots dY_2(\ell) \tag{F-18}$$

$$= \int_{-\infty}^{+\infty}\int \frac{K_1 C_2 \sqrt{\pi}}{2C_1\sqrt{C_1}} \left[\frac{1}{C_2} + \frac{C_2}{2C_1}\right] e^{-[C_3 - \frac{C_2^2}{4C_1}]} \frac{X_2^2(\ell)}{[X_2^2(\ell)+Y_2^2(\ell)]^2} dX_2(\ell)dY_2(\ell) \quad \text{(F-19)}$$

$$E\left\{\frac{Y_1^2(\ell)Y_2^2(\ell)}{[X_2^2(\ell)+Y_2^2(\ell)]^2}\right\} = \int_{-\infty}^{+\infty}\int \frac{K_2 C_6 \sqrt{\pi}}{2C_4\sqrt{C_4}} \left[\frac{1}{C_5} + \frac{C_5}{2C_4}\right] \frac{Y_2^2(\ell)}{[X_2^2(\ell)+Y_2^2(\ell)]^2} e^{-[C_6 - \frac{C_5^2}{4C_4}]} dX_2(\ell)dY_2(\ell)$$

(F-20)

$$E\left\{\frac{X_1^2(\ell)Y_2^2(\ell)}{[X_2^2(\ell)+Y_2^2(\ell)]^2}\right\} = \int_{-\infty}^{+\infty}\int \frac{K_1 C_2 \sqrt{\pi}}{2C_1\sqrt{C_1}} \left[\frac{1}{C_2} + \frac{C_2}{2C_1}\right] \frac{Y_2^2(\ell)}{[X_2^2(\ell)+Y_2^2(\ell)]^2} e^{-[C_3 - \frac{C_2^2}{4C_1}]} dX_2(\ell)dY_2(\ell)$$

(F-21)

$$E\left\{\frac{Y_1^2(\ell)X_2^2(\ell)}{[X_2^2(\ell)+Y_2^2(\ell)]^2}\right\} = \int_{-\infty}^{+\infty}\int \frac{K_2 C_6 \sqrt{\pi}}{2C_4\sqrt{C_4}} \left[\frac{1}{C_5} + \frac{C_5}{2C_4}\right] \frac{X_2^2(\ell)}{[X_2^2(\ell)+Y_2^2(\ell)]^2} e^{-[C_6 - \frac{C_5^2}{4C_4}]} dX_2(\ell)dY_2(\ell)$$

(F-22)

APPENDIX G: MOMENTS OF THE S MATRIX ELEMENTS

Expectations of S_{11}^2, S_{12}^2, S_{22}^2, $S_{11}S_{12}$, $S_{11}S_{22}$, and $S_{12}S_{22}$ are required for the evaluation of certain terms appearing in chpater six. These terms will be evaluated in the stated order here.

$$S_{11}^2 = g_x^2 - 2g_x(g_x-g_y)\left(\frac{V_\infty}{V_r}\right)^2 + (g_x-g_y)^2\left(\frac{V_\infty}{V_r}\right)^4 \tag{G-1}$$

$$E\{S_{11}^2\} = E\{g_x^2\} - 2E\left\{g_x(g_x-g_y)\left(\frac{V_\infty}{V_r}\right)^2\right\} + E\left\{(g_x-g_y)^2\left(\frac{V_\infty}{V_r}\right)^4\right\} \tag{G-2}$$

$$E\{g_x^2\} = \int_0^\infty d_0^6\,[8.25 - 0.244d_0^2 + 0.023d_0^3]\,\frac{\gamma^3}{2}\,d_0^2\,e^{-\gamma d_0}\,dd_0$$

$$= \left(\frac{\gamma^3}{2}\right)\left[\frac{3.25 \times 8!}{\gamma^9} - \frac{0.244 \times 10!}{\gamma^{11}} + \frac{0.023 \times 11!}{\gamma^{12}}\right] \tag{G-3}$$

$$E\left\{g_x(g_x-g_y)\left(\frac{V_\infty}{V_r}\right)^2\right\} = E\left\{g_x^2\left(\frac{V_\infty}{V_r}\right)^2\right\} - E\left\{g_xg_y\left(\frac{V_\infty}{V_r}\right)^2\right\} \tag{G-4}$$

$$E\left\{g_x^2\left(\frac{V_\infty}{V_r}\right)^2\right\} = \left(\frac{\gamma^3}{2}\right)\left(\frac{10.105}{V_r}\right)^2 \left\{\left[\frac{8.25 \times 8!}{\gamma^9} - \frac{0.244 \times 10!}{\gamma^{11}} + \frac{0.023 \times 11!}{\gamma^{12}}\right]\right.$$

$$- 2\left[\frac{8.25 \times 8!}{(\frac{1}{2}+\gamma)^9} - \frac{0.244 \times 10!}{(\frac{1}{2}+\gamma)^{11}} + \frac{0.023 \times 11!}{(\frac{1}{2}+\gamma)^{12}}\right]$$

$$\left. + \left[\frac{8.25 \times 8!}{(1+\gamma)^9} - \frac{0.244 \times 10!}{(1+\gamma)^{11}} + \frac{0.023 \times 11!}{(1+\gamma)^{12}}\right]\right\} \tag{G-5}$$

$$E\left\{g_x g_y \left(\frac{V_\infty}{V_r}\right)^2\right\} = \left(\frac{\gamma^3}{2}\right)\left(\frac{10.105}{V_r}\right)^2$$

$$\cdot\left\{\left[\frac{8.29\times 8!}{\gamma^9} - \frac{0.0672\times 10!}{\gamma^{11}} + \frac{0.0115\times 11!}{\gamma^{12}} - \frac{0.002075\times 12!}{\gamma^{13}}\right]\right.$$

$$- 2\left[\frac{8.29\times 8!}{(\frac{1}{2}+\gamma)^9} - \frac{0.0672\times 10!}{(\frac{1}{2}+\gamma)^{11}} + \frac{0.0115\times 11!}{(\frac{1}{2}+\gamma)^{12}} - \frac{0.002075\times 12!}{(\frac{1}{2}+\gamma)^{13}}\right]$$

$$\left.+\left[\frac{8.29\times 8!}{(1+\gamma)^9} - \frac{0.0672\times 10!}{(1+\gamma)^{11}} + \frac{0.0115\times 11!}{(1+\gamma)^{12}} - \frac{0.002075\times 12!}{(1+\gamma)^{13}}\right]\right\} \qquad (G\text{-}6)$$

$$E\left\{(g_x-g_y)^2\left(\frac{V_\infty}{V_r}\right)^4\right\} = \left(\frac{\gamma^3}{2}\right)\left(\frac{10.105}{V_r}\right)^4$$

$$\cdot\left\{\left[\frac{0.0024\times 10!}{\gamma^{11}} + \frac{0.00415\times 12!}{\gamma^{13}}\right] - 4\left[\frac{0.0024\times 10!}{(\frac{1}{2}+\gamma)^{11}} + \frac{0.00415\times 12!}{(\frac{1}{2}+\gamma)^{13}}\right]\right.$$

$$+ 6\left[\frac{0.0024\times 10!}{(1+\gamma)^{11}} + \frac{0.00415\times 12!}{(1+\gamma)^{13}}\right] - 4\left[\frac{0.0024\times 10!}{(\frac{3}{2}+\gamma)^{11}} + \frac{0.00415\times 12!}{(\frac{3}{2}+\gamma)^{13}}\right]$$

$$\left.+\left[\frac{0.0024\times 10!}{(2+\gamma)^{11}} + \frac{0.00415\times 12!}{(2+\gamma)^{13}}\right]\right\} \qquad (G\text{-}7)$$

The following notation is adcpted in order to simplify representation of the following work.

$A_1 = \gamma^3/2$

$A_2 = 8.25\times 8!$

$A_3 = 0.244\times 10!$

$A_4 = 0.023\times 11!$

$A_5 = (10.105/V_r)^2$

$A_6 = 8.29\times 8!$

$A_7 = 0.0672\times 10!$

$A_8 = 0.0115\times 11!$

$A_9 = 0.002075\times 12!$

$A_{10} = 0.0024\times 10!$

$A_{11} = 0.00415\times 12!$

$A_{12} = 8.33\times 8!$

$A_{13} = 0.112\times 10!$

$G_1 = \gamma^9$

$G_2 = \gamma^{11}$

$G_3 = \gamma^{12}$

$G_4 = \gamma^{13}$

$G_5 = (\frac{1}{2}+\gamma)^9$

$G_6 = (\frac{1}{2}+\gamma)^{11}$

$G_7 = (\frac{1}{2}+\gamma)^{12}$

$G_8 = (\frac{1}{2}+\gamma)^{13}$

$G_9 = (1+\gamma)^9$

$G_{10} = (1+\gamma)^{11}$

$G_{11} = (1+\gamma)^{12}$

$G_{12} = (1+\gamma)^{13}$

$G_{13} = (\frac{3}{2}+\gamma)^9$

$G_{14} = (\frac{3}{2}+\gamma)^{11}$

$G_{15} = (\frac{3}{2}+\gamma)^{12}$

$G_{16} = (\frac{3}{2}+\gamma)^{13}$

$G_{17} = (2+\gamma)^9$

$G_{18} = (2+\gamma)^{11}$

$G_{19} = (2+\gamma)^{12}$

$G_{20} = (2+\gamma)^{13}$

$G_{21} = (\frac{5}{2}+\gamma)^{11}$

$G_{22} = (\frac{5}{2}+\gamma)^{13}$

$$S_{12}^2 = (g_x-g_y)^2 \left(\frac{V_\infty}{V_r}\right)^2 - (g_x-g_y)^2 \left(\frac{V_\infty}{V_r}\right)^4 \qquad (G-8)$$

$$E\{S_{12}^2\} = E\left\{(g_x-g_y)^2 \left(\frac{V_\infty}{V_r}\right)^2\right\} - E\left\{(g_x-g_y)^2 \left(\frac{V_\infty}{V_r}\right)^4\right\} \qquad (G-9)$$

$$E\left\{(g_x-g_y)^2 \left(\frac{V_\infty}{V_r}\right)^2\right\} = A_1A_5 \left\{\left[\frac{A_{10}}{G_2} + \frac{A_{11}}{G_4}\right] - 2\left[\frac{A_{10}}{G_6} + \frac{A_{11}}{G_8}\right] + \left[\frac{A_{10}}{G_{10}} + \frac{A_{11}}{G_{12}}\right]\right\} \qquad (G-10)$$

$E\left\{(g_x-g_y)^2 (V_\infty/V_r)^4\right\}$ is evaluated in equation (G-7).

$$S_{22}^2 = (g_x-g_y)^2 \left(\frac{V_\infty}{V_r}\right)^4 + 2g_y(g_x-g_y)\left(\frac{V_\infty}{V_r}\right)^2 + g_y^2 \qquad (G-11)$$

$$E\{S_{22}^2\} = E\left\{(g_x-g_y)^2\left(\frac{V_\infty}{V_r}\right)^4\right\} + 2E\left\{g_y(g_x-g_y)\left(\frac{V_\infty}{V_r}\right)^2\right\} + E\{g_y^2\} \qquad (G-12)$$

$$E\left\{g_y(g_x-g_y)\left(\frac{V_\infty}{V_r}\right)^2\right\} = E\left\{g_xg_y\left(\frac{V_\infty}{V_r}\right)^2\right\} - E\left\{g_y^2\left(\frac{V_\infty}{V_r}\right)^2\right\} \qquad (G-13)$$

$E\left\{g_xg_y\left(\frac{V_\infty}{V_r}\right)^2\right\}$ is evaluated in equation (G-6).

$$E\left\{g_y^2\left(\frac{V_\infty}{V_r}\right)^2\right\} = A_1A_5 \left\{\left[\frac{A_{12}}{G_1} + \frac{A_{13}}{G_2}\right] - 2\left[\frac{A_{12}}{G_5} + \frac{A_{13}}{G_6}\right] + \left[\frac{A_{12}}{G_{13}} + \frac{A_{13}}{G_{14}}\right]\right\} \qquad (G-14)$$

$$S_{11}S_{12} = g\,(g_x-g_y)\left(\frac{V_\infty}{V_r}\right) - \left(\frac{1}{2}\right) g_x(g_x-g_y)\left(\frac{V_\infty}{V_r}\right)^3$$

$$- (g_x-g_y)^2 \left(\frac{V_\infty}{V_r}\right)^3 + (\tfrac{1}{2})\ (g_x-g_y)^2 \left(\frac{V_\infty}{V_r}\right)^5 \qquad \text{(G-15)}$$

$$E\{S_{11}S_{12}\} = E\left\{g_x(g_x-g_y)\left(\frac{V_\infty}{V_r}\right)\right\} - (\tfrac{1}{2})\ E\left\{g_x(g_x-g_y)\left(\frac{V_\infty}{V_r}\right)^3\right\}$$

$$- E\left\{(g_x-g_y)^2 \left(\frac{V_\infty}{V_r}\right)^3\right\} + (\tfrac{1}{2})\ E\ (g_x-g_y)^2 \left(\frac{V_\infty}{V_r}\right)^5\Bigg\} \qquad \text{(G-16)}$$

$$E\left\{g_x(g_x-g_y)\left(\frac{V_\infty}{V_r}\right)\right\} = E\left\{g_x^2\left(\frac{V_\infty}{V_r}\right)\right\} - E\left\{g_x g_y\left(\frac{V_\infty}{V_r}\right)\right\} \qquad \text{(G-17)}$$

$$E\left\{g_x^2\left(\frac{V_\infty}{V_r}\right)\right\} = A_1\sqrt{A_5}\left\{\left[\frac{A_2}{G_1} - \frac{A_3}{G_2} + \frac{A_4}{G_3}\right] - \left[\frac{A_2}{G_5} - \frac{A_3}{G_6} + \frac{A_4}{G_7}\right]\right\} \qquad \text{(G-18)}$$

$$E\left\{g_x g_y\left(\frac{V_\infty}{V_r}\right)\right\} = A_1\sqrt{A_5}\left\{\left[\frac{A_6}{G_1} - \frac{A_7}{G_2} + \frac{A_8}{G_3} - \frac{A_9}{G_4}\right] - \left[\frac{A_6}{G_5} - \frac{A_7}{G_6} + \frac{A_8}{G_7} - \frac{A_9}{G_8}\right]\right\} \qquad \text{(G-19)}$$

$$E\left\{g_x(g_x-g_y)\left(\frac{V_\infty}{V_r}\right)^3\right\} = E\left\{g_x^2\left(\frac{V_\infty}{V_r}\right)^3\right\} - E\left\{g_x g_y\left(\frac{V_\infty}{V_r}\right)^3\right\} \qquad \text{(G-20)}$$

$$E\left\{g_x^2\left(\frac{V_\infty}{V_r}\right)^3\right\} = A_1 A_5^{3/2}\left\{\left[\frac{A_2}{G_1} - \frac{A_3}{G_2} + \frac{A_4}{G_3}\right] - 3\left[\frac{A_2}{G_5} - \frac{A_3}{G_6} + \frac{A_4}{G_7}\right]\right.$$

$$\left. + 3\left[\frac{A_2}{G_9} - \frac{A_3}{G_{10}} + \frac{A_4}{G_{11}}\right] - \left[\frac{A_2}{G_{13}} - \frac{A_3}{G_{14}} + \frac{A_4}{G_{15}}\right]\right\} \qquad \text{(G-21)}$$

$$E\left\{g_x g_y\left(\frac{V_\infty}{V_r}\right)^3\right\} = A_1 A_5^{3/2}\left\{\left[\frac{A_6}{G_1} - \frac{A_7}{G_2} + \frac{A_8}{G_3} - \frac{A_9}{G_4}\right] - 3\left[\frac{A_6}{G_5} - \frac{A_7}{G_6} + \frac{A_8}{G_7} - \frac{A_9}{G_8}\right]\right.$$

$$+ 3\left[\frac{A_6}{G_9} - \frac{A_7}{G_{10}} + \frac{A_8}{G_{11}} - \frac{A_9}{G_{12}}\right] - \left[\frac{A_6}{G_{13}} - \frac{A_7}{G_{14}} + \frac{A_8}{G_{15}} - \frac{A_9}{G_{16}}\right]\Bigg\} \quad \text{(G-22)}$$

$$E\left\{(g_x-g_y)^2\left(\frac{V_\infty}{V_r}\right)^3\right\} = A_1 A_5^{3/2}\left\{\left[\frac{A_{10}}{G_2} + \frac{A_{11}}{G_4}\right] - 3\left[\frac{A_{10}}{G_6} + \frac{A_{11}}{G_8}\right]\right.$$

$$\left. + 3\left[\frac{A_{10}}{G_{10}} + \frac{A_{11}}{G_{12}}\right] - \left[\frac{A_{10}}{G_{14}} + \frac{A_{11}}{G_{16}}\right]\right\} \quad \text{(G-23)}$$

$$E\left\{(g_x-g_y)^2\left(\frac{V_\infty}{V_r}\right)^5\right\} = A_1 A_5^{5/2}\left\{\left[\frac{A_{10}}{G_2} + \frac{A_{11}}{G_4}\right] - 5\left[\frac{A_{10}}{G_6} + \frac{A_{11}}{G_8}\right] + 10\left[\frac{A_{10}}{G_{10}} + \frac{A_{11}}{G_{12}}\right]\right.$$

$$\left. - 10\left[\frac{A_{10}}{G_{14}} + \frac{A_{11}}{G_{16}}\right] + 5\left[\frac{A_{10}}{G_{18}} + \frac{A_{11}}{G_{20}}\right] - \left[\frac{A_{10}}{G_{21}} + \frac{A_{11}}{G_{22}}\right]\right\} \quad \text{(G-24)}$$

$$S_{11}S_{22} = g_x(g_x-g_y)\left(\frac{V_\infty}{V_r}\right)^2 - (g_x-g_y)^2\left(\frac{V_\infty}{V_r}\right)^4 + g_x g_y - g_y(g_x-g_y)\left(\frac{V_\infty}{V_r}\right)^2 \quad \text{(G-25)}$$

$$E\{S_{11}S_{22}\} = E\left\{g_x(g_x-g_y)\left(\frac{V_\infty}{V_r}\right)^2\right\} - E\left\{(g_x-g_y)^2\left(\frac{V_\infty}{V_r}\right)^4\right\}$$

$$+ E\{g_x g_y\} - E\left\{g_y(g_x-g_y)\left(\frac{V_\infty}{V_r}\right)^2\right\} \quad \text{(G-26)}$$

$E\left\{g_x(g_x-g_y)\left(\frac{V_\infty}{V_r}\right)^2\right\}$ is given in equations (G-4), (G-5), and (G-6),

and $E\left\{(g_x-g_y)^2\left(\frac{V_\infty}{V_r}\right)^4\right\}$ is evaluated in equation (G-7).

$$E\{g_x g_y\} = A_1\left[\frac{A_6}{G_1} - \frac{A_7}{G_2} + \frac{A_8}{G_3} - \frac{A_9}{G_4}\right] \qquad (G\text{-}27)$$

Note also that $E\left\{g_y(g_x-g_y)\left(\frac{V_\infty}{V_r}\right)^2\right\}$ is expressed in equations (G-6) and (G-14).

APPENDIX H: NUMERICAL INTEGRATION TECHNIQUES

Numerical integration will be used to evaluate the required moments of $G'(k)$. The work of Appendix G has shown that the desired moments may be expressed as two dimensional integrals extending over $(-\infty, +\infty)$, but for the purposes of numerical integration it is desirable that the range of integration by (0, 1). The change of integration range is accomplished in the following manner.

$$\int_{-\infty}^{+\infty} f(x)\,dx = \int_{-\infty}^{0} f(x)\,dx + \int_{0}^{\infty} f(x)\,dx \qquad \text{(H-1)}$$

In the range $(-\infty, 0)$, let $x = \ln y$ so that

$$\int_{-\infty}^{0} f(x)\,dx = \int_{0}^{1} f(\ln y)\,\frac{dy}{y}\,, \qquad \text{(H-2)}$$

and in the range $(0, +\infty)$, let $x = -\ln y'$ so that

$$\int_{0}^{\infty} f(x)\,dx = -\int_{1}^{0} f(-\ln y)\,\frac{dy'}{y'} = \int_{0}^{1} f(-\ln y')\,\frac{dy'}{y'} \qquad \text{(H-3)}$$

Thus,

$$\int_{-\infty}^{+\infty} f(x)\,dx = \int_{0}^{1} \frac{[f(\ln y) + f(-\ln y)]}{y}\,dy. \qquad \text{(H-4)}$$

This type of transformation is suggested by Davis and Rabinowitz [51].

The actual numerical integration scheme is basically a Monte Carlo technique, but instead of using a multidimensional random variable generator

to provide the independent variables, a set of linearly independent equidistributed sequences is used. A justification for and discussion of this technique is provided by Davis and Rabinowitz [51]. Integration was carried out using one thousand points of evaluation in each quadrant of the independent variable space, and checks on the accuracy of integration were developed as indicated in the following figures.

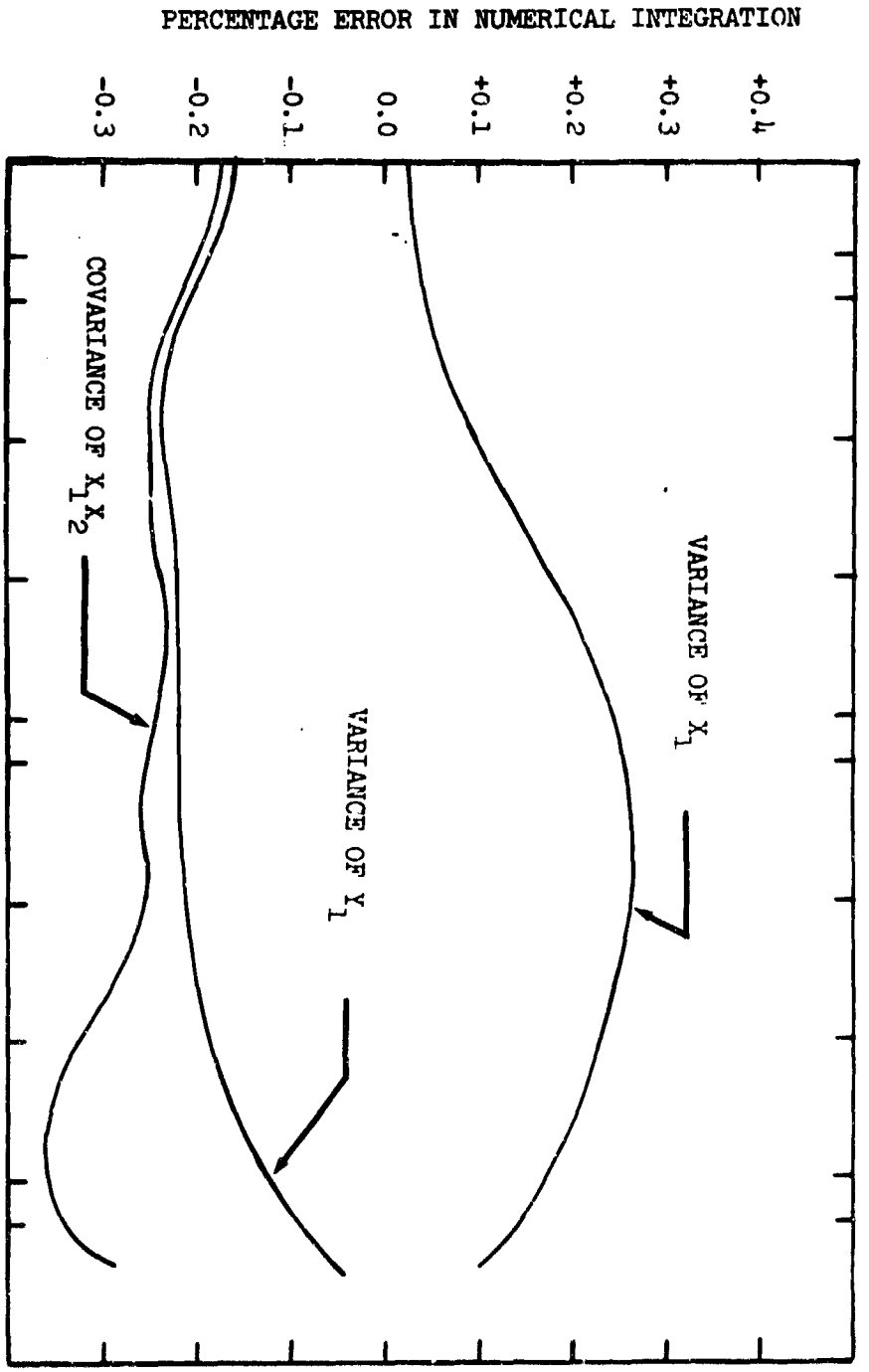

Fig. H-1. Accuracy of numerical integration.

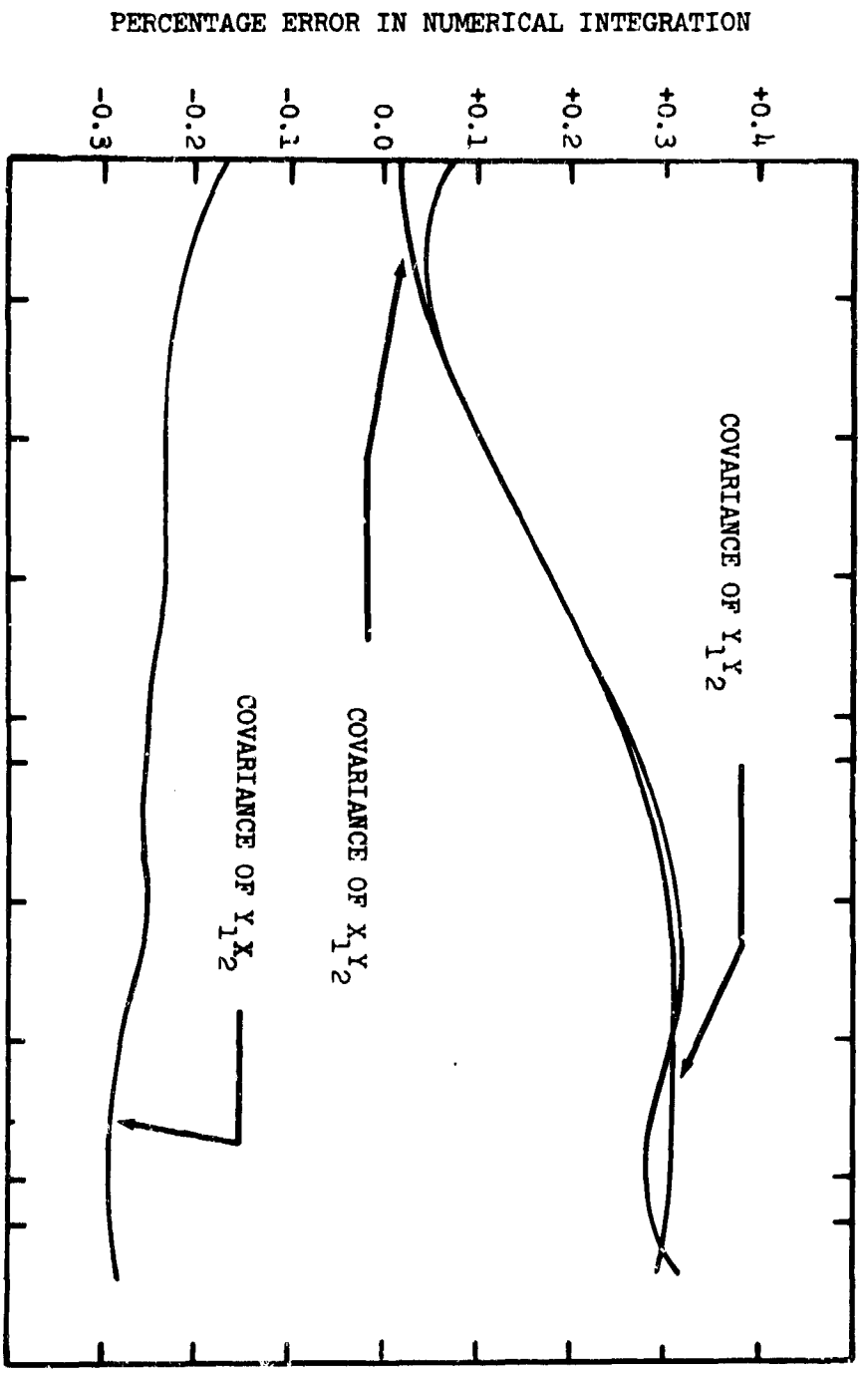

Fig. 42. Accuracy of numerical integration.

MISSION
of
Rome Air Development Center

RADC is the principal AFSC organization charged with planning and executing the USAF exploratory and advanced development programs for information sciences, intelligence, command, control and communications technology, products and services oriented to the needs of the USAF. Primary RADC mission areas are communications, electromagnetic guidance and control, surveillance of ground and aerospace objects, intelligence data collection and handling, information system technology, and electronic reliability, maintainability and compatibility. RADC has mission responsibility as assigned by AFSC for demonstration and acquisition of selected subsystems and systems in the intelligence, mapping, charting, command, control and communications areas.